



*Marcin K. Widomski, Dariusz Kowalski,
Małgorzata Iwanek, Grzegorz Łagód*

Modeling of Water Flow and Pollutants Transport in Porous Media

With Exemplary Calculations in FEFLOW

M
O
N
O
G
R
A
F
I
E

Modeling of Water Flow and Pollutants Transport in Porous Media

With Exemplary Calculations in FEFLOW

Monografie – Politechnika Lubelska



HUMAN CAPITAL
NATIONAL COHESION STRATEGY

EUROPEAN UNION
EUROPEAN
SOCIAL FUND



Publication co-financed by the European Union
under the European Social Fund

Marcin K. Widomski, Dariusz Kowalski,
Małgorzata Iwanek, Grzegorz Łagód

Modeling of Water Flow and Pollutants Transport in Porous Media

With Exemplary Calculations in FEFLOW



Politechnika Lubelska
Lublin 2013

Reviewer:
Prof. dr hab. Henryk Sobczuk



The publication distributed free of charge. 200 copies.
Published as part of the Modern education – the development
of didactic potential of the Lublin University of Technology.
Number of agreement POKL.04.01.01-00-108/08 UDA – financed
by the European Union under the European Social Fund.

Publication approved by the Rector of Lublin University of Technology

© Copyright by Lublin University of Technology 2013

ISBN: 978-83-63569-59-4

Publisher: Lublin University of Technology
ul. Nadbystrzycka 38D, 20-618 Lublin, Poland
Realization: Lublin University of Technology Library
ul. Nadbystrzycka 36A, 20-618 Lublin, Poland
tel. (81) 538-46-59, email: wydawca@pollub.pl
www.biblioteka.pollub.pl
Printed by: TOP Agencja Reklamowa Agnieszka Łuczak
www.agencjatorp.pl

Elektroniczna wersja książki dostępna w Bibliotece Cyfrowej PL www.bc.pollub.pl
Nakład: 200 egz.

Table of contents

Notation	6
Introduction	8
1 Fundamentals of water flow in soils	11
1.1 Soil and water	11
1.2 Water retention curve	14
1.3 Hydraulic conductivity of soils	18
1.4 Darcy's law	20
1.5 Richard's equation	21
2 Fundamentals of mass transport in soils	23
2.1 Equation of hydrodynamic dispersion	23
2.2 Hydrodynamic dispersion coefficient	25
2.3 Models of sorption	27
2.4 Decay reactions	28
3 Brief description of FEFLOW	30
3.1 Software characteristics	30
4 Exemplary calculations of water flow and mass (pollutants) transport in soil by FEFLOW	45
4.1 Simulation of fine sand column wetting by capillary rise	45
4.2 Simulation of water capillary rise in two-layered soil profile	58
4.3 Simulation of water capillary rise in three-layered soil profile	67
4.4 Simulation of cadmium transport in fine sand column wetting by capillary rise	73
4.5 Simulation of chromium transport in two-layered soil profile	82
4.6 Simulation of water and contaminant balance for the soil profile consisting of four layers	91
5 Bibliography	105

Notation

- a – anisotropy ratio [-],
 a – fitting parameter,
 b – fitting parameter,
 $clay$ – percentage clay fraction content [%],
 D – soil water diffusivity [m^2/s],
 d – micropore diameter [m],
 h – hydraulic pressure head [m],
 h_a – air entry pressure head [m],
 h_s – soil matric suction pressure [cm],
 K – hydraulic conductivity [m/s],
 \mathbf{K} – permeability tensor,
 K_H – horizontal hydraulic conductivity [m/s],
 K_{ij} – hydraulic conductivity tensor, $i, j = 1, 2$ [m/s],
 k – permeability [m^2],
 K_r – relative hydraulic conductivity of soil [-],
 K_s – saturated hydraulic conductivity [m/s],
 K_v – vertical hydraulic conductivity [m/s],
 $K(\theta)$ – hydraulic conductivity [m/s],
 l – fitting parameter ,
 m – fitting parameter [-],
 m – fitting parameter,
 m_t – mass of soil [kg],
 m_w – mass of water contained in soil [kg],
 n – fitting parameter [-], (eq. 1.10),
 p – groundwater pressure [N/m^2],
 pF – logarithmic water retention curve [-],
 q – water flux [m/s],
 q – groundwater flux [m/s],
 \mathbf{qi} – groundwater flux vector [m/s],
 S – degree of saturation [-],
 $sand$ – percentage sand fraction content [%],
 S_0 – specific storage compressibility [1/m],
 S_r – residual saturation [-],
 S_s – saturated saturation [-],
 $S(\theta)$ – sink or source term [1/s],
 t – time [s],
 V_t – total volume of soil [m^3],
 V_v – void volume [m^3],
 V_w – volume of water contained in soil [m^3],
 x – spatial coordinate [m],
 z – elevation height [m],
 x, y, z – Cartesian coordinates [m],

- α – wetting angle [deg],
 α – fitting parameter [1/m] or [1/cm],
 ∇ – 3D gradient operator,
 Δh – pressure drop [m],
 Δx – flow length [m],
 η – porosity ratio [-],
 μ – dynamic viscosity of fluid [kg/(m·s)],
 θ – volumetric water content [m³/m³],
 θ – volumetric water content [m³/m³],
 θ_a – actual volumetric water content [m³/m³],
 θ_m – gravimetric water content [kg/kg],
 θ_r – residual volumetric water content [m³/m³],
 θ_s – saturated volumetric water content [m³/m³],
 ρ – water density [kg/m³],
 σ – water surface tension [N/m],
 Ψ – water potential [N/m²] or [m],
 Ψ_g – gas pressure potential [N/m²],
 Ψ_m – matric potential [N/m²],
 Ψ_o – osmotic potential [N/m²],
 Ψ_z – gravity potential [N/m²],
 Ψ_{op} – overburden potential [N/m²],

Introduction

This elaboration, prepared in the textbook form, may be treated as a learning aid for computer laboratory of numerical modeling of groundwater movement and mass transport in soils, especially for the Environmental Engineering students. Our main purpose was to present the theoretical fundamentals and practical applications of groundwater flow and pollutants transport in soils, both in the saturated and unsaturated zones and the main rules of numerical model development. Definition of required input data, water-transport parameters of soil, initial and boundary conditions, simulation calculations as well as results presentation were practically illustrated by exemplary calculations elaborated by the Authors and conducted in demo version of FEFLOW, DHI-WASY.

Rapid development of computer techniques in the last three decades (1980–2010) enabled popularization of numerical modeling application, understood as description of natural systems by the language of mathematics. Thus, mathematical models represent concept description or estimations describing physical systems or processes by mathematical equations. Modeling may cover different types of systems: biological, economic and physical-electric, mechanical, hydraulic and thermodynamic etc.

Technical literature presents different definitions of model, usually with different aspect underlined: mathematical, numerical or computer (*Kulbik, 2004*).

The Polish encyclopedical definition (*Encyklopedia, 2002*) states that model is a physical system or mathematical description of several properties and characteristics relating to the selected properties or characteristics of modeled object, and modeling is an experimental method of research based on constructed models.

Usually models present simplified, to some extent, reflection of the real-world studied phenomena. The efficiency of applications of models reflecting processes of physical phenomena results directly from accepted level of model simplification. Thus, true and full understanding of modeled phenomena and simplifications applied to the mathematical equations describing the studied process are required to obtain the statistically relevant results. Then, the definition of required set of input data allowing to develop the initial and boundary conditions is necessary (*Bear et al. 1992, Grabarczyk, 2000*).

The dynamic, deterministic mathematical models of water movement and mass transport in soils use mathematical equations based on several assumptions simplifying the real systems, covering usually: geometry of the system (basin or aquifer) with the proper physical description. The heterogeneity of medium as well as properties of applied liquids, direction of flow, transport mechanisms and equations of chemical reactions occurring inside the liquid body are considered (*Wind, 1979; Maciejewski 1998*).

Taking the above into consideration, we may state that mathematical model of groundwater movement and pollutants transport based on several assumptions and requiring significant number of input data, which obtainment may be strained by measure and calculation errors, should be treated as simplified attempts of physical phenomena description, but not as their precise projections. The available scientific reports (e.g. *Olszta and Zaradny, 1994; Kowalik, 1995; Maciejewski, 1998; Zhao et al., 2005*) show that, despite the purposeful described simplifications and possible inaccuracy, modeling may be treated as a successful aid in scientific and engineering activities.

Known applications of mathematical models into scientific and engineering activities considering porous media cover:

- water movement in porous media (soil, building materials),
- water balance of catchments or aquifers,
- dynamics of water content distribution in unsaturated zone of soil profile,
- influence of changes in water balance on ecosystems e.g. plants growth, water availability etc.,
- pollutants transport originated from point and surface sources in porous media, applicable at designing of direct and indirect protection zone of underground and surface water intakes or in determination of engineering object on local environment (e.g. municipal solid waste landfill site),
- heat transport in porous media of different saturation (by water or various chemical solutions).

The presented above exemplary applications of numerical modeling in scientific and engineering activities of, commonly understood, environmental engineering show that modeling may be treated as an important element in designing of engineering objects and may be successfully introduced into management of developed environmental systems.

Employment of various mathematical models into engineering practice enables management of the real, existing systems or analysis of operational conditions of systems being just at the stage of design or development.

Numerous authors (e.g. *de Wit and Goudriaan, 1978; Heinrich and Pepper, 1999; Grabarczyk, 2000; Karafiat, 2000; Knapik, 2000; Cook, 2002; Kulbik, 2004; Król, 2006; Gromiec, 2007, Widomski et al., 2010*) state that modeling may be very useful and convenient in irrigation and drainage of agricultural areas planning, designing of building excavations drainage, localization of various objects of water supply or sewage systems, spatial planning of objects potentially hazardous to the natural environment (municipal solid waste landfill sites, petrol stations, fertilizers and pesticides warehouses and reloading points). Modeling may also improve the assessment of agricultural and transport operations effects on water resources con-

dition and characteristics, calculation of required pressure head of pumping devices, selection of disinfectants doses, analysis of water quality outside distribution systems, assessment of thermal isolation efficiency etc. Thus, introduction of modeling may result in reduction of management costs and shortening of designing time, in many cases eliminating the expensive and time-consuming pilot, in-situ tests.

1 Fundamentals of water flow in soils

This chapter contains the basic information concerning the subjects of water in soil (as a porous medium), soil matric pressure, water retention curve, hydraulic conductivity, as well as soil water movement.

1.1 Soil and water

Soil is a natural body consisting of layers (soil horizons) of mineral constituents of variable thicknesses different from the parent materials in their morphological, physical, chemical, and mineralogical characteristics (*Birkeland, 1999*). Soil is also a multiphase mineral and organic porous media consisting of three phases: solid, liquid and gaseous. The solid phase consists of particles of various distribution generated by partitioning of rocks by different environmental (erosion, transport, deposition), thermal and chemical processes. There are three main types of soil particles distinguished: sand, silt and clay. The relative amount of each fraction in the soil sample, sorted according to its size (particle diameter) are presented by particle size distribution or grain size distribution (*Jillavenkatesa et al., 2001*).

Soil particles are usually packed loosely, with different, even unique three dimensional spatial orientation, thus creating a soil solid structure filled with empty pores, which may be occupied by fluids – liquids or/and gases. The fraction of void space in the porous material/soil is defined by porosity ratio (e.g. *Orzechowski et al., 1997*).

$$\eta = \frac{V_v}{V_t} \quad (1.1)$$

where: η – porosity ratio [-], V_v – void volume [m^3], V_t – total volume of soil [m^3].

The exemplary values of porosity for different rocks are presented in Table 1.1.

Table 1.1. Porosity of different rocks (*Wieczysty, 1982*)

Type of rock	Porosity [-]
Gravel	0.25–0.30
Sand	0.36–0.45
Clayey sand	0.45–0.49
Granite	0.0005–0.0090
Basalt	0.006–0.013
Limestone	0.006–0.169
Peat	0.70–0.96

Water in soil is located below the soil surface and fills the empty spaces among solid grains – soil pores. Two different zones of soil saturation may be observed: saturated and unsaturated zone, divided by ground water table. If the water fills all space of pores the zone is recognized as saturated zone. In the other case, when water fills the pore spaces partially, above the water table the zone is described as unsaturated zone.

The amount of water contained in soil may be characterized by water content or moisture content. Volumetric water content θ is defined by a fraction:

$$\theta = \frac{V_w}{V_t} \quad (1.2)$$

where: θ – volumetric water content [m^3/m^3], V_w – volume of water contained in soil [m^3].

Thus, gravimetric water content θ_m may be defined as:

$$\theta_m = \frac{m_w}{m_t} \quad (1.3)$$

where: θ_m – gravimetric water content [kg/kg], m_w – mass of water contained in soil [kg], m_t – mass of soil [kg].

Additionally, we may define the degree of saturation S understood as fraction of actual volumetric content to the volumetric water content of tested soil in saturated conditions (e.g. *Kowalik, 2007*):

$$S = \frac{\theta_a}{\theta_s} \quad (1.4)$$

where: S – degree of saturation [-], θ_a – actual volumetric water content [m^3/m^3], θ_s – saturated volumetric water content [m^3/m^3].

Water in unsaturated zone is held in micropores by various capillary forces connected to the surface tension of water – soil interface. Forces holding water in close distance to solid particles and inside the narrow interstices between particles are strong adsorptive forces known as van der Waal-London forces as well as the osmotic forces exerted by solutes on nearby water molecules (*Chesworth, 2008*).

Scheme of capillary rise in narrow micropore and equation describing the height of capillary rise are presented in Fig. 1.1., where H is calculated as:

$$H = \frac{2 \cdot \sigma}{\rho \cdot g \cdot d} \cos \alpha \quad (1.5)$$

where: σ – water surface tension (0,073 [N/m] at 20°C), d – micropore diameter [m], ρ – water density [kg/m^3], α – wetting angle [deg].

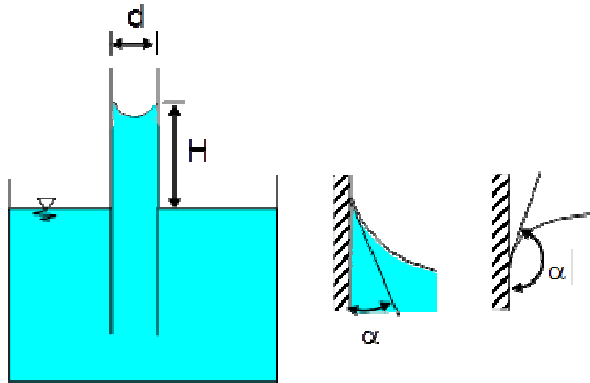


Fig. 1.1. Scheme of capillary rise phenomenon

Complicated structure of porous media and nature of various forces holding water in soil makes quantification of retentive forces hardly possible (Chesworth, 2008). Thus, instead the term of water potential was introduced.

According to numerous international sources (e.g. Hillel, 1982; Zaradny, 1990; Kowalik, 2007; Chesworth, 2008) water potential Ψ (in $[N/m^2]$) is consisting of several components:

- matric potential, Ψ_m : a negative value of work necessary to remove water from soil sample overcoming the forces of surface tension and particle surface forces,
- osmotic potential, Ψ_o : a negative value of work necessary to remove water from ions in the soil solution,
- gravity potential, Ψ_z : a negative or positive value of work necessary to move water in soil from one elevation to reference level,
- gas pressure potential, Ψ_g : value of work needed to overcome soil gas pressure gradient,
- overburden potential, Ψ_{op} : involves the weight of movable soil particles which exert the pressure on soil water.

Thus, equation representing water potential may have a form:

$$\Psi = \Psi_m + \Psi_o + \Psi_z + \Psi_g + \Psi_{op} \quad (1.6)$$

Soil matric pressure, commonly described as pore water pressure is the sum of matric and pneumatic pressures (ISO 11276:1995).

Another commonly used variable to describe potential of groundwater is pressure head h representing the internal energy of water due to the pressure exerting on the soil (the container of groundwater). Pressure head may be explained as:

$$h = \frac{p}{\rho \cdot g} \quad (1.7)$$

where: p – groundwater pressure [N/m²].

After assuming action of gravity, we may transform pressure head to groundwater hydraulic head:

$$h = \frac{p}{\rho \cdot g} + z \quad (1.8)$$

1.2 Water retention curve

Water retention curve, also known as soil moisture characteristics is a relationship between volumetric water content θ and water potential Ψ .

The introduction of soil matric suction pressure h_s [cm], according to ASTM D 5298 understood as a sum of matric and osmotic suction, allows to present the water retention curve in logarithmic form, as presented below (e.g. *Zaradny, 1990; Kowalik, 2007*).

$$pF = \log_{10} h_s \quad (1.9)$$

where: pF – logarithmic water retention curve [-], h_s – soil matric suction pressure [cm].

The exemplary shape of water retention curve in the form of pF curve is presented in Fig. 1.2.

Water retention curve is commonly used in soil, hydrological and agricultural science to predict the amount of water stored in the soil profile, to calculate the water field capacity, water availability to plants and soil aggregate stability (e.g. *Zaradny, 1990; Raikai et al., 2004*).

Fig. 1.2. presents also two crucial points applied in water retention curves analyses – water field capacity (FC , $pF = 2.0$) and wilting point (WP , $pF = 4.2$). Water field capacity is the amount of water content held in soil after the excess water drained gravitationally downward. Wilting point defines the minimal amount of available water to plant not to unrecoverable wilt.

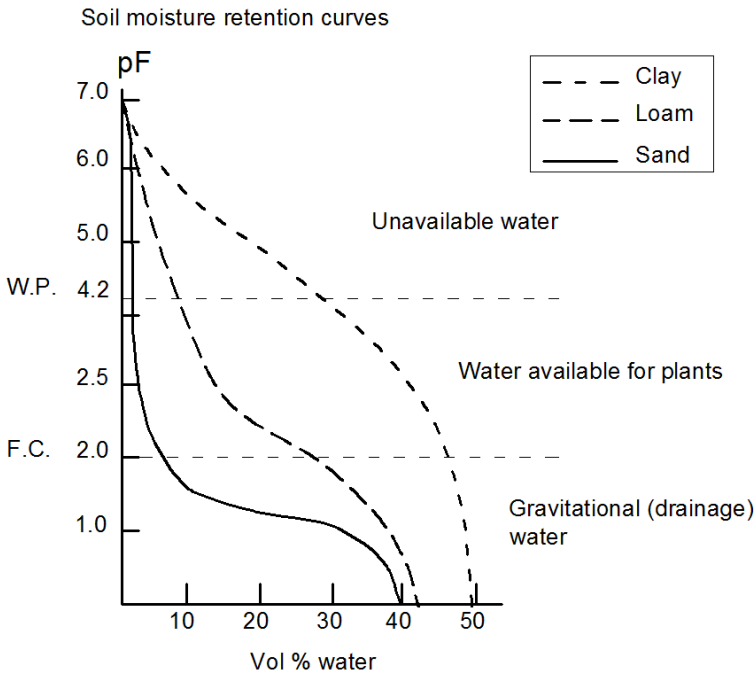


Fig. 1.2. Exemplary pF curves for various soils (modified from www.nivaa.nl/uk)

Usually, the hysteresis effect of water retention curve may be observed – see Fig. 3.3. The drying curve is located above the wetting curve – this means that drying soil preserves higher amounts of water that soil during water filling the pores at the same value of soil pressure (pF). Different approaches are observed in practical application of hysteresis phenomenon – often only wetting curve is used, or calculation are based on mean values for wetting-drying cycle (*Brzostowski and Olszta, 1996; Stauffer and Kinze, 2001; Werner and Lockington, 2003; Kowalik, 2007*).

The most popular mathematical description of water retention curve shape was presented by van Genuchten (1980):

$$\theta = \frac{\theta_s - \theta_r}{[1 + (\alpha h)^n]^m} + \theta_r \quad (1.10)$$

where: θ_r – residual volumetric water content [m^3/m^3], representing the amount of water present in soil sample after drying in 105°C , α , n , m – fitting parameters, $m = 1 - n^{-1}$, α in [$1/\text{m}$] or [$1/\text{cm}$], the others – dimensionless.

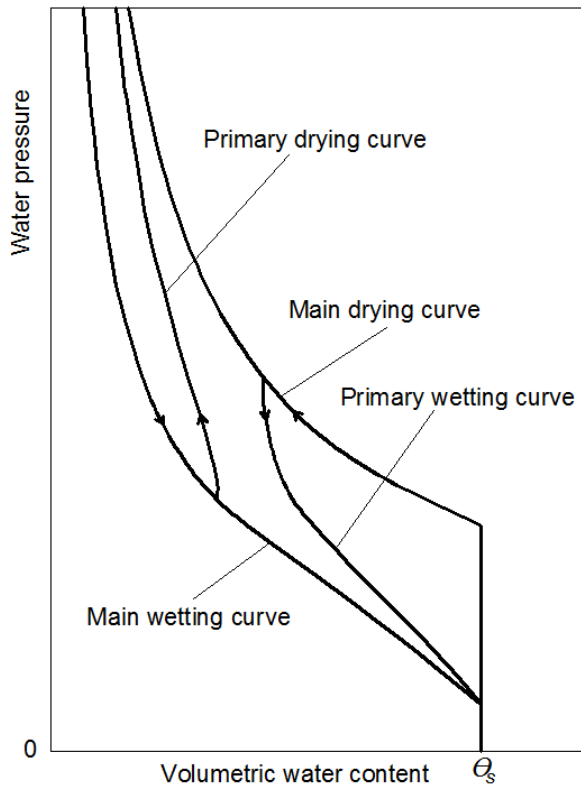


Fig. 1.3. Exemplary hysteresis effect of water retention curve (*Maqsoud et al., 2004*)

The exemplary fitting parameters for water retention curve in the van Genuchten's model are presented in Tab. 1.2.

The above formula may be also presented in degree of saturation based form like applied in FEFLOW (*Diersch, 2005*):

$$S = \frac{S_s - S_r}{[1 + (\alpha\psi)^n]^m} + S_r, (\psi < 0) \quad (1.11)$$

where: S_r – residual saturation [-].

Table 1.2. Exemplary parameters of water retention curves for various soils (modified from Zand-Parsa and Sepaskhah, 2004; Schaap and van Genuchten, 2006)

Soil type	Saturated soil moisture θ_s	Residual soil moisture θ_r	Fitting parameters	
			α	n
	[m ³ /m ³]	[m ³ /m ³]	[1/cm]	[-]
Sands (average for Sand, Loamy Sand, Sandy Loam, Sandy Clay Loam)	0.396	0.052	0.0263	2.23
Loams (average for Loam and Clay Loam)	0.512	0.056	0.0407	1.19
Silts (average for Silty Loam and Silt)	0.428	0.031	0.0120	1.38
Clays (average for Clay, Sandy Clay, Silty Clay and Silty Clay Loam)	0.512	0.098	0.0178	1.30
Sand	0.380	0.110	0.0260	7.700
	0.250	0.153	0.0079	10.400
Silt loam	0.550	0.161	0.0367	1.572
Loam	0.500	0.060	0.0261	1.441
	0.520	0.218	0.0115	2.030
Sandy loam	0.042	0.010	0.0094	1.632
	0.335	0.074	0.0153	1.265
Fine sand	0.380	0.030	0.0226	7.339
Sandy loam	0.335	0.074	0.0153	1.265
Silt loam	0.388	0.173	0.0471	1.461
	0.469	0.190	0.0050	7.090
	0.369	0.131	0.0042	2.060
Sandy clay loam	0.402	0.112	0.0082	1.275
Clay	0.589	0.109	0.0007	1.419
	0.446	0.000	0.0015	1.170

1.3 Hydraulic conductivity of soils

Hydraulic conductivity of porous media (often marked as K) represents the ease with which water can move through pore spaces or fractures. In other words, the hydraulic conductivity is a measure of the porous media (e.g. soil) ability to transmit water when submitted to a hydraulic gradient.

Hydraulic conductivity is related to porous media permeability (property of soil, or other porous media, permitting the transmission of fluids) according to the relation:

$$K = k \frac{\rho g}{\mu} \quad (1.12)$$

where: K – hydraulic conductivity [m/s], k – permeability [m²], μ – dynamic viscosity of fluid [kg/(m·s)].

Saturated hydraulic conductivity, commonly marked as K_{sat} or K_s , describes water flow through saturated porous media (all pores filled with water). The exemplary ranges of K_s for selected types of soil are presented in Tab. 1.3.

Table 1.3. Approximated saturated conductivity of soils (modified from <http://web.ead.anl.gov> and <http://web.ead.anl.gov/resrad/datacoll/conduct.htm>)

Soil type	Saturated hydraulic conductivity [m/day]
Gravel	30–30 000
Clear sand	0.3–300
Silty sand	0.03–30
Silt, loess	$3.0 \cdot 10^{-5}$ –0.3
Glacial till	$3.0 \cdot 10^{-8}$ –0.03
Unweathered marine clay	$3.0 \cdot 10^{-8}$ – $3.0 \cdot 10^{-5}$

According to the significant time and workload necessary to obtain the K_s value by means of in situ and laboratory methods as well as in relation to the obtained results variability, numerous empirical functions (pedotransfer functions) allowing to obtain hydraulic conductivity of saturated soils basing on their particle composition are available (e.g. *Tietje and Hennings, 1996; Sobieraj et al., 2000; Wagner et al., 2001; Rajkai et al., 2004*). Below, the selected pedotransfer empirical functions allowing to easily obtain K_s as input data to hydrological modeling are presented:

- Cosby (*Cosby et al., 1984*):

$$K_s = 7.0556 \cdot 10^{-6} \cdot 10^{(-0,6+0,0126sand-0,0064clay)} \quad (1.13)$$

- Saxton (*Saxton et al., 1986*):

$$K_s = 2.778 \cdot 10^{-6} \exp(x)$$

$$x = 12.0121 - 7.55 \cdot 10^{-2} sand + \frac{-3.895 + 3.671 \cdot 10^{-2} sand - 0.1103clay + 8.7546 \cdot 10^{-4} clay^2}{\theta_s} \quad (1.14)$$

- Brakensiek (*Brakensiek et al., 1984*):

$$K_s = 2.78 \cdot 10^{-6} \cdot \exp(x)$$

$$x = 19.52348 \cdot \theta_s - 8,96847 - 0.028212clay + 1.8107 \cdot 10^{-4} sand^2 - 9.4125 \cdot 10^{-3} clay^2 - 8.395215 \cdot \theta_s^2 + 0.077718sand \cdot \theta_s - 0.00298sand^2 \cdot \theta_s^2 - 0.019492clay^2 \cdot \theta_s^2 + 1.73 \cdot 10^{-5} sand^2 clay + 0.02733clay^2 \cdot \theta_s + 0.001434sand^2 \cdot \theta_s - 3.5 \cdot 10^{-6} clay^2 sand \quad (1.15)$$

where: *sand* – percentage sand fraction content [%], *clay* – percentage clay fraction content [%].

Knowledge of hydraulic conductivity in unsaturated conditions is crucial in modeling of ground water movement and pollutants propagation in soils. But value of hydraulic conductivity in unsaturated soil varies according to changes in soil saturation by water or/and soil pressure. The relation describing the changes of K in dependence to *S*, θ , Ψ or finally *h* (saturation, water content, soil potential and soil pressure), necessary to mathematical description of water movement in unsaturated porous media is difficult to obtain by laboratory and, especially, in-situ methods. Thus, several empirical models allowing to calculate the value of unsaturated hydraulic conductivity are available (*Bohne and Olszta, 1988*). Table 3 presents the most popular formulas frequently used to obtain the relative conductivity of unsaturated soil, understood as:

$$K_r = \frac{K}{K_s} \quad (1.16)$$

where: K_r – relative hydraulic conductivity of soil [-], *K* – hydraulic conductivity [m/s].

Table 1.3. The most popular formulas of unsaturated hydraulic conductivity empirical models (*Wind, 1955; Gardner, 1958; Brooks and Corey, 1964; Rijtema, 1965, Van Genuchten, 1980*)

Name	Formula
Brooks and Corey (1964)	$K_r = K_s, h \geq h_a$ $K_r = \left(\frac{h_a}{h}\right)^{-n}, h < h_a$
Rijtema (1965)	$K = K_s, h \geq h_a$ $K_r = e^{\alpha(h-h_a)}, h_1 \leq h \leq h_a$ $K = K_1 \left(\frac{h}{h_1}\right)^{-n}, h < h_1$
Wind (1955)	$K = \alpha h ^{-n}$
Gardner (1958)	$K_r = e^{\alpha h}, K = \frac{a}{ h ^n + b}$
Van Genuchten (1980)	$K = K_s S^l \left[1 - \left(1 - S^{\frac{1}{m}} \right)^m \right]^2$

where: h_a – air entry pressure head [m], S – degree of saturation [-], a, b, α, n, m, l – fitting parameters.

1.4 Darcy's law

Darcy's law (1856) is a basic law describing flow of water or the other fluids in porous, permeable media (soils, rocks, timber, concrete and other building materials, membranes etc.). The general idea of Darcy's law is that water flux in the porous material is proportional to the water potential in this point (*Gliński et. al., 2011*). Coefficient of water conductivity is a coefficient of proportionality in this equation.

Generally, Darcy's law for water flow in unsaturated medium may be expressed as:

$$\vec{q} = -K(\Psi) \cdot \text{grad } \Psi \quad (1.17)$$

or

$$\vec{q} = -K(\Psi) \cdot \frac{\partial \Psi}{\partial x} \quad (1.18)$$

where: q – water flux [m/s], x – spatial coordinate [m].

In the case of groundwater flow in saturated conditions, the unsaturated hydraulic conductivity of soil $K(\Psi)$ is replaced by coefficient of its saturated hydraulic conductivity K_s .

In case of three dimensional groundwater flow, equation of Darcy's flow transforms to (e.g. *Migolo et al., 2003*):

$$\mathbf{q} = -\mathbf{K}\nabla \Psi \tag{1.19}$$

where, \mathbf{K} – permeability tensor, ∇ – 3D gradient operator.

Gradient operator ∇ , also known as nabla operator is a differential operator understood in Cartesian coordinate system (x,y,z) as:

$$\nabla = \left(\frac{\partial}{\partial x}, \frac{\partial}{\partial y}, \frac{\partial}{\partial z} \right). \tag{1.20}$$

In the simplest cases of groundwater flow through the saturated soil (e.g. flow through the aquifer) the Darcy's law equation may be transformed to the following form:

$$v = K_s \frac{\Delta h}{\Delta x} \tag{1.21}$$

where: v – saturated water flow velocity (Darcy's velocity) [m/s], Δh – pressure drop [m], Δx – flow length (length of which the pressure drop Δh was observed) [m].

1.5 Richard's equation

Modeling calculations of water movement in the studied soil profile is usually based on standard form of Darcy's and Richard's equations (i.e. *Richards, 1931; Raats, 2001; Pachepsky et al., 2003*):

$$q = -K(\theta)\nabla \Psi \tag{1.22}$$

$$\frac{\partial \theta}{\partial t} = \nabla(K(\theta)\nabla \Psi) - S(\theta) \tag{1.23}$$

where: q – groundwater flux [m/s], θ – volumetric water content [m^3/m^3], t – time [s], $K(\theta)$ – hydraulic conductivity [m/s], Ψ – water potential [N/m^2] or [m] when expressed as pressure head, $S(\theta)$ – sink or source term [1/s].

The sink or source term reflects local increase or decrease of water content according to local inflows or outflows of water to the modeled domain, e.g. water uptake by plants' roots, evapotranspiration, infiltration and exfiltration etc.

For the simplest one-dimensional flow of water in soils the Richards' equation may have the form (*Pachepsky et al., 2003*):

$$\frac{\partial \theta}{\partial t} = \frac{\partial}{\partial z} \left(D(\theta) \frac{\partial \theta}{\partial z} \right) \quad (1.24)$$

where: D – soil water diffusivity [m^2/s].

Modeling calculations of two dimensional water movement in the FEFLOW are based on standard forms of Darcy's and Richard's equations (e.g. *Richards, 1931; Raats, 2001; Pachepsky et al., 2003; Diersh, 2005*):

$$\mathbf{q}_i = -\mathbf{K}_{ij} \frac{\partial h}{\partial x_j} \quad (1.25)$$

$$S_0 \frac{\partial h}{\partial t} = -\frac{\partial \mathbf{q}_i}{\partial x_i} \mp Q \quad (1.26)$$

where: \mathbf{q}_i – groundwater flux vector [m/s], h – hydraulic pressure head [m], t – time [s], \mathbf{K}_{ij} – hydraulic conductivity tensor [m/s], $i, j = 1, 2$, Q – sink or source term [$1/\text{s}$], S_0 – specific storage compressibility [$1/\text{m}$], $S_0 = 1 \cdot 10^{-4} 1/\text{m}$.

The hydraulic conductivity tensor along the main, principal directions in two dimensional model may be expressed as diagonal matrix, reflecting the anisotropy of soil:

$$\mathbf{K}_{ij}^p = \begin{bmatrix} K_1^p & 0 \\ 0 & K_2^p \end{bmatrix} \quad (1.27)$$

Which can be transformed to the Cartesian system by the rotation matrix containing the angle of rotation ϕ between the involved directional axes:

$$b_{ij} = \begin{bmatrix} b_{11} & b_{12} \\ b_{21} & b_{22} \end{bmatrix} = \begin{bmatrix} \cos\phi & \sin\phi \\ -\sin\phi & \cos\phi \end{bmatrix} \quad (1.28)$$

The resultant hydraulic conductivity tensor may be calculated as follows (*Diersch, 2005*):

$$\mathbf{K}_{ij} = b_{li} K_{lk}^p \quad (1.29)$$

So, the maximum value of hydraulic conductivity (e.g. horizontal or vertical), anisotropy factor, understood as e.g. $K_{max} K_{min}^{-1}$ or $K_H K_V^{-1}$, and rotation angle are required (*Diersch, 2005*). Thus, anisotropy factor is used to calculate the value of the second element of the diagonal matrix presented in Eq. 1.30:

$$K_2^p = a \cdot K_1^p \quad (1.30)$$

where: a – a dimensionless anisotropy ratio.

2 Fundamentals of mass transport in soils

The mass of water and substances dissolved in water moves in soil porous medium in natural environment continually. The fundamentals of water flow mathematical description were presented in the previous chapter. The following chapter contains the presentation of description of transport of substances dissolved in water.

2.1 Equation of hydrodynamic dispersion

For any element moving in the porous medium space the principle of mass conservation must be preserved, which can be described as a continuity equation (e.g. *Dagan, 1989; Maciejewski, 1998; Diersch, 2005*):

$$\frac{\partial \rho^k}{\partial t} = -\frac{\partial q_i^k}{\partial x_i} + S^k \quad (2.1)$$

where: q^k – intensity of flux of particles of species k , S^k – volumetric source term of species k , t – time, x – Cartesian coordinate.

One of the basic parameters describing a content of a substance dissolved in water is a concentration according to the formula:

$$C = \frac{dm}{dV^w} \quad (2.2)$$

where: m denotes mass of a substance dissolved in the volume of V^w of ground water.

The dependence between a concentration C of the substance and its density ρ can be expressed as:

$$\rho = \frac{dm}{dV} = \frac{dm}{dV^w} \frac{dV^w}{dV} = C\theta \quad (2.3)$$

where: θ – volumetric water content (moisture), $\theta = \frac{dV^w}{dV}$, V – volume of soil medium.

Velocities of particles of individual components of ground water are usually different. The difference between velocity of particles of one component and average velocity of all fluid particles in the elementary representative volume is called *dispersion velocity* (*Maciejewski, 1998; Diersch, 2005*):

$$v^d = v - \bar{v} \quad (2.4)$$

where: v^d – dispersion velocity, v – velocity of particles of the component under consideration, \bar{v} – average mass velocity of fluid (e.g. ground water).

In the general case, an average mass velocity of multicomponent fluid may be defined as:

$$\bar{v} = \frac{\sum_{k=1}^n v^k \rho^k}{\sum_{k=1}^n \rho^k} = \frac{\sum_{k=1}^n v^k \rho^k}{\rho^c} \quad (2.5)$$

where: v^k – velocity of particles of species k , ρ^k – density of species k , ρ^c – density of liquid phase, n – number of liquid components.

Problems of flow of water with only one low-concentrated dissolved component are usually considered in modeling the mass transport. Thus, a parameter describing the relevant component is often omitted and it is assumed that the average mass velocity of a solution equals the velocity of ground water.

On the basis of the equation (1.56) defining a dispersion velocity, a dispersion flux can be determined as (Maciejewski, 1998; Diersch, 2005):

$$q^d = \rho v^d = \rho v - \rho \bar{v} = q - \bar{q} \quad (2.6)$$

where: q – flux of flow of the component mass in soil, \bar{q} – flux of the component particles assuming that the particles move at a velocity equal to average velocity of the liquid, ρ – density of the component.

The total intensity of flux q of mass of a substance dissolved in ground water can be divided into a convective flux \bar{q} connected to an average mass velocity of liquid flow in porous medium and a dispersion flux q^d . In the as such complex medium as soil is, it can be assumed that velocities of individual liquid particles oscillate around the average flow velocity. In the such medium, a dispersion flux is assumed to be proportional to the gradient of concentration C (e.g. Hassanizadeh, 1986; Maciejewski, 1998; Sawicki, 2003; Diersch, 2005):

$$q_i^d = -D_{ij} \theta \frac{\partial C}{\partial x_j} \quad (2.7)$$

where: D_{ij} – elements of tensor of hydrodynamic dispersion.

On the basis of the relation (1.7), the total flux of mass of any substance dissolved in soil water can be described as:

$$q_i = q_i^d + q = -D_{ij}\theta \frac{\partial \bar{C}}{\partial x_j} + C\theta v_i \quad (2.8)$$

Applying the relation (1.8) into the continuity equation (1.1) results in the equation of hydrodynamic dispersion with a source term S . This equation is commonly used to describe hydrodynamic dispersion. The mentioned source term reflects external sources and sinks of a dispersing substance. For the liquid phase of saturated and unsaturated porous medium the mentioned equation has the following form:

$$\frac{\partial(C\theta)}{\partial t} = \frac{\partial}{\partial x_i} \left(D_{ij}\theta \frac{\partial C}{\partial x_j} \right) - \frac{\partial(C\bar{v}_i\theta)}{\partial x_i} + S \quad (2.9)$$

For the case of flow in the saturated zone of homogeneous soil, where $\theta = \theta_s = \text{const}$, the equation of hydrodynamic dispersion can be expressed as (Maciejewski, 1998):

$$\frac{\partial(C)}{\partial t} = \frac{\partial}{\partial x_i} \left(D_{ij} \frac{\partial C}{\partial x_j} \right) - \frac{\partial(C\bar{v}_i)}{\partial x_i} + \frac{S}{\theta_{sat}} \quad (2.10)$$

In the above description of movement of a substance dissolved in water it is assumed that the all ground water attends the movement and that velocities of individual fluid particles inside a representative elementary volume vary around an average value accidentally.

2.2 Hydrodynamic dispersion coefficient

Hydrodynamic dispersion coefficient expresses the ability of a dissolved substance to mix with water in the soil medium (e.g. Wilson and Gelhar, 1981). The mixing depends on a molecular diffusion, geometry of soil pores and a distribution of soil water velocity, which in turn depends on the content of water in the medium. If the velocity of water equals zero, the process of mixing occurs as a result of a molecular diffusion only. The extent of diffusing particles of a solution in porous medium is lesser than the extent in open water, because particles of dissolved substance move in the tortuous pores of soil, wherethrough effective displacement of the particles diminishes.

According to ground water velocity increase, the fluid mixing rate caused by differences of flow velocity in individual soil pores increases. This phenomenon is called mechanical or convective dispersion. Thus, mechanical dispersion characterizes the influence of fluctuation of a fluid velocity field in soil medium on a mixing process. Hydrodynamic dispersion coefficient D in porous medium is a sum of mechanical dispersion coefficient D_m and molecular diffusion coefficient D_d , what can be expressed as:

$$D = D_m + D_d \quad (2.11)$$

Molecular diffusion coefficient in soil is given by:

$$D_d = D_{*d} \cdot \tau \quad (2.12)$$

where: D_{*d} – diffusion coefficient in water, τ – tortuosity of porous medium, which is defined as:

$$\tau = \left(\frac{L}{L_c} \right)^2 < 1 \quad (2.13)$$

where: L – straight line distance of a diffusing particle, L_c – real distance covered by a diffusing particle moving through pores among solid particles of soil.

In a general case molecular diffusion coefficient is a tensor. For a flow in an isotropic medium it can be assumed that hydrodynamic dispersion coefficient depends on characteristics of both soil pores and field of flow velocity. This coefficient is a tensor of the second order even for homogeneous and isotropic soil. Basic properties of a hydrodynamic dispersion coefficient are the result of the following simple physical assumptions:

- during flow in porous medium fluid mixes in all directions,
- in homogeneous and isotropic medium only one direction is distinguished,
- in isotropic medium molecular diffusion process does not depend on flow direction.

A process of mixing in the distinguished direction (flow direction) is called *longitudinal dispersion*. The mixing in other directions is called *lateral dispersion*. Thus, in the coordinate system for which the direction of the X'_1 axis agrees with the direction of a vector of a velocity of ground water flow, components of a hydrodynamic dispersion tensor can be given as:

$$D'_{ij} = D_L \delta_{j1} \delta_{i1} + D_T (\delta_{j2} \delta_{i2} + \delta_{j3} \delta_{i3}) + D_d \delta_{ij} \quad (2.14)$$

where: D_L – longitudinal dispersion coefficient, D_T – lateral dispersion coefficient, D_d – molecular diffusion coefficient, δ_{ij} – Kronecker's delta.

2.3 Models of sorption

Liquid particles in soil medium interact with the surface of grains and particles of solid phase. Most colloidal soil particles have negative surface charge, so the positive ions are adsorbed on their surface during soil water flow. The equilibrium of adsorption and desorption of ions on the surface of soil particles occurs virtually immediately. Thus, in this case the model of static sorption should be applied.

Analyzing the phenomena, adsorption and desorption processes can be considered in microscopic and macroscopic terms. In microscopic analysis the processes are complex and their description is complicated. So usefulness of this analysis to solve macroscopic problems of flow in the porous medium is limited. In the macroscopic term phenomenological approach basing on investigation of connections between concentration of a substance solved in ground water and mass of adsorbed substance is practically applied. Therefore, models of Henry, Langmuir and Freundlich are used in this approach.

The theory of the Henry adsorption isotherm assumes the existence of steady state conditions in the adsorption process, low concentration of an adsorbate and low value of surface coverage. The isotherm can be expressed as (*Prutton, 1994*):

$$m^a = K \cdot C \tag{2.15}$$

where: m^a – mass of an adsorbate on the surface of sorbent (soil particles), C – concentration of an adsorbate in the liquid phase in the state of equilibrium (unit of adsorbate mass per unit of solution volume), K – Henry's adsorption constant, that expresses adsorption ability of an adsorbate and denotes the amount of mass that is adsorbed per a mass unit of a sorbent at the unit concentration of an adsorbate.

If the concentration of an adsorbate is higher, the Langmuir equation (also known as the Langmuir isotherm) is applied (*Zangwill, 1988*):

$$\frac{m^a}{m^g} = \frac{K \cdot C}{1 + K \cdot C} \tag{2.16}$$

where: m^g – mass of soil particles, the rest of designations is the same as in the equation of the Henry's isotherm.

The generalization of the Langmuir equation was proposed by Freundlich (e.g. *Sheindorf i in., 1981; Maciejewski, 1998; Sawicki, 2003*). It can be expressed as:

$$\frac{m^a}{m^g} = (KC)^n \tag{2.17}$$

where: n – parameter depending on sort of soil and sort of solute dissolved in ground water, the rest of designations is the same as in the equations of the Henry and Langmuir isotherms.

The Freundlich adsorption isotherm is applied wider than the Henry and Langmuir isotherms. It is assumed in the equations of the Freundlich isotherm that a sorbent has unlimited sorption capacity and the concentration of a sorbate can rise in the state of equilibrium. This assuming is correct for low concentrations only, because each sorbent has limited surface able to adsorb some maximum amount of a sorbate.

The n parameter expresses degree of nonlinearity of adsorption isotherm. It was experimentally determined that for very low concentrations of a sorbate n approaches 1 and the graph of an adsorption isotherm as a relation $C(m^a/m^s)$ is a straight line.

The adsorption constant K expresses intensity of adsorption and its absolute value depends on the selection of measurement units. The constant K is usually determined in a laboratory and used in models simulating behaviour of a solute during water flow in soil medium.

2.4 Decay reactions

A decay of components of a solution flowing in soil medium can occur as a chemical or physical process. It is a complex phenomenon, so simplified models are used to its description. The model of first-order is the simplest one.

An example of a decay reaction is a decomposition of both solute particles and particles adsorbed by soil. The amount of this decay can be expressed introducing a negative source term in the following form (*Sawicki, 2003; Diersch, 2005*):

$$s^w + s^s = -\lambda(\rho^s + \rho^a) \quad (2.18)$$

where: λ – denotes decay constant, s^w – source term expressing sources and sinks for a substance dissolved in ground water, s^s – source term expressing sources and sinks for a substance adsorbed by the solid phase, ρ^a – density of adsorbed substance, ρ^s – dry bulk density.

In the case of a decay of a substance in an enzyme-catalyzed reaction the Michaelis-Menten mechanism is applied (*Diersch, 2005*). The enzyme-catalyzed reactions have the same properties and the most important one is maximum saturation of an enzyme by a substrate, limiting a rate of a reaction. It can be expressed by the Michaelis-Menten model given as:

$$v = v_{\max} \frac{C}{C + K_m} \quad (2.19)$$

where: v – rate of reaction, v_{\max} – maximum rate of reaction, K_m – Michaelis constant.

In the FEFLOW software the option of consecutive reactions (also called decay chains) typical for radioactive elements with long time of decay is available. In this option it is necessary to define a decay chain of these elements.

3 Brief description of FEFLOW

FEFLOW (*Finite Element subsurface FLOW systems*) developed by WASY Institute for Water Resources Planning and Systems Research Ltd., nowadays owned by DHI Germany is an interactive, based on graphical user interface (GUI) tool for two (2D) and three dimensional (3D) modeling of water flow in saturated, partially saturated or unsaturated, isotropic or anisotropic soil domain.

3.1 Software characteristics

FEFLOW allows also the numerical calculations of mass and heat transport in porous media. The model is based on finite elements/volumes method – FEM/FVM (Huebner, 2001; Zienkiewicz *et al.* 2005a; Zienkiewicz *et al.*, 2005b) and was developed in ANSI C/C++ which allows its application by Windows and Linux OS users. Fig. 3.1. shows the GUI of FEFLOW in the demo version*.

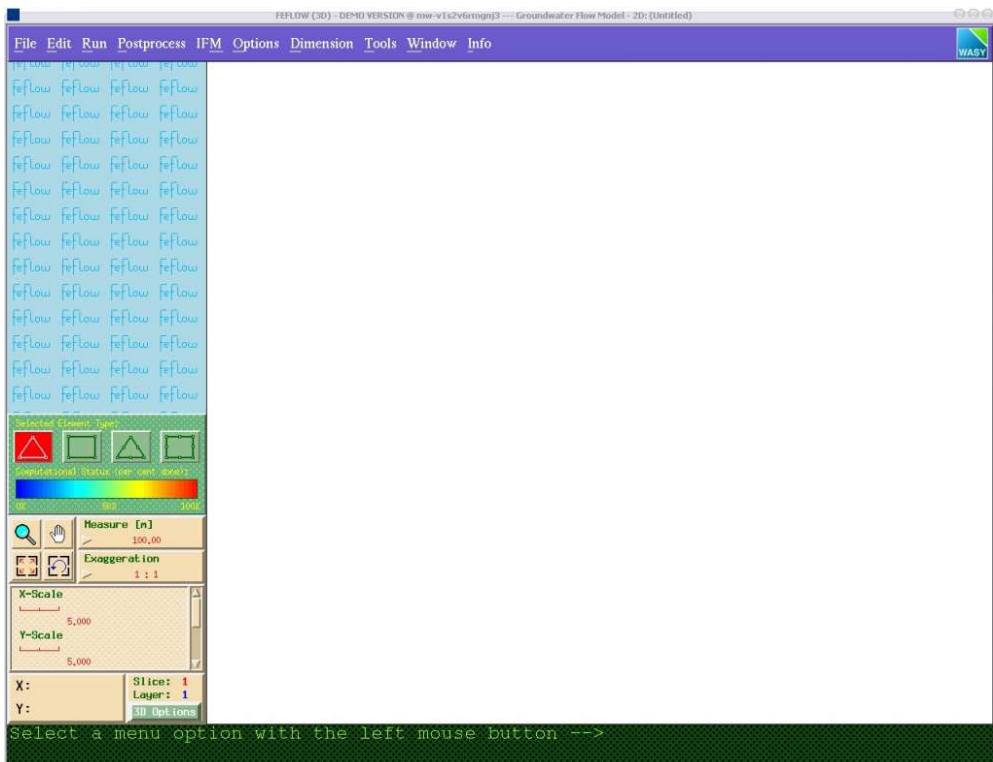


Fig. 3.1. FEFLOW's GUI

* All the figures presenting FEFLOW GUI are the printscreens of the demo version of FEFLOW 6.0 by DHI-WASY.

FEFLOW was many times positively verified in numerous scientific and engineering applications (e.g. *Diersch and Kolditz, 2002; Zhao et al., 2005; Mazzia and Putti, 2006; Trefry and Muffels, 2007; Widomski, 2007, Widomski et al., 2010; Widomski et al., 2013*).

The known applications of FEFLOW cover:

- researches focused on propagation of anthropogenic pollutants from point and surface sources,
- development of remediation and decontamination strategies,
- studies on changes in water resources in mining regions,
- modeling of mines drainage,
- designing of groundwater, surface water and infiltration water uptakes
- projects of power plants using geothermal water,
- infiltration and exfiltration from and to pipelines located in the soil,
- water seepage through dams and floodbanks,
- numerical simulations of infiltration and capillary rise in soil columns,
- assessment of available soil water resources,
- validation and managing of water management strategies,
- designing the safe zones surrounding water supply units requiring direct and indirect protection preventing the contamination,
- reporting the influence of investment on natural environment.

The main advantages of FEFLOW:

- proven high quality of computations,
- wide variety of applications:
 - saturated, partially saturated and unsaturated water flow, supported by mass and heat transport,
 - application of variable media density to calculations
 - sorption modeling,
 - random chemical reactions.

FEFLOW allows (*Diersch, 2005a*):

- import and export of model data and maps to and from files ASCII, GIS, CAD and TIF (Fig. 3.2),
- partial or total automatization of finite elements/volumes elements mesh with the possibility of manual adjustments and validation of the mesh quality (Fig. 3.3),
- built-in regionalization of all applied parameters,

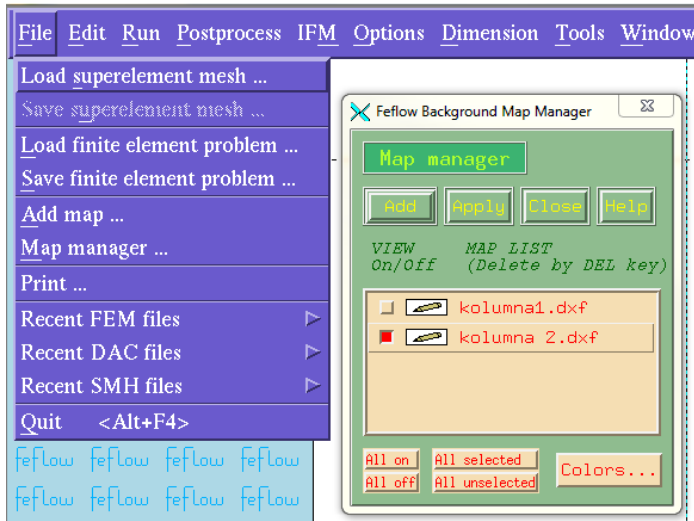


Fig. 3.2. FEFLOW map manager

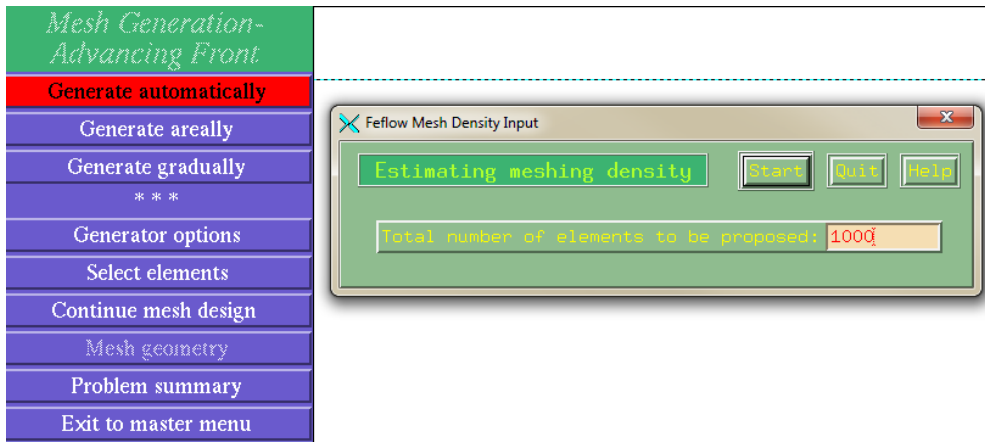


Fig. 3.3. Mesh generator

- application of sophisticated simulation algorithms in calculations for complex, multi parameters processes,
- visualization and analyses of calculations results,
- tracking of flowing fluid element (particle tracking),
- application of iso-surfaces to modeling,
- open environment of programming,
- simulations for steady and unsteady flow conditions,

- various methods of time step determination: constant and variable time step, including fully automated procedures of time step length adjustments (Fig. 3.4),

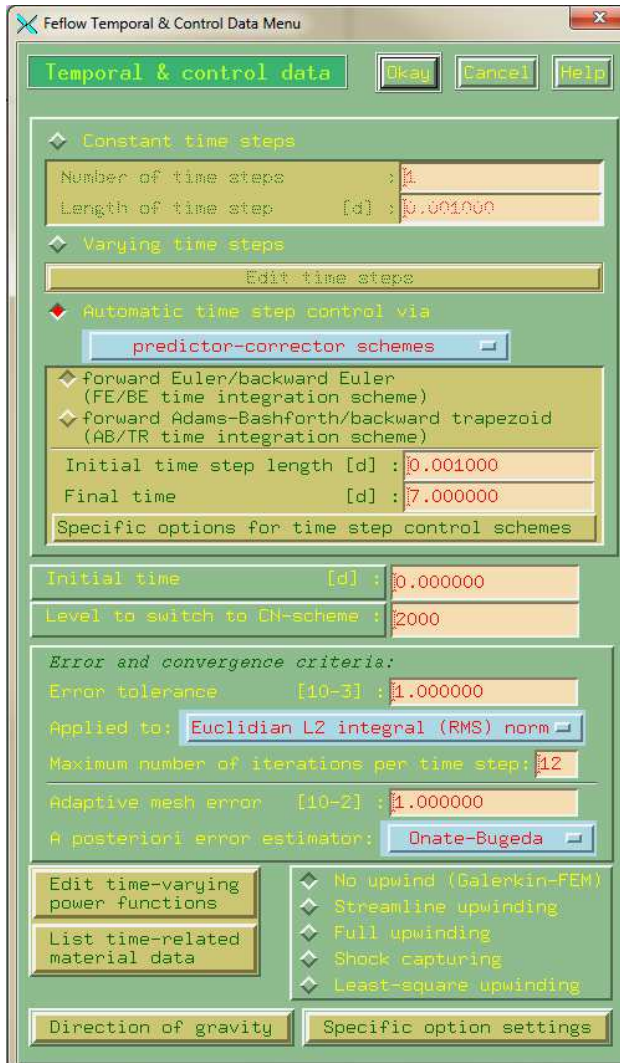


Fig. 3.4. FEFLOW temporal and control data menu

- various models for the free water table: movable mesh of finite elements/volumes, linear relation between saturation and hydraulic conductivity and modeling of unsaturated or partially saturated conditions according to the Richards' equation,
- PEST-based automatic calibration,

- variable solvers based on the Newton and Picard iteration technique, fast and direct iteration PCG and Restarted-OR-THOMIN and alternative algebraic solver SAMG,
- mass transport calculations for unlimited number of pollutants, diluted or absorbed, based on linear or non-linear equation of hydrodynamic dispersion,
- application of the first order reactions and Michaelis-Menten reactions model,
- available sorption models: Henry, Freundlich and Langmuir,
- user defined rate and degree of the reaction,
- simulation of radioactive mass transport with applied time of decay.

Mathematical description of water flow in porous media applied to FEFLOW is based on Darcy and Richards equations, also with sink/source term, solved basing on soil media parametrization, applied set of input data, initial and boundary conditions.

Parametrization of the modeled porous media may be performed according to the following models: van Genuchten, Brooks-Corey, Haverkamp, exponential and linear (Fig. 3.5 – Fig. 3.9) (Diersch, 2005; Diersch 2005a). It is also possible to reflect the phenomenon of capillary hysteresis in the calculations.

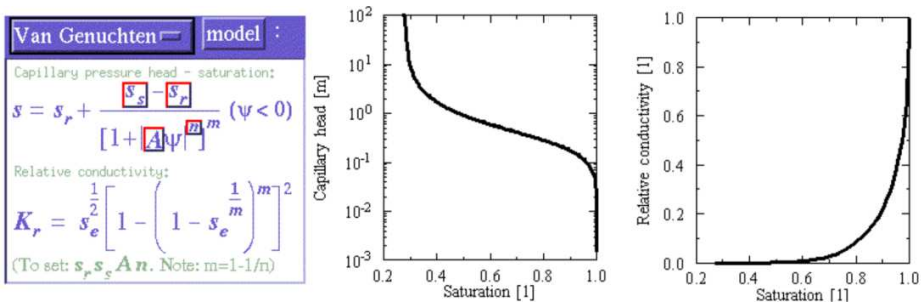


Fig. 3.5. Van Genuchten model

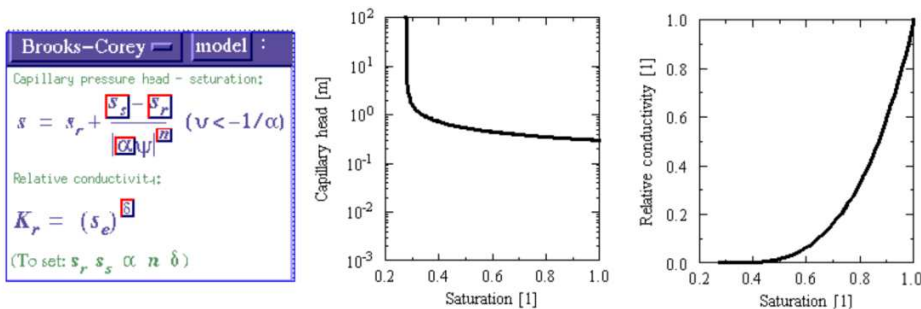


Fig. 3.6. Brooks-Corey model

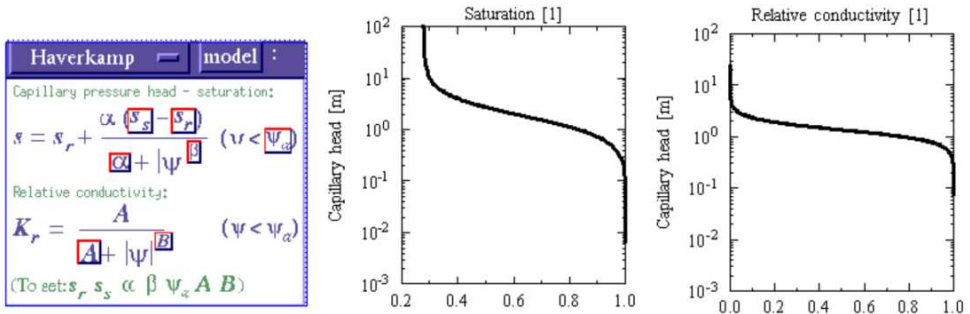


Fig. 3.7. Haverkamp model

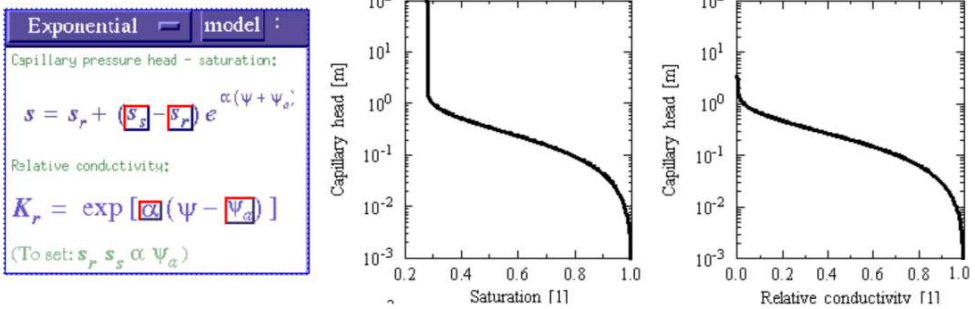


Fig. 3.8. Exponential model

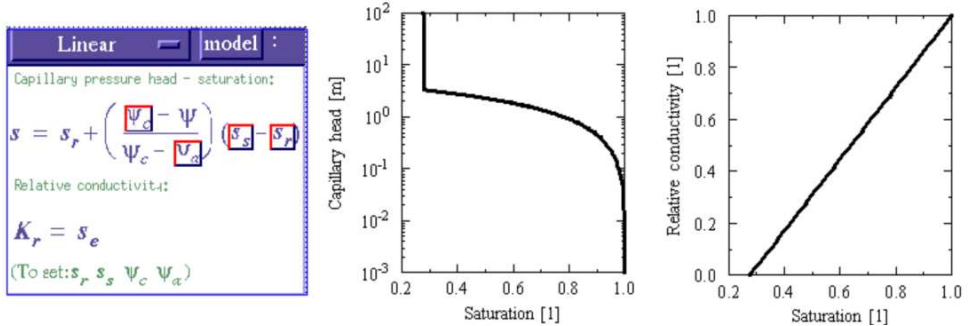


Fig. 3.9. Linear model

FEFLOW, based on finite elements/volumes method, requires creation of the model in three different stages described below (Diersch, 2005a):

- preprocessor allowing determination of geometric characteristics of modeled domain, generation of finite elements mesh, edition of problem class, method of solution, temporal and control data setting, determination of hydraulic properties of the domain, characteristics of pollutants and models of

their propagation, definition of initial and boundary conditions. Mentioned settings options are presented in the Fig. 3.10, Fig. 3.11 and Fig. 3.12.

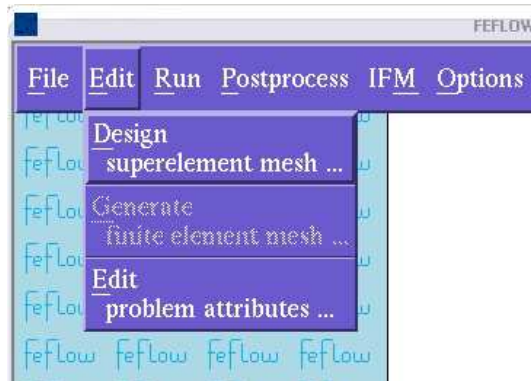


Fig. 3.10. Main menu of FEFLOW preprocessor

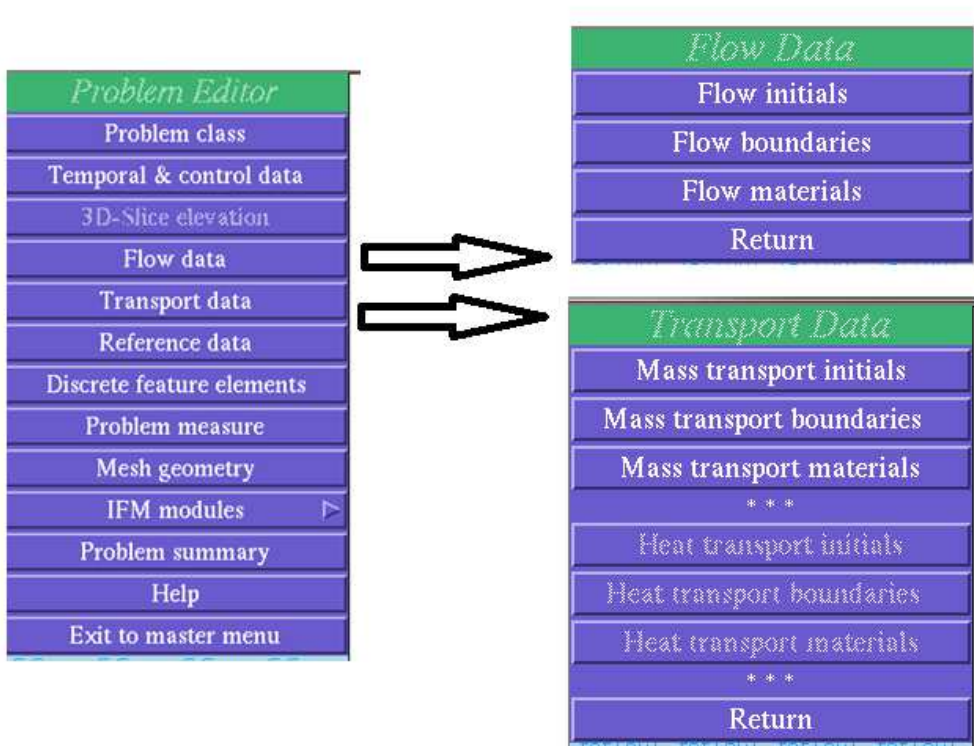


Fig. 3.11. Problem editor menu with Flow Data and Transport Data submenus

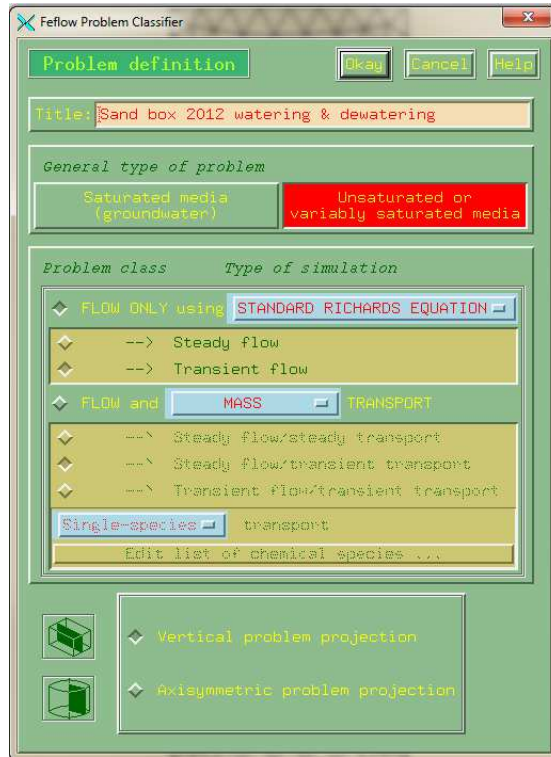


Fig. 3.12. Problem class definition for unsaturated 2D water flow in FEFLOW

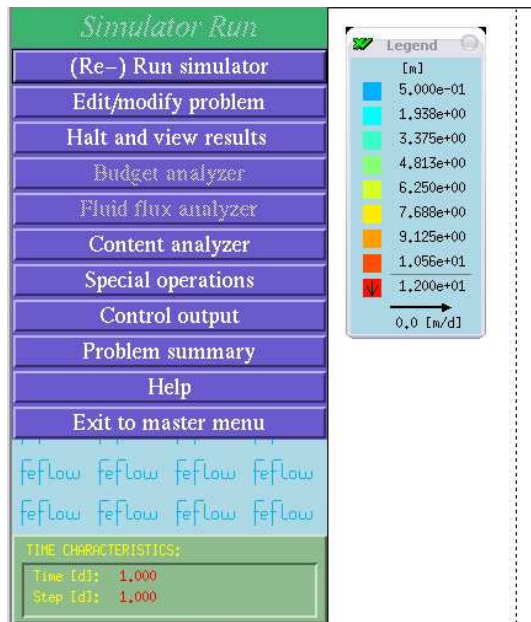


Fig. 3.13. Menu of FEFLOW processor

- processor allowing the main numerical calculations of water flow, saturation dynamics and mass transport in the studied domain of porous media, Fig. 3.13,
- postprocessor (Fig. 3.14) allowing graphical or numerical visualization of calculation results.

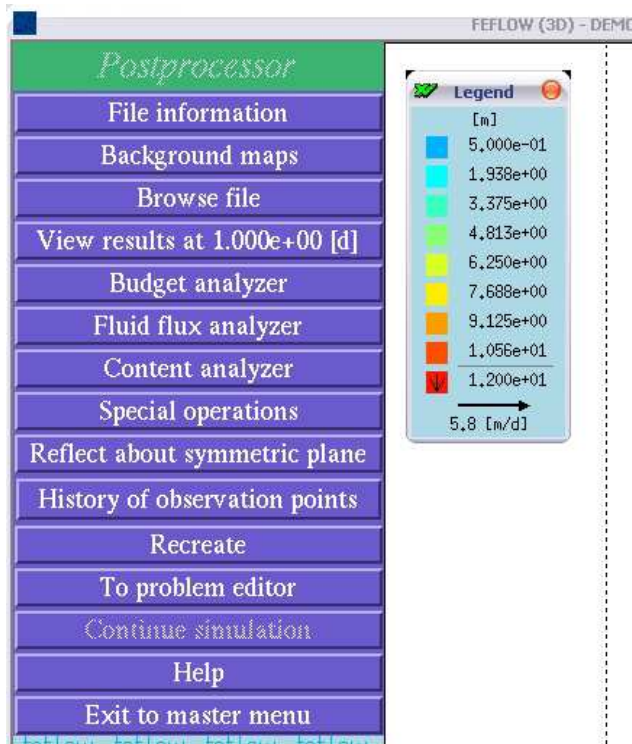


Fig. 3.14. Postprocessor menu of FEFLOW

The data set required to numerical calculations in FEFLOW's finite elements method covers (e.g. *Diersh, 2005a; Widomski, 2007; Widomski et al., 2010*):

- physical and hydraulic parameters of soil: porosity, hydraulic conductivity in saturated conditions, anisotropy ratio, saturated and residual saturation as well as shape parameters of water retention curve and unsaturated hydraulic conductivity model (Fig. 3.15 and Fig. 3.16),
- initial conditions for water flow: saturation, volumetric moisture content, pressure head and pressure are allowable (Fig. 3.17).

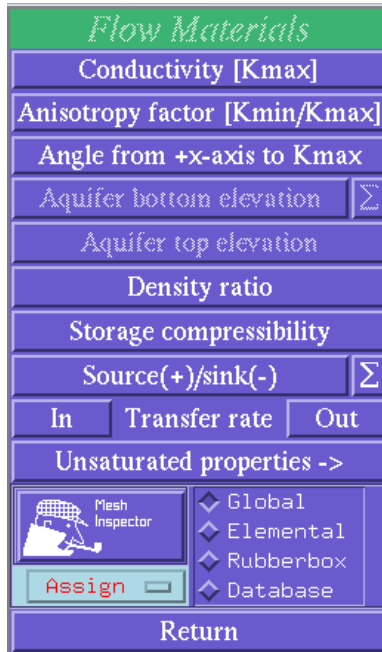


Fig. 3.15. Saturated properties of soil

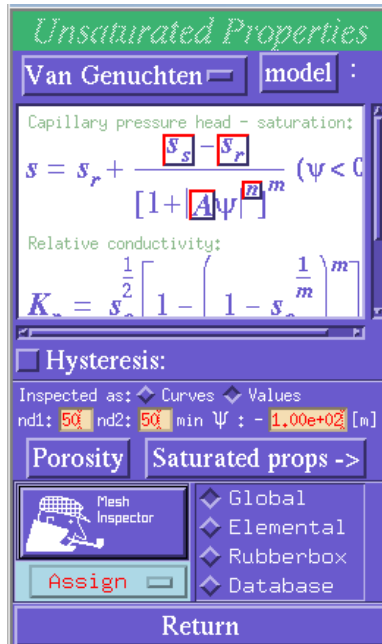



Fig. 3.16. Unsaturated properties of soil

Flow Initials

Hydraulic head

Alternate:

Content analyzer

 Mesh Inspector

- Global
- Elemental
- Nodal
- Rubberbox
- Database

Return

Fig. 3.17. Initial conditions for water flow

- mass transport parameters of soils, including porosity, sorption model, longitudinal and transverse dispersivity, model of dispersion, molecular diffusion coefficient and type and coefficients for decay reaction (Fig. 3.18),

Mass Materials

Aquifer thickness

Porosity

Sorption

Molecular diffusion

Longitudinal dispersivity

Transverse dispersivity

Linear dispersion

First-order decay Rate

Source(+)/sink(-) Σ

 Mesh Inspector

- Global
- Elemental
- Rubberbox
- Database

Return

Fig. 3.18. Input data for mass transport modeling

- initial condition for mass transport (Fig. 3.19).

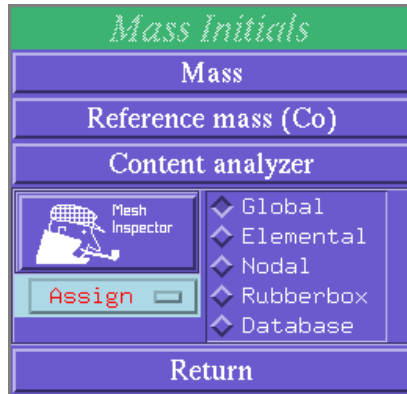


Fig. 3.19. Mass transport initial conditions

The initial conditions and characteristics of soil may be prescribed to model area in several ways: to the single nodes, to selected elements of FEM mesh, to the greater area selected by the popular window tool, globally to the whole area and finally data may be imported from data base prepared in ESRI, dBASE or ASCII formats.

Introduction of the boundary conditions to models in FEFLOW is based on selection of one of four offered types of boundary condition, definition of its value (constant of time varied) and assignment of the condition to FEM mesh.

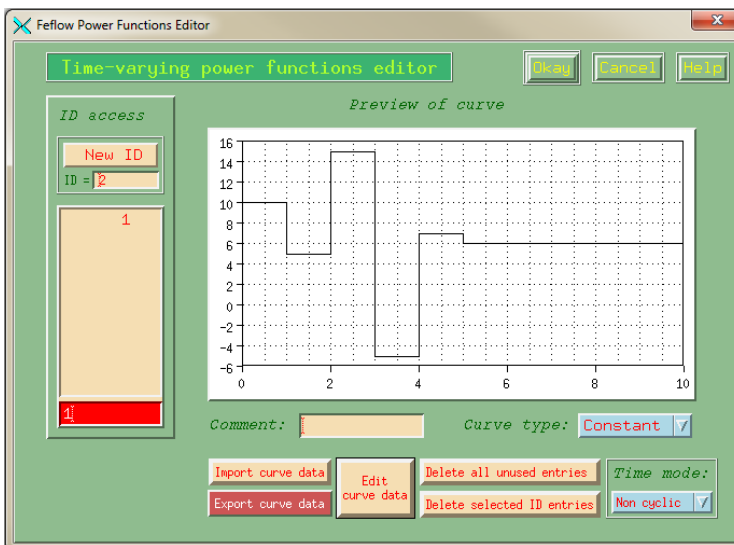


Fig. 3.20. Time-varying functions editor

Available in FEFLOW types of boundary conditions for water and mass transport (Fig. 3.21 and Fig. 3.22) are as follows (Diersch, 2005; Diersch, 2005a):

- First type (Dirichlet) describing pressure head (water) and concentration (mass) for the given node.
- Second type (Neuman) determining water flux or mass flux leaving or entering the modeled domain through the selected limit of the model.
- Third type (Couchy) defining reference pressure head (water) and concentration (mass) of the area located outside the modeled domain allowing inflow or outflow.
- Fourth type, a single well allowing water and mass inflow or outflow through a single node.

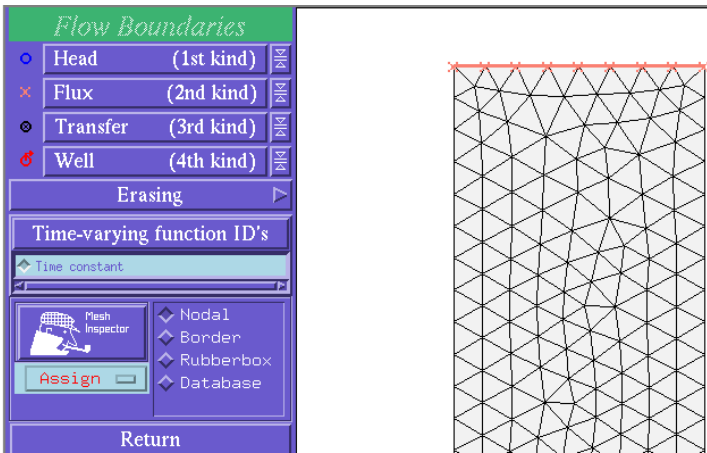


Fig. 3.21. Boundary conditions for water flow in FEFLOW

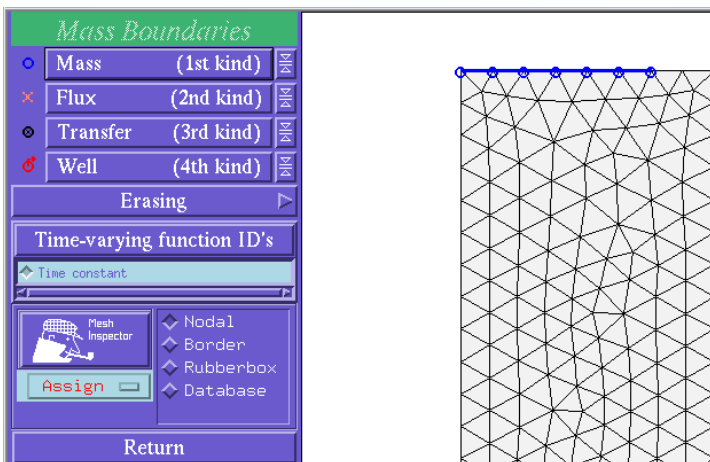


Fig. 3.22. Boundary conditions for mass transport in FEFLOW

The results of numerical calculations in FEFLOW may be presented in many ways. The software allows visualization by isolines, contours (both BW or in color), velocity field, time dependant curves etc. etc. (Fig. 3.23 – Fig. 3.26).

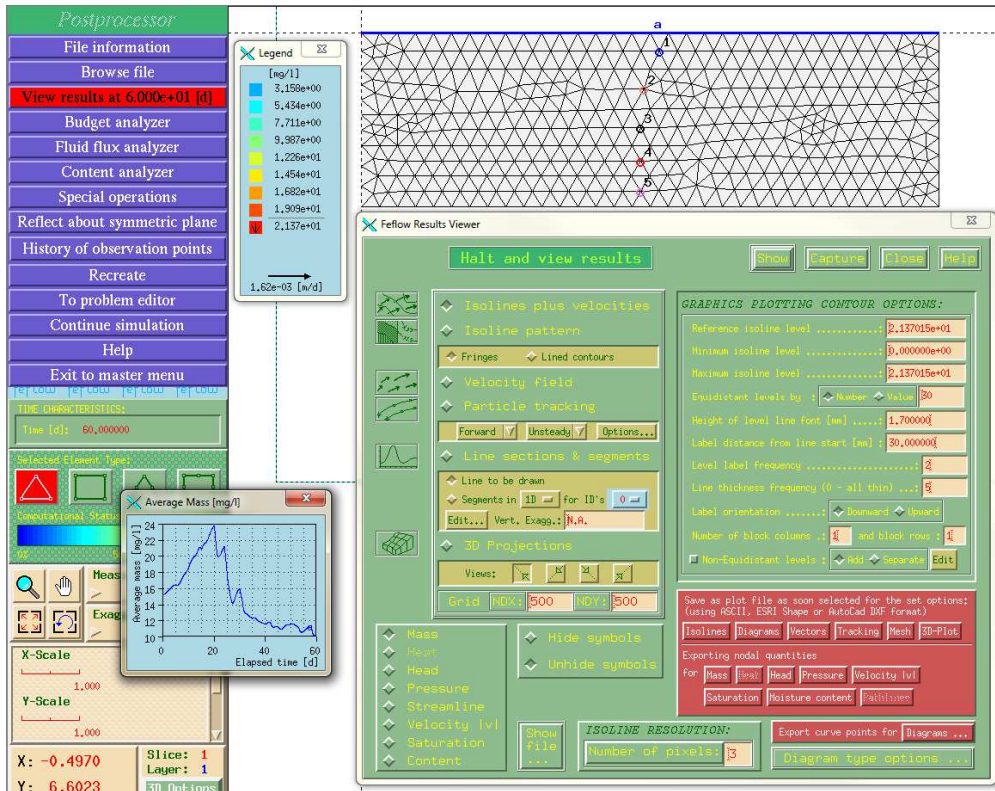


Fig. 3.23. Visualization setup for mass transport modeling results – isolines fringes and velocity vectors

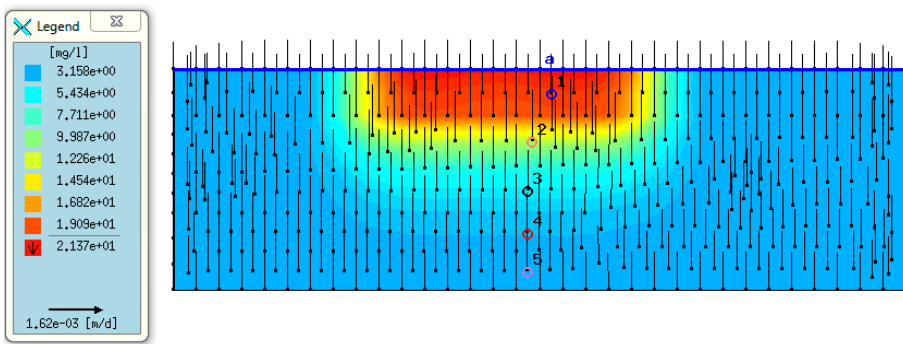


Fig. 3.24. Resultant mass distribution 2D contour plot

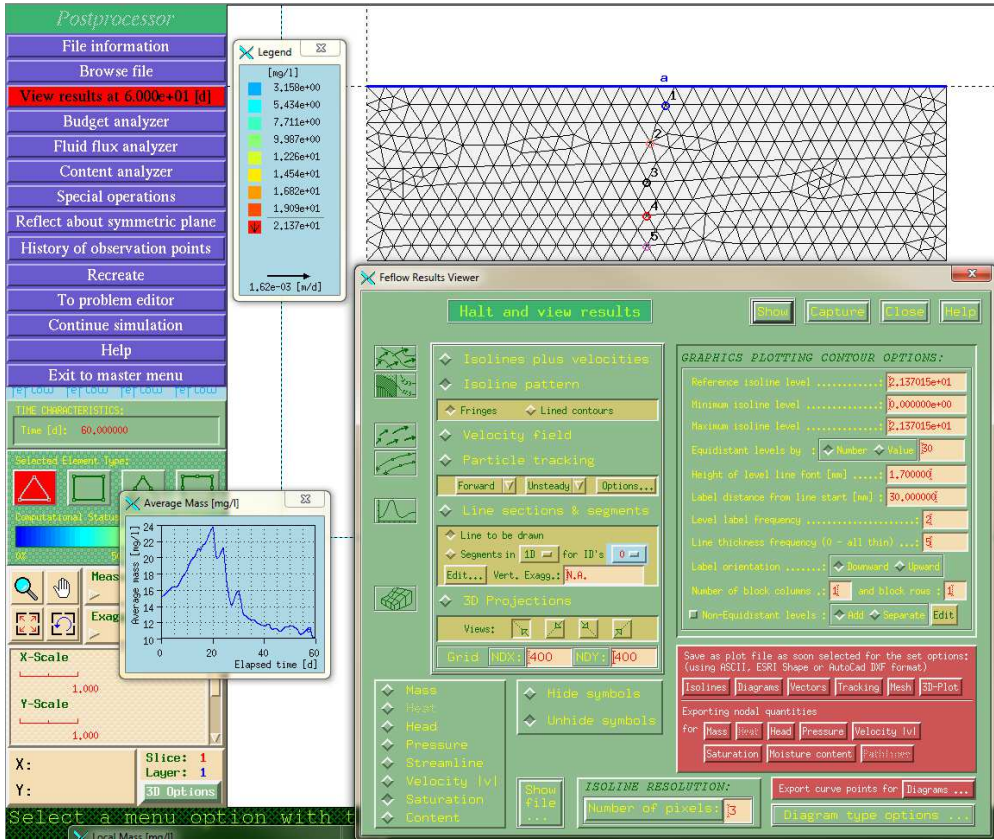


Fig. 3.25. Settings for saturation distribution 2D plot

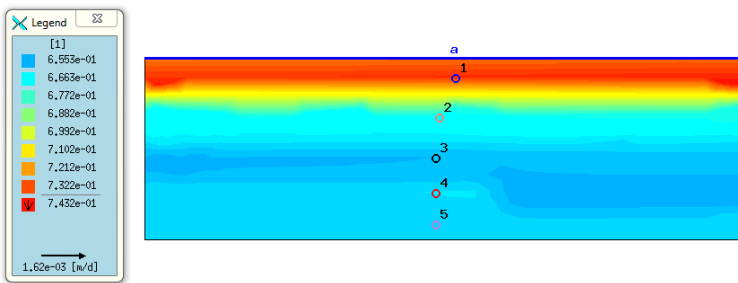


Fig. 3.26. Calculated saturation distribution

More precise information concerning FEFLOW GUI, creation of the model domain, generation of FEM mesh, input data as well as initial and boundary conditions assignment, performing the numerical calculations, viewing and exporting of the results, various ways of results analyses by build-in FEFLOW tools, re-creating and re-hacking of the simulation are available in the software documentation and FEFLOW help files.

4 Exemplary calculations of water flow and mass (pollutants) transport in soil by FEFLOW

4.1 Simulation of fine sand column wetting by capillary rise

Perform numerical simulation of fine sand column (0.3x1.0m) wetting by capillary rise during 6 hours of the experiment. Present soil saturation for the final time step and time dependant graphs for soil moisture content. Calculate the water volume for the first and final time step.

The column is saturated by water in 20% at the start of the experiment. The bottom boundary of modeled column is set at the level of water free surface. There is no water flux through the side boundaries, the top boundary is also sealed.

Table 4.1. Required soil input data (after *Eching et al., 1994*) for fine sand

Type of soil	Saturated water content θ_s [-]	Residual water content θ_r [-]	Saturated hydraulic conductivity K_s [m/s]	WRC fitting parameter A [1/m]	WRC fitting parameter n [-]
Fine sand	0.380	0.03	6.2E-06	2.26	7.339

We assume:

- fine sand applied to modeling is an isotropic material,
- no hysteresis for pF (WR) curves,
- porosity equal to maximum saturation,
- automatic time step control.

Solution

- Create the finite element mesh (or load existing, developed earlier) representing the modeled soil profile (Fig. 4.1).
- Open **Problem editor** (preprocessor) and set type of model – edit **Problem class** – set **Unsaturated or variably saturated media** and **Flow only using standard Richards equation, transient flow** (Fig. 4.2).
- Define time and time step control for the simulation in **Temporal & control data**, according to Fig. 4.3, set time of simulation 0.25 day.

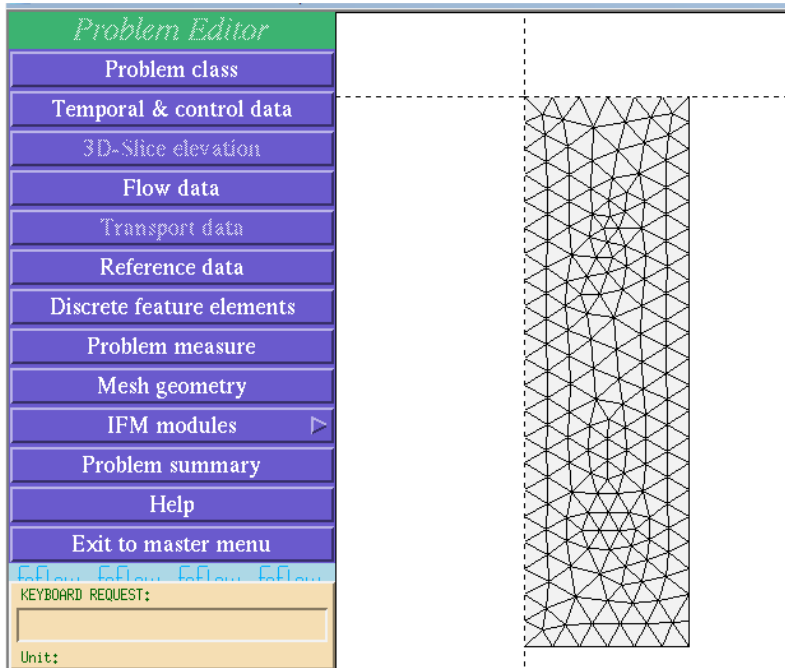


Fig. 4.1. Modeled domain and finite elements mesh

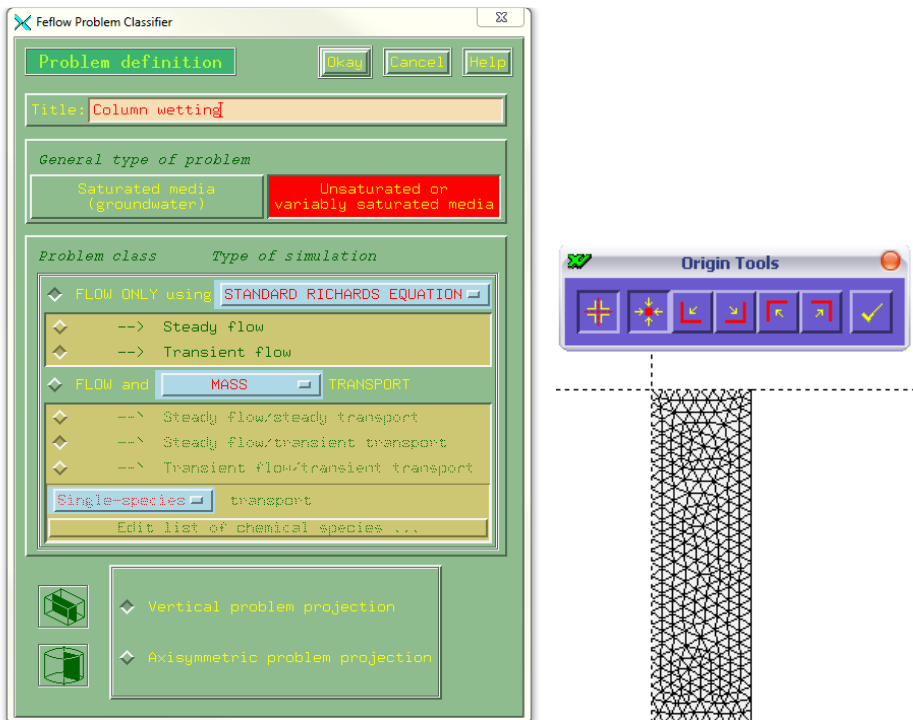


Fig. 4.2. Problem class settings

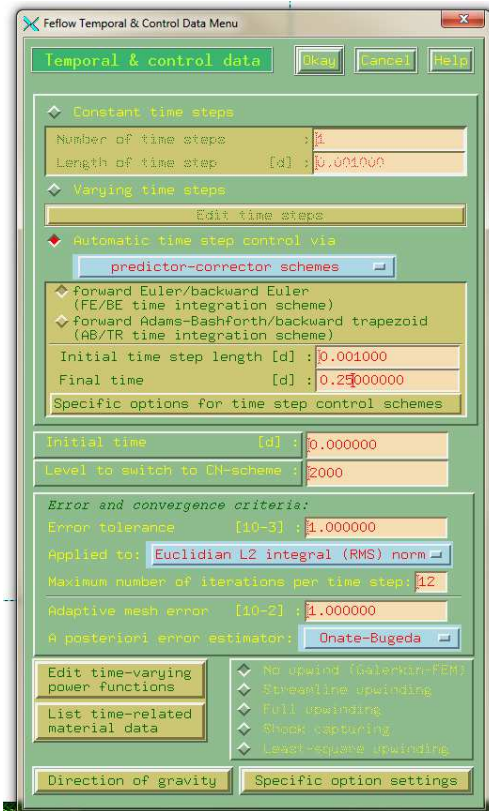


Fig. 4.3. Temporal & control data

- Enter **Flow data** according to Fig. 4.4.

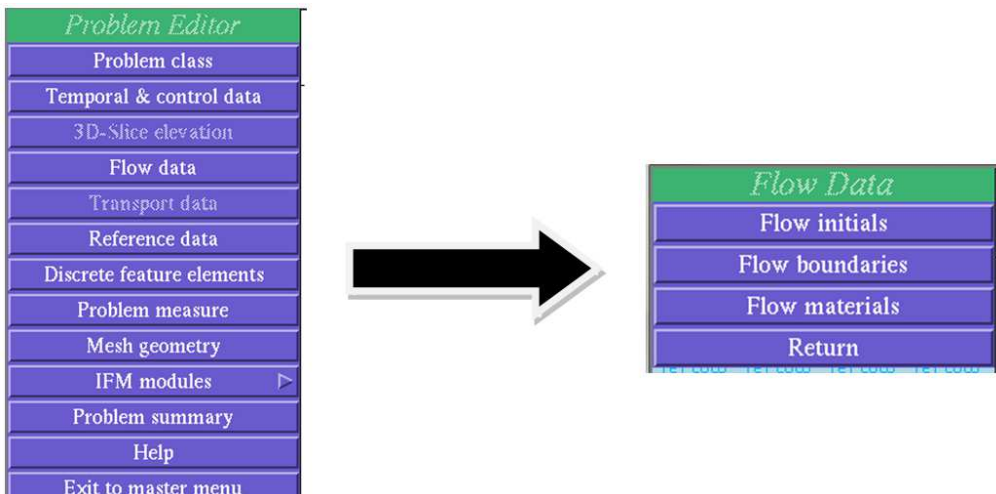


Fig. 4.4. Flow Data menu

- Open **Flow materials** to assign characteristics of soil to model.
- Set saturated hydraulic conductivity $6.2E-06$ m/s as **Kmax** (be careful about the format of the data – $0.062E-4$ m/s is required – Fig. 4.5) in **Saturated properties**, then go to **Unsaturated props** (assume isotropic soil).

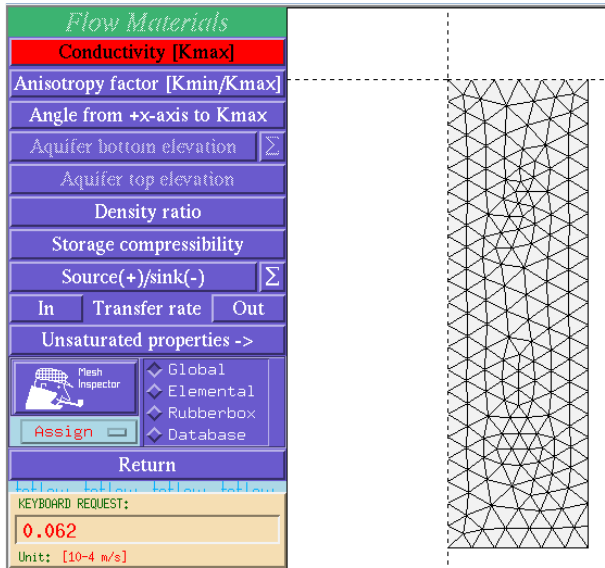


Fig. 4.5. Input data – saturated conductivity

- In **Unsaturated properties** assign **Porosity** as 0.38 (Fig. 4.6).

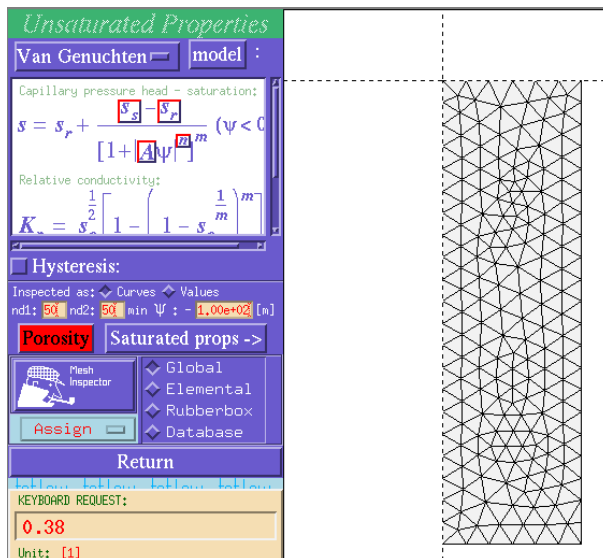


Fig. 4.6. Input data – porosity

- Now we need to assign van Genuchten’s water retention curve parameters, starting from Saturated degree of saturation (S_s) equal to 1.0 (Fig. 4.7).

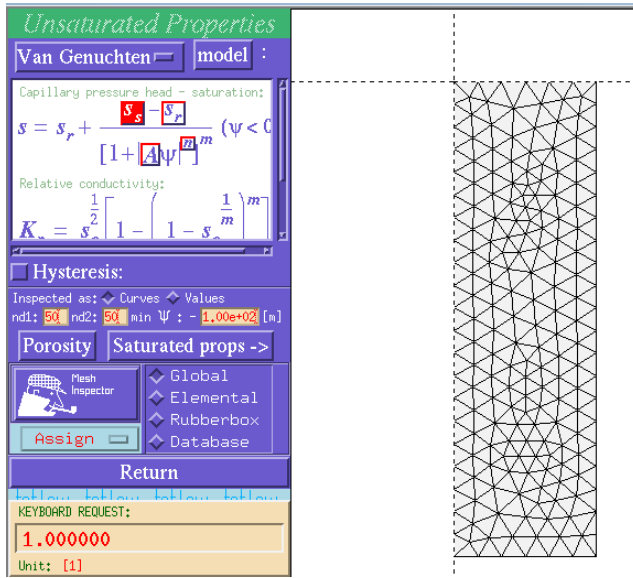


Fig. 4.7. Assignment of saturated degree of saturation

- Next we input residual saturation (S_r) which can be calculated by division of residual water content by the saturated water content (Fig. 4.8).

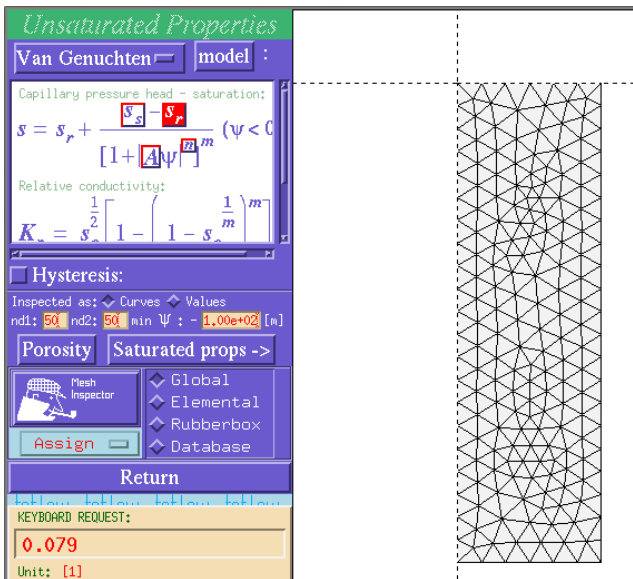


Fig. 4.8. Input of residual saturation

- Next we assign the A in $[1/m]$ according to Fig. 4.9.

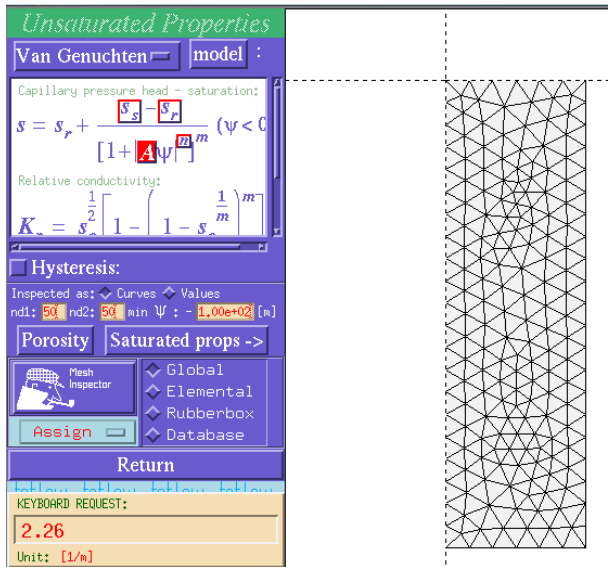


Fig. 4.9. Fitting parameter A $[1/m]$

- And, finally, we can add dimensionless fitting parameter n (Fig. 4.10).

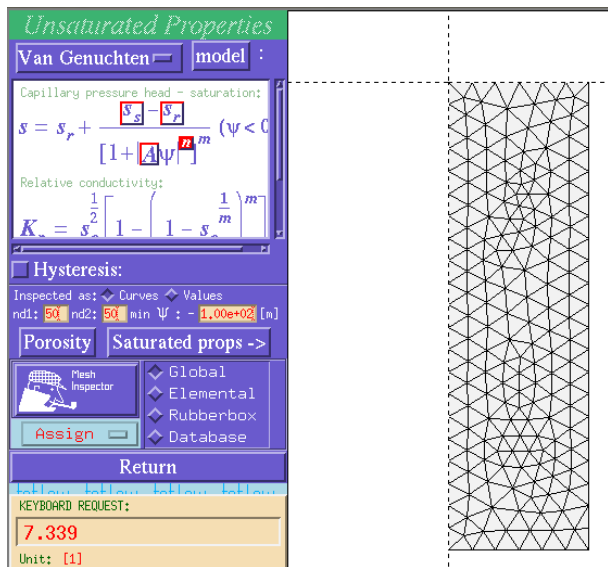


Fig. 4.10. Fitting parameter n

- Let's check the input data for soil water retention characteristics. Select **Mesh inspector** and move the cursor over the modeled domain (Fig. 4.11).

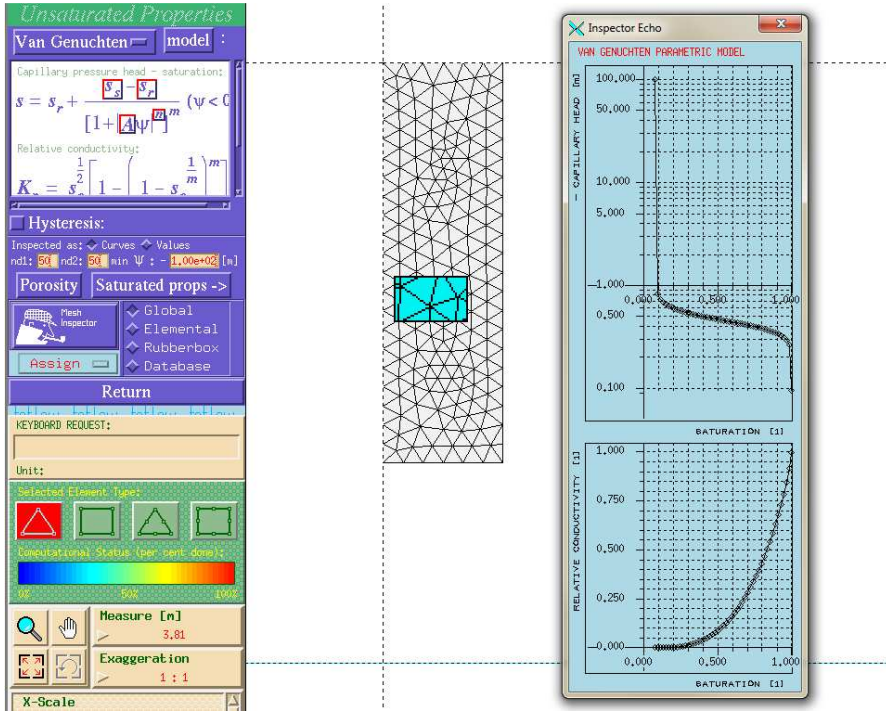


Fig. 4.11. Inspection of WRC input data

- Now go back to **Flow data** and select **Flow initials** (Fig. 4.12). Then select **Saturation** and assign 0.2 [-] representing 20% of saturation for time $t = 0$ to the whole model domain (by setting **Global**).

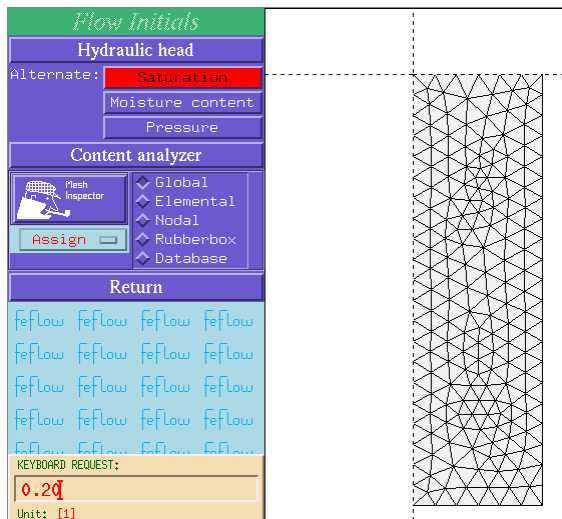


Fig. 4.12. Assignment of initial conditions

- Go back to **Flow data** and enter **Flow boundaries**, then select **Head** and assign head equal to 0.0 m to the nodes of the bottom boundary of the modeled domain (Fig. 4.13), to reflect the localization of groundwater table.

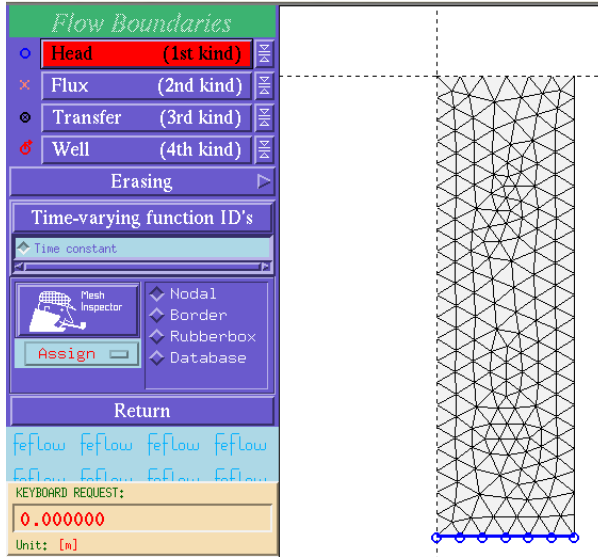


Fig. 4.13. Bottom boundary conditions

- Go back to the main window of **Problem Editor** and enter **Reference data** – **Observation single points** and set observation points by choosing the command **Set at nodal points** according to Fig. 4.14.

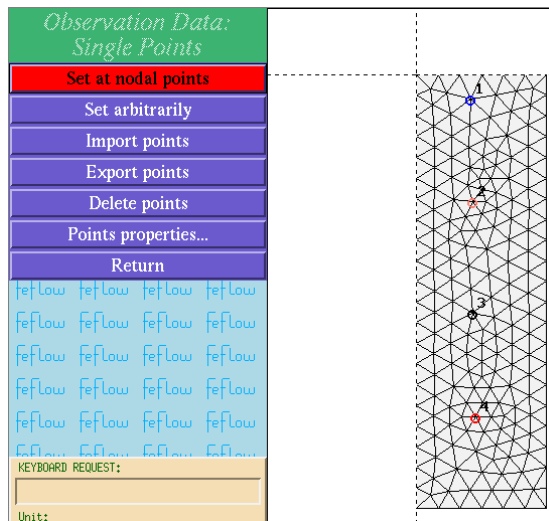


Fig. 4.14. Observation points

- Now our model is ready, go to the main menu of FEFLOW and enter the solver by selecting **Run – Start simulator** (Fig. 4.15).

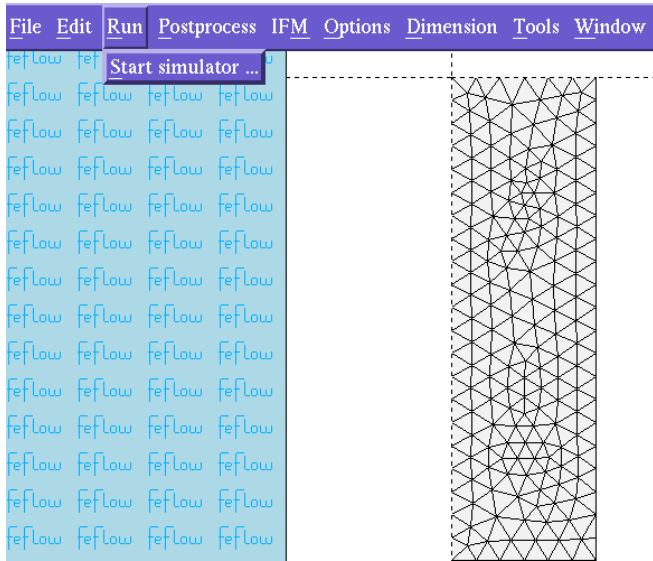


Fig. 4.15. Starting the simulation

- Select **Control output**, choose format and location of data file (Fig. 4.16).

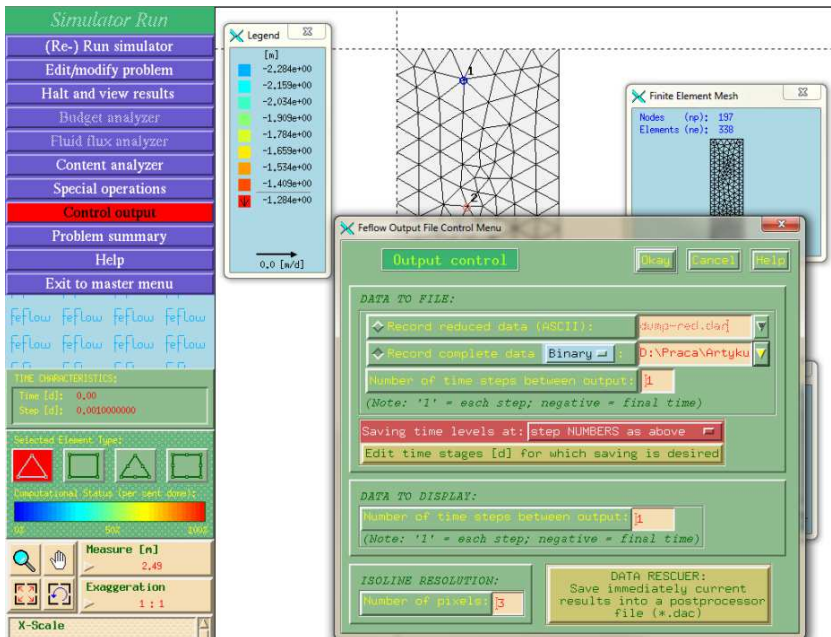


Fig. 4.16. Setting output control

- Run the simulation and check the results in solver or postprocessor (Fig. 4.17, Fig. 4.18 and Fig. 4.19) – after loading the resultant output data file.

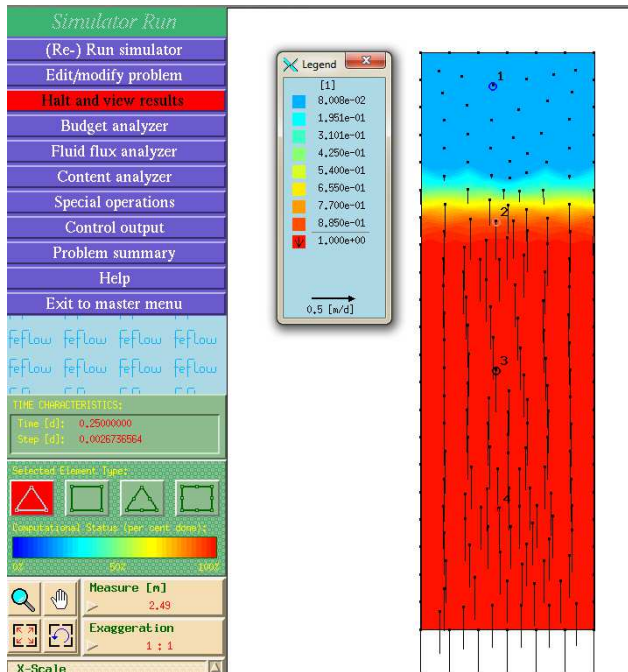


Fig. 4.17. Saturation distribution in modeled soil profile for time $t = 0.25$ day (6 hrs)

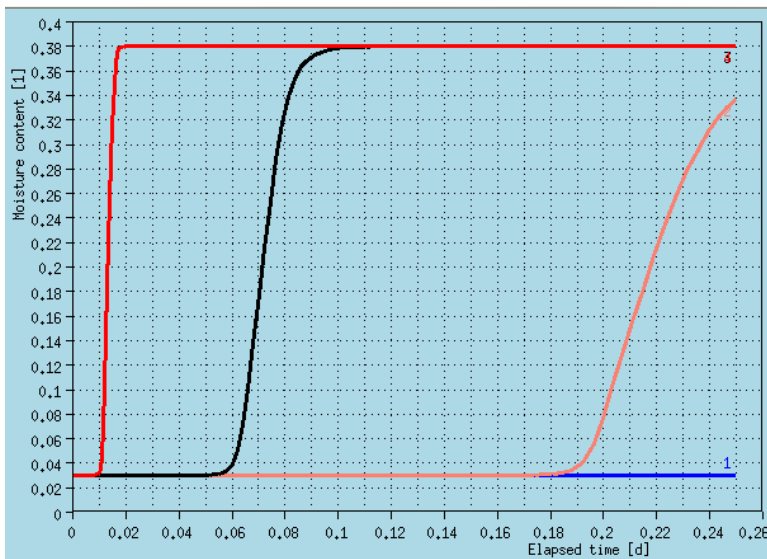


Fig. 4.18. Time dependant soil water content for selected observation points

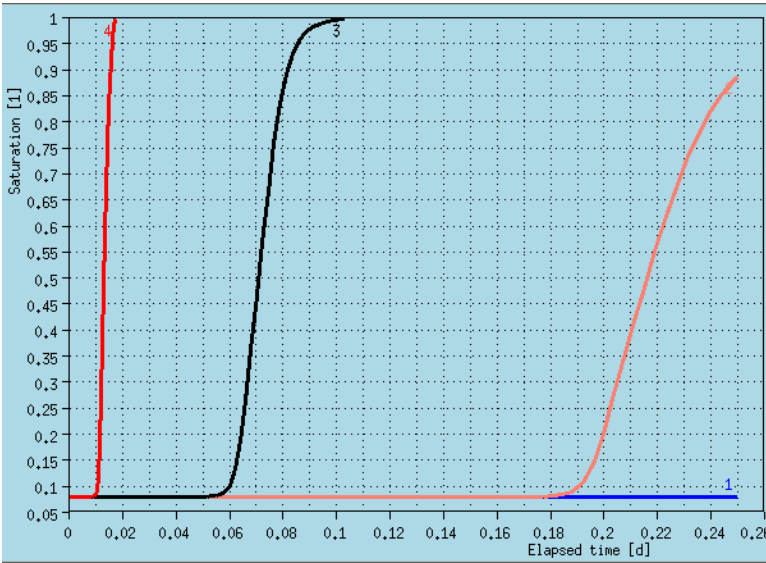


Fig. 4.19. Time dependant soil saturation for selected observation points

- To calculate the water volume for the first and final time step we need to open the postprocessor by selecting **Postprocess – Load and run...**, according to Fig. 4.20.

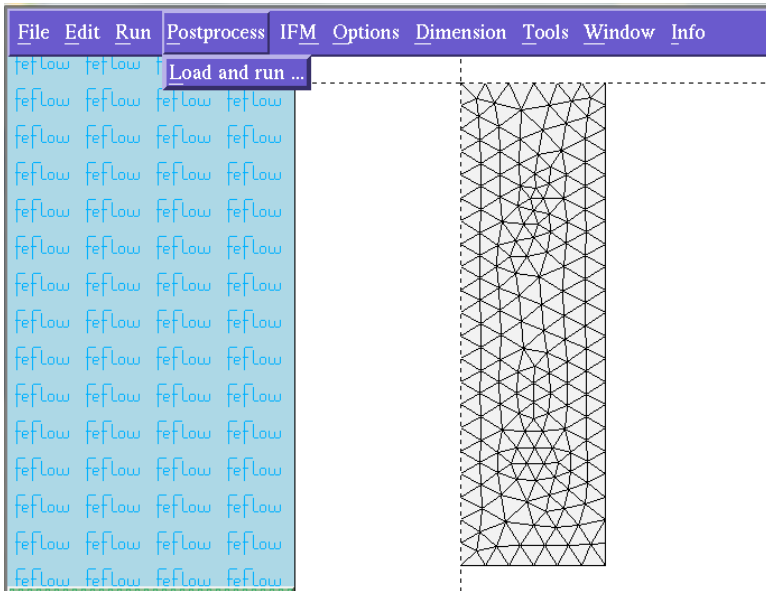


Fig. 4.20. Entering postprocessor

- In **Postprocessor** select **Browse file** and choose time step $t = 0$, than press **Apply** and **Close** (Fig. 4.21).

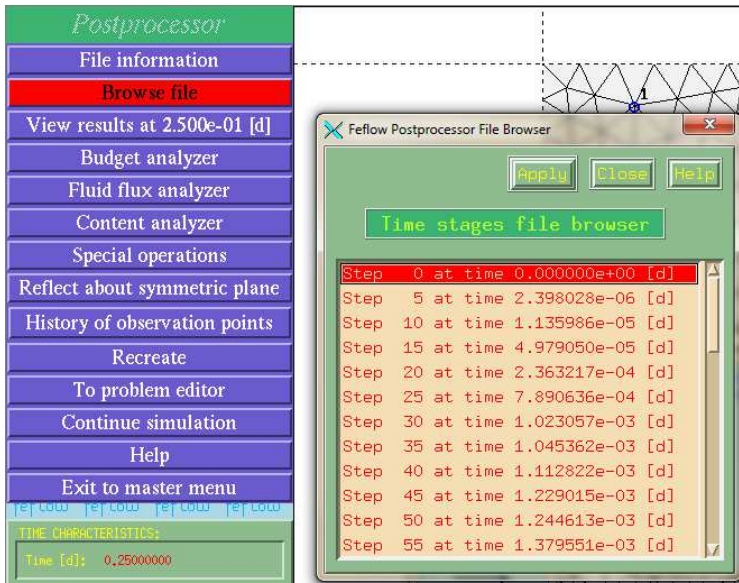


Fig. 4.21. Selecting the required time step

- Select **Content analyzer** and calculate **Fluid content** [m³] by selecting it from the list and pressing **Apply** according to Fig. 4.22.

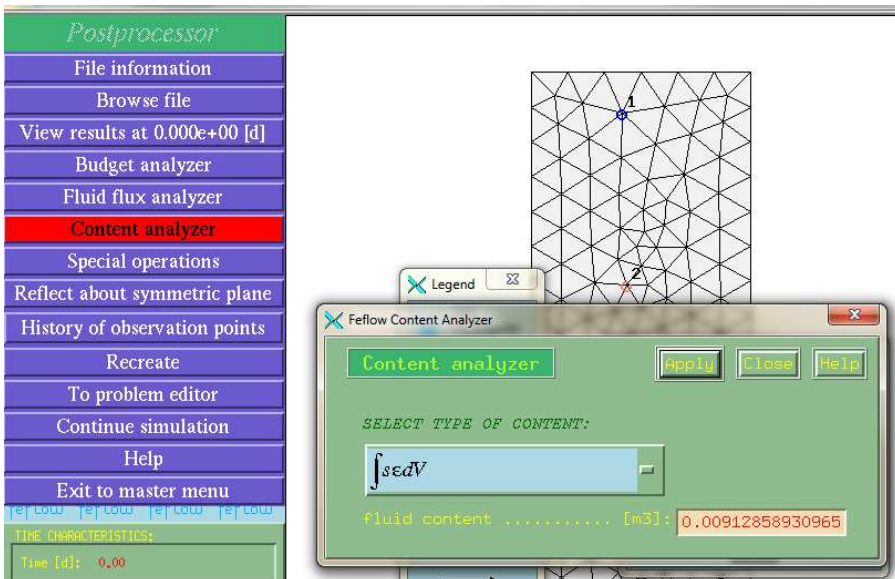


Fig. 4.22. Calculation of water volume for the first time step

- Press Close and repeat points 20 and 21 for the last time step, for $t = 0.25$ day, as it is presented at Fig. 4.23 and Fig. 4.24.

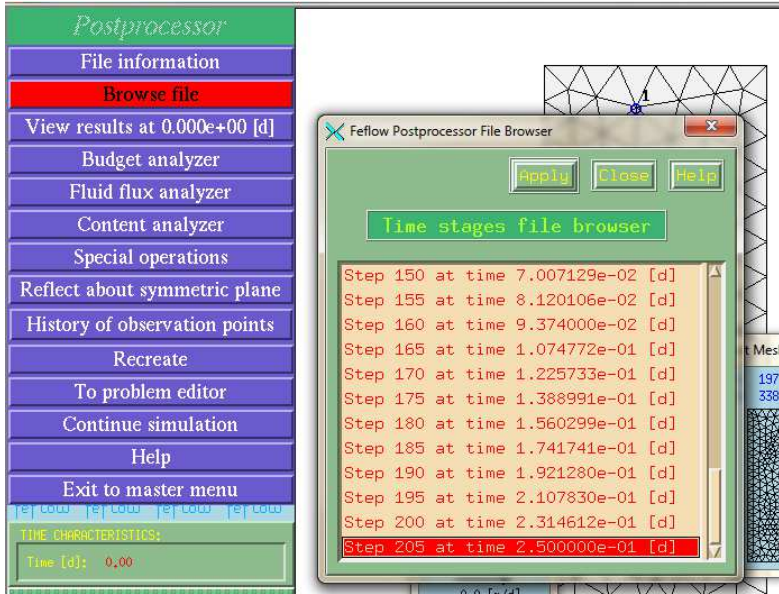


Fig. 4.23. Selecting the final time step

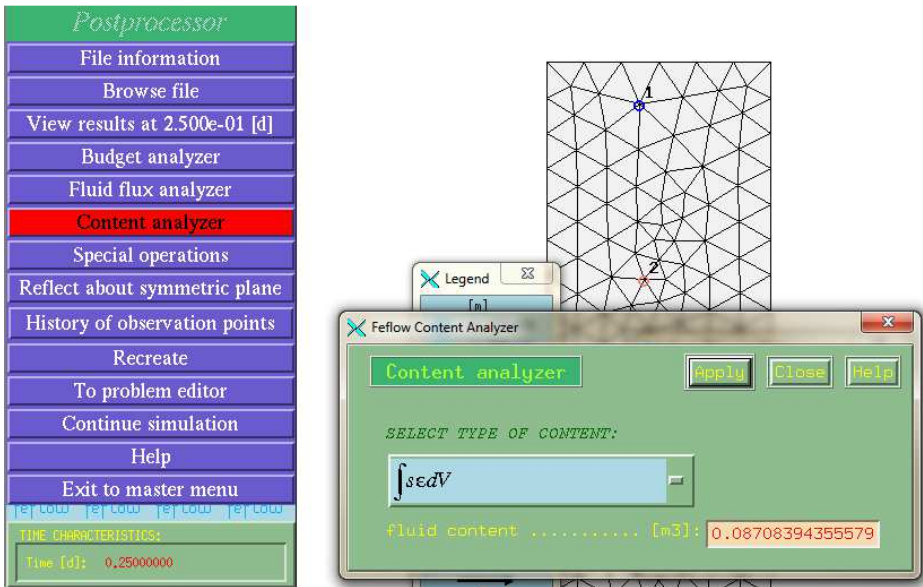


Fig. 4.24. Calculated water volume for the last time step

4.2 Simulation of water capillary rise in two-layered soil profile

Perform numerical calculations of water capillary rise in two-layered soil profile of dimensions 0.3x1.0 m during 10 days of experiment. Water enters the bottom boundary of the modeled domain with the head of -200 cm, while the upper boundary shows the constant flux of evapotranspiration 0.5 mm per day.

Check soil saturation by water distribution after 1, 5 and 10 days of simulation and calculate water flow through the horizontal surface located in the middle of the column.

Table 4.2. Required input soil data

Soil	Depth	Saturated hydraulic conductivity K_s (cm/d)	Saturated water content θ_s [-]	WRC fitting parameter A [1/cm]	WRC fitting parameter n [-]
Layer 1	0–50 cm	18	0.433	0.00596	1.24892
Layer 2	50–100 cm	2	0.37	0.00113	1.2946

Soil profile at the beginning of the experiment is saturated by water in 50% (the upper layer) and 60% (bottom layer).

We assume:

- residual saturation $S_r = 0$,
- soils applied to modeling are an isotropic material,
- no hysteresis for pF (WR) curves,
- porosity equal to maximum saturation,
- automatic time step control,
- two observation points in the vertical axis of the column and observation line in the border of two layers.

Solution

- Create the finite element mesh (or load existing, developed earlier) representing the modeled soil profile – two layers of soil in 0.3x1.0 m profile (see Fig. 4.25).

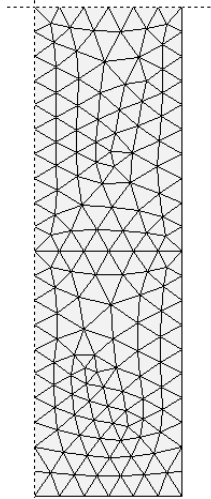


Fig. 4.25. Developed modeled domain and finite elements mesh

- Set type of simulation (Fig. 4.26), time duration (Fig. 4.27) and time control options (Fig. 4.28).

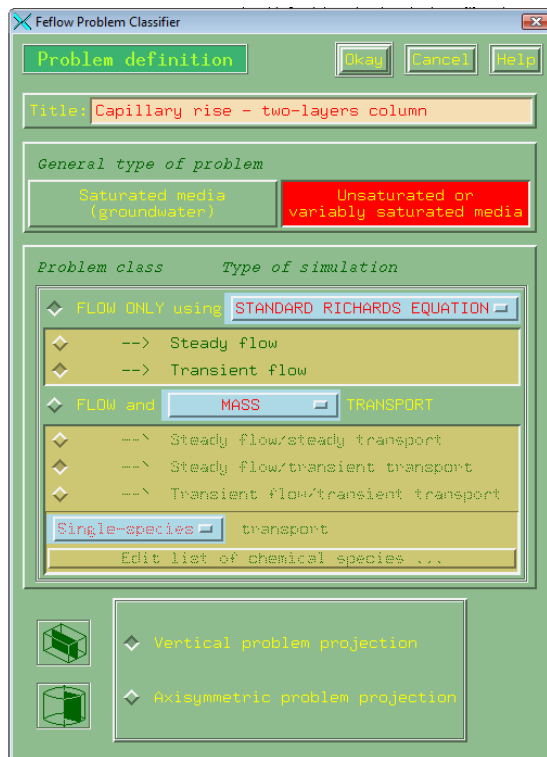


Fig. 4.26. Problem class editor

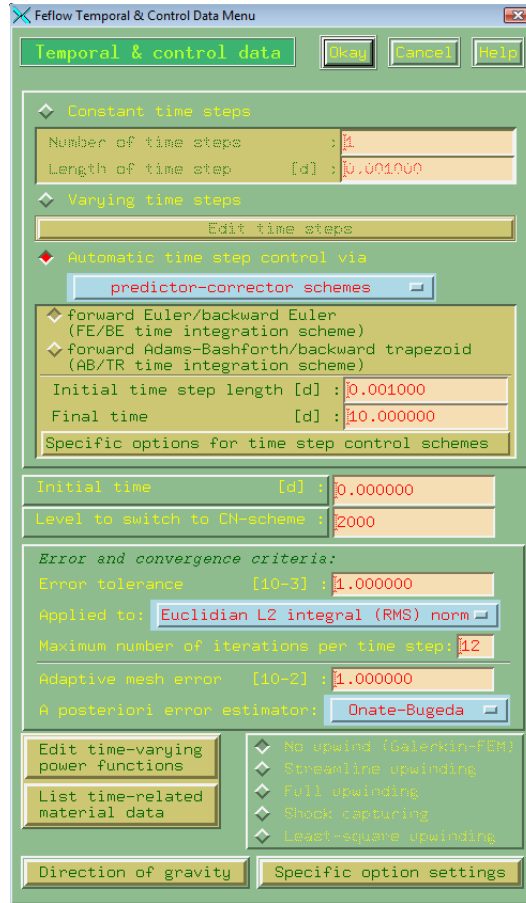


Fig. 4.27. Temporal and control data settings

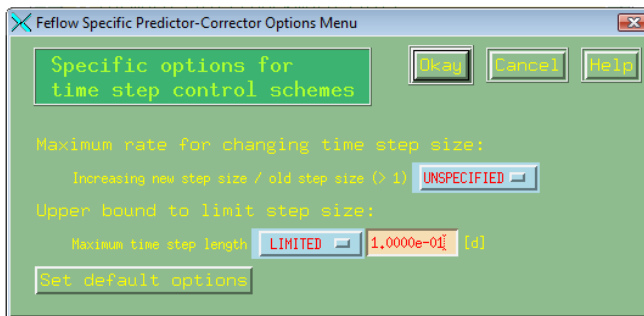


Fig. 4.28. Specific options for time control settings

- In **Flow data** menu assign saturated and unsaturated hydraulic characteristics to soil profile, separately for each layer, saturated conductivity and water retention curve (pF) parameters, according to Fig. 4.29.

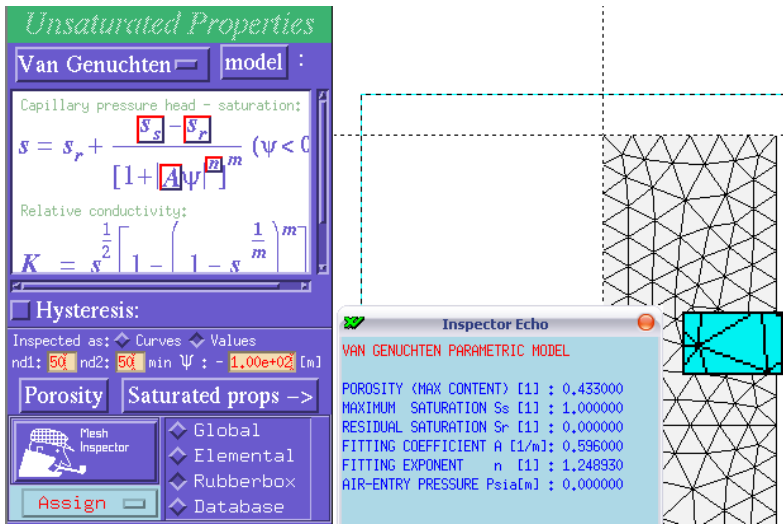


Fig. 4.29. Unsaturated properties assignment

- Go back to **Flow data** and select **Flow initials**. Then select **Saturation** and assign 0.5 [-] representing 50% of saturation for time $t = 0$ to the upper layer and 0.6 [-] (60%) saturation to the bottom layer (Fig. 4.30).

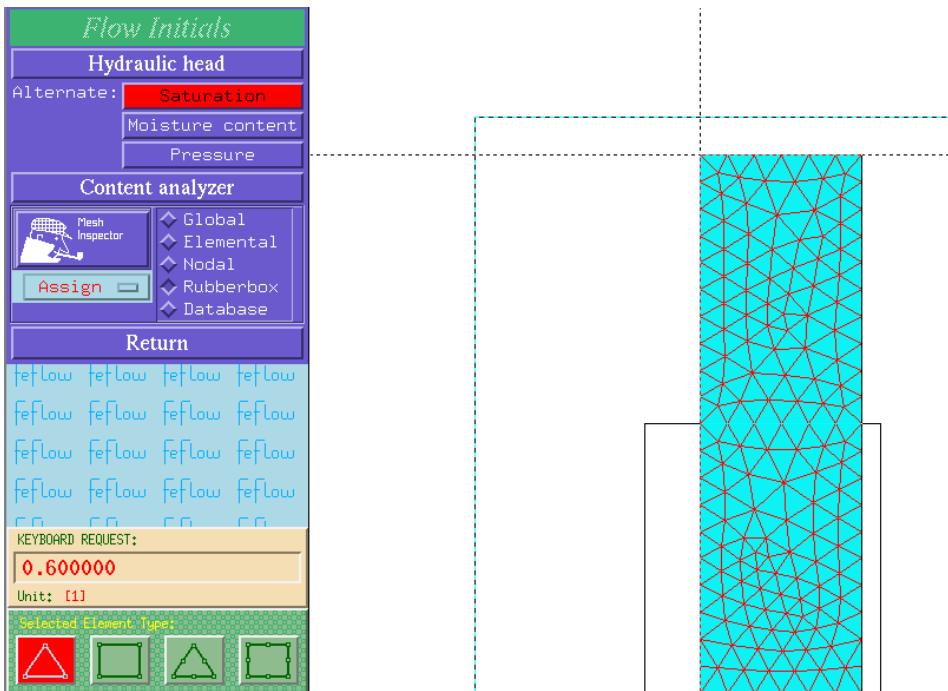


Fig. 4.30. Initial conditions

- Go to Flow boundaries and assign the bottom boundary condition as Head = -2.0 m, according to Fig. 4.31 and the top boundary condition as Flux = 0.005 m/day, as it is presented in Fig. 4.32. Note: + and – signs are crucial here.

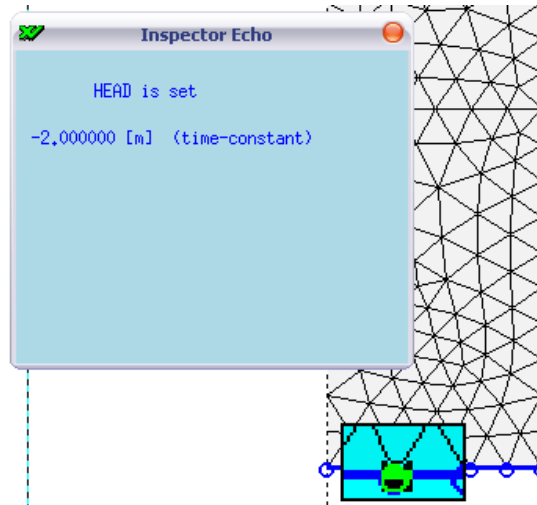


Fig. 4.31. Bottom boundary condition

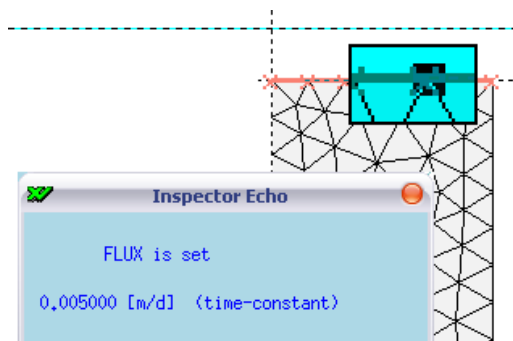


Fig. 4.32. Top boundary condition

- Now go to the **Reference data – Observation single points** and set observation points and observation line according to Fig. 4.33.

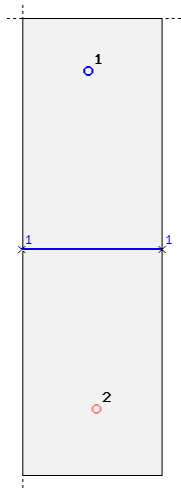


Fig. 4.33. Observation points and surface (line)

- Save finite element problem, go to the **Simulator**, input **Control output** settings and run the simulation (Fig. 4.34).

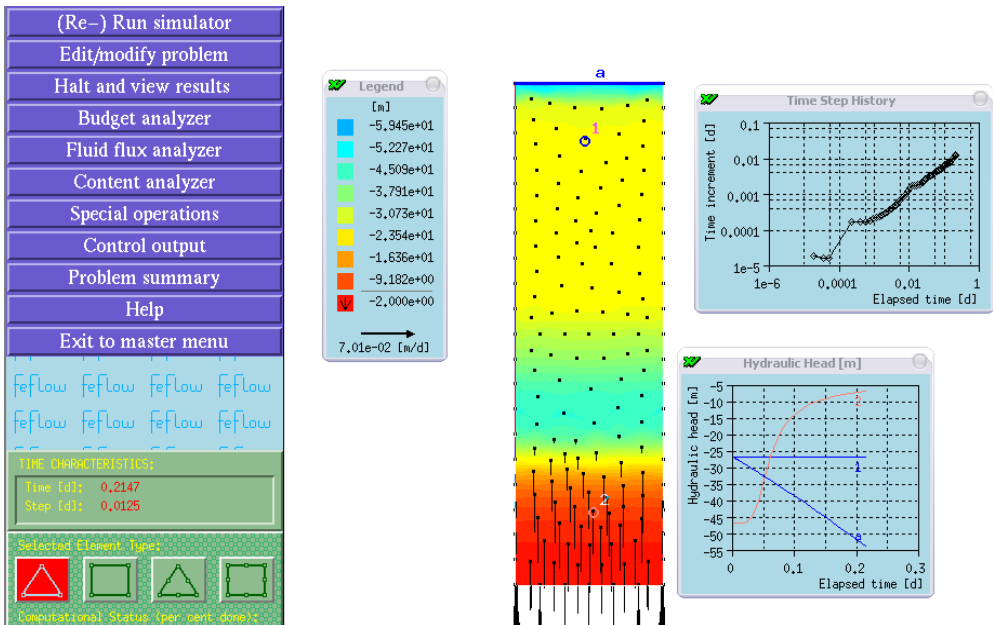


Fig. 4.34. Working model in Simulator (solver) – note vectors of soil water velocities

- Having finished the calculations, enter **Postprocess** and load results data (Fig. 4.35).

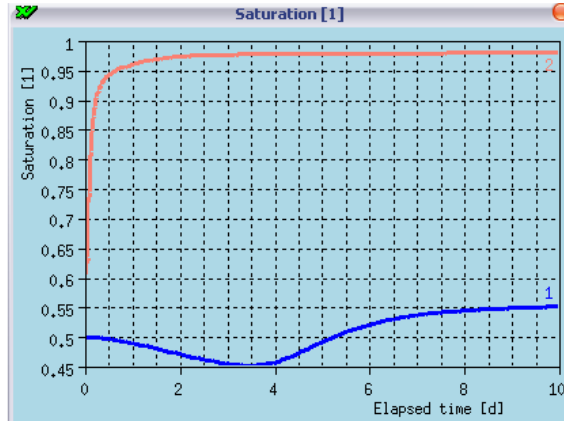


Fig. 4.35. Time varied saturation in observation points

- Using **Browse file** and **View results** check distributions of soil saturations by water for 1 (Fig. 4.36), 5 (Fig. 4.37) and 10 day of simulation (Fig. 4.38).

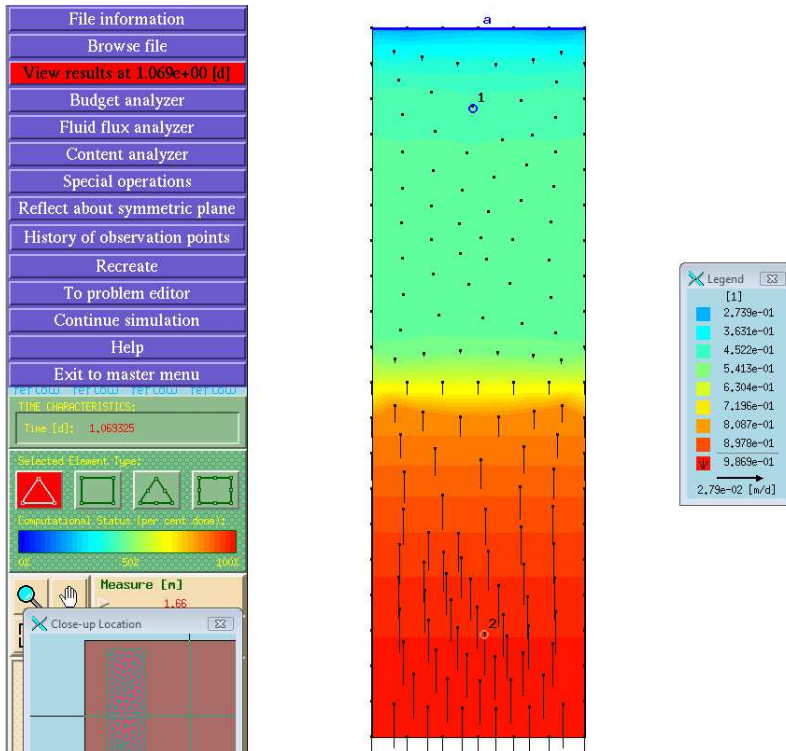


Fig. 4.36. Soil saturation distribution for 1 day time duration

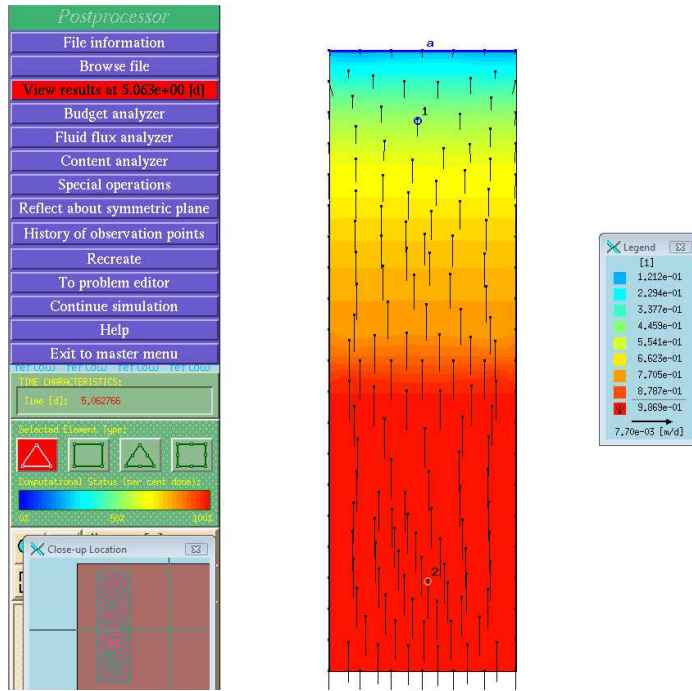


Fig. 4.37. Soil saturation distribution for 5 days time duration

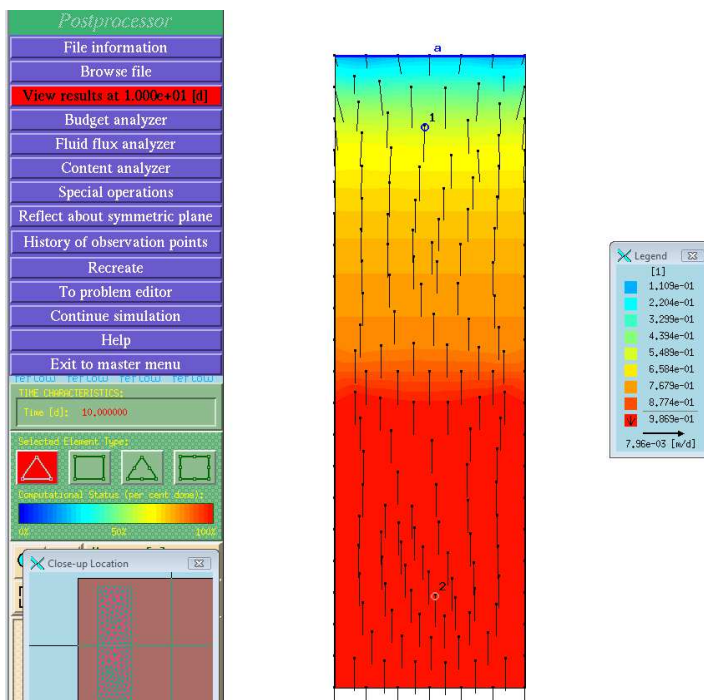


Fig. 4.38. Soil saturation distribution for 10 days time duration

- Select **Fluid flux analyzer** and calculate the water flux through selected observation line (surface) according to Fig. 4.39 – **Segment 1** for the whole time duration of simulation (Fig. 4.40).

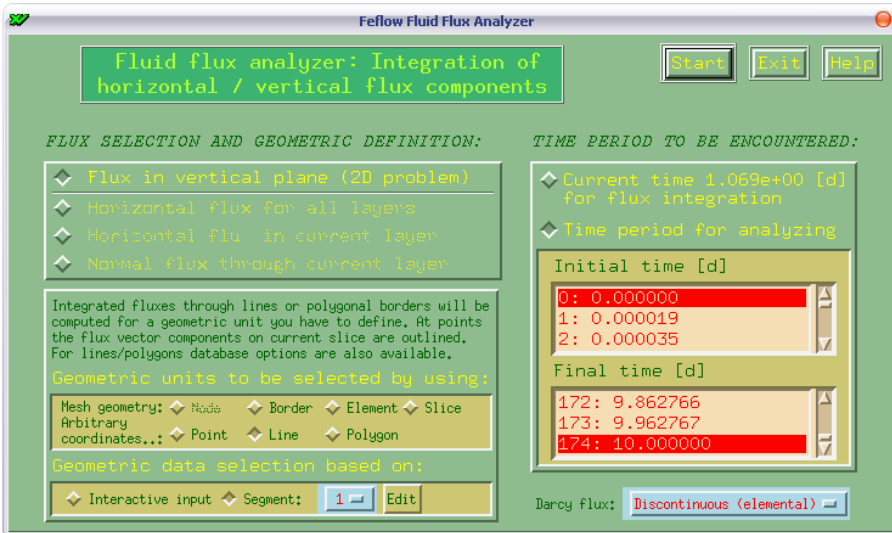


Fig. 4.39. Fluid flux analyzer settings

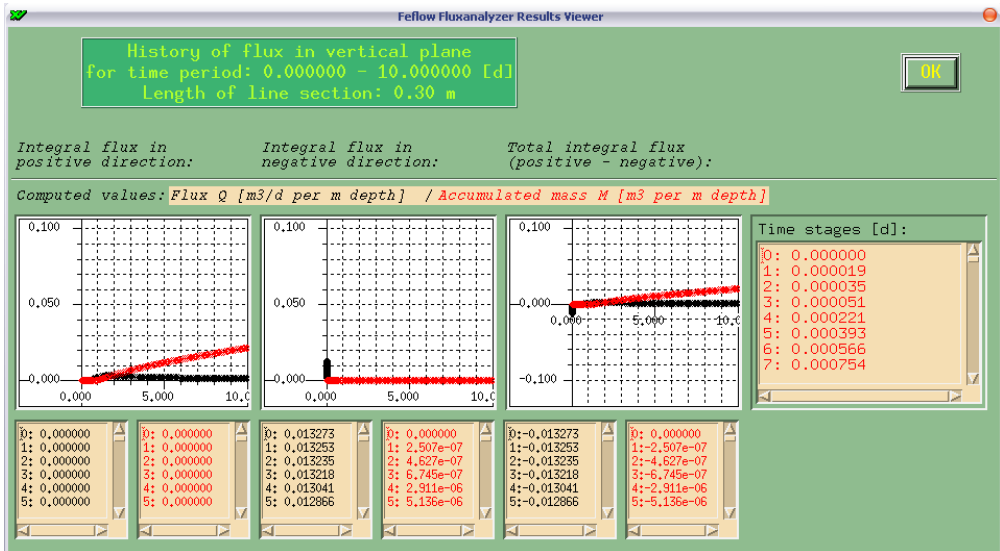


Fig. 4.40. Calculated water flow and accumulated volume for the full period of simulation

4.3 Simulation of water capillary rise in three-layered soil profile

Perform numerical calculations of water movement in three-layered soil profile of dimensions 0.3x1.0 m during 20 days of the experiment (variable time step – the Euler/Euler scheme) for input soil data presented in Table 4.3.

Table 4.3. Input soil data required for simulation

Soil	Depth cm	Saturated hydraulic conductivity K_s [cm/d]	Saturated water content θ_s [-]	Residual water content θ_r [-]	WRC fitting parameter α [1/cm]	WRC fitting parameter n [-]
Layer 1	0–100	52.91	0.43	0.02	0.0234	1.801
Layer 2	100–180	14.07	0.40	0.00	0.0194	1.250
Layer 3	180–300	12.98	0.42	0.01	0.0084	1.441

Initial and boundary conditions:

The initial condition – saturation of the soil column – layer 1 – 30%, layer 2 – 35%, layer 3 – 31%.

The top boundary condition – varying day transpiration according to Table 4.4.

Table 4.4. Top boundary condition for simulation

Day of experiment	Average day transpiration [mm]
1–4	1.2
5–12	1.8
13–16	2.5
17–20	2.7

Additionally, in the 15th day of the simulation period at 12.00 the precipitation (12 mm per 1 hour) occurred. The surface runoff coefficient equals 0.1.

The bottom boundary condition – constant potential head of water equals 150 cm.

We assume:

- variable time step,
- maximal length of time step – 0.1 day,
- model of unsaturated conductivity calculation – the van Genuchten model.
- two observation lines on the borders of the layers,

- no hysteresis for pF (WR) curves,
- residual saturation $S_r = 0$,
- porosity equal to maximum saturation.

Determine the balance of water flow through the assumed observation planes.

Solution

- Load the map of the profile developed earlier in the *.dxf file according to Fig. 4.41.

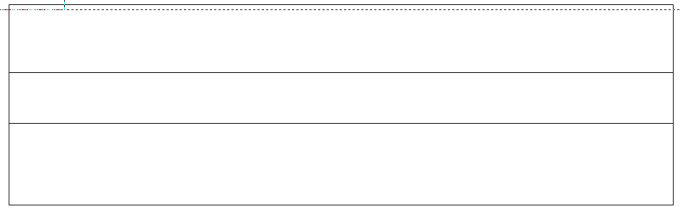


Fig. 4.41. Loaded electronic map of calculation area

- On the basis of the loaded map create the finite element mesh and locate the coordinate origin on the soil surface (Fig. 4.42).

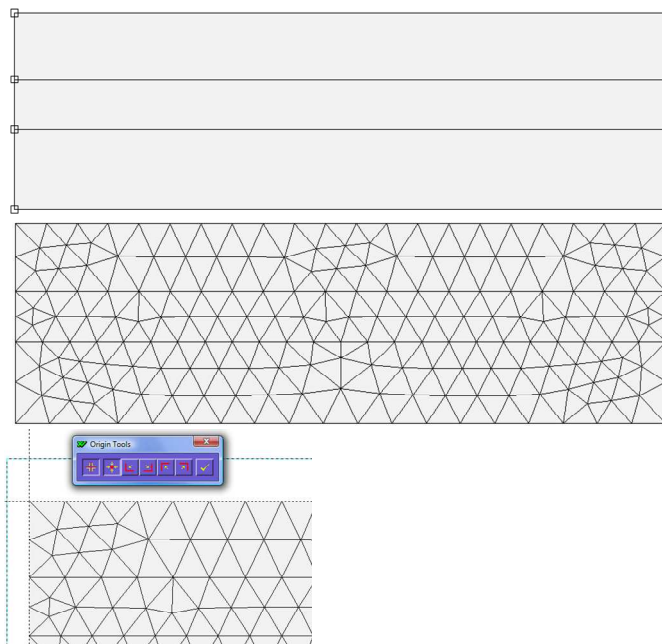


Fig. 4.42. Creation of the finite element mesh and change of the coordinate origin localization

- Define the initial conditions according to the text of the exercise – Saturation – layer 1 – 0.3 [-], layer 2 – 0.35 [-], layer 3 – 0.31 [-] (Fig. 4.43).

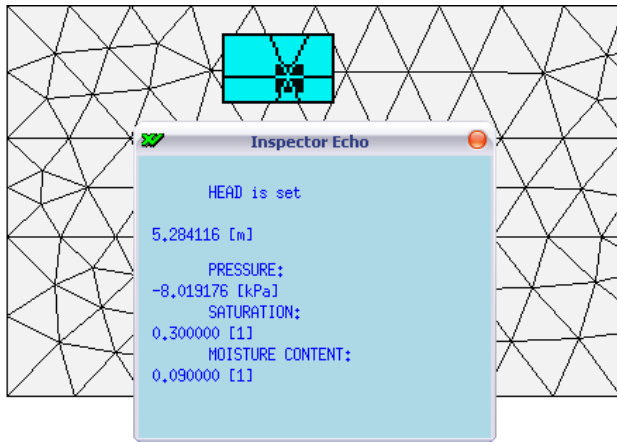


Fig. 4.43. Defining of initial conditions

- Assign physics and hydraulic – saturated and unsaturated – parameters of soil to the mesh elements (Fig. 4.44).

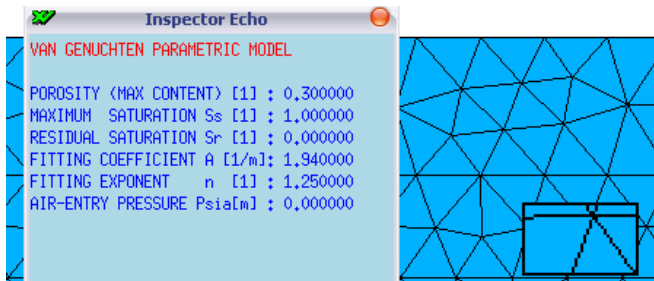


Fig. 4.44. Assignment of physics and hydraulic parameters of soil to the mesh elements

- Assign the boundary condition of the first type – Head = -1.5 m, to the bottom edge of the finite element mesh (Fig. 4.45).

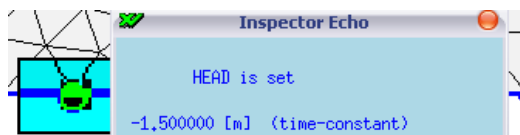


Fig. 4.45. Bottom boundary condition

- Define a function determining the top boundary condition (Fig. 4.46).

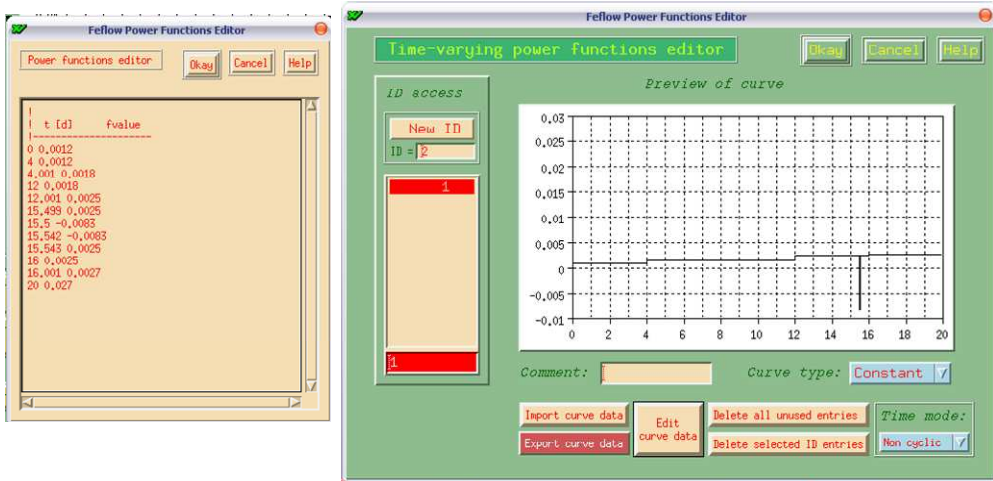


Fig. 4.46. Function of top boundary condition, variable in time

- Assign the variable boundary condition Flux – the ID 1 function in figure below (Fig. 4.47) – to the top edge of the finite element mesh.

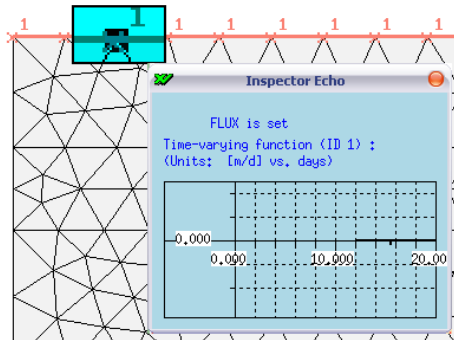


Fig. 4.47. Top boundary condition

- Locate the observation lines (Fig. 4.48).

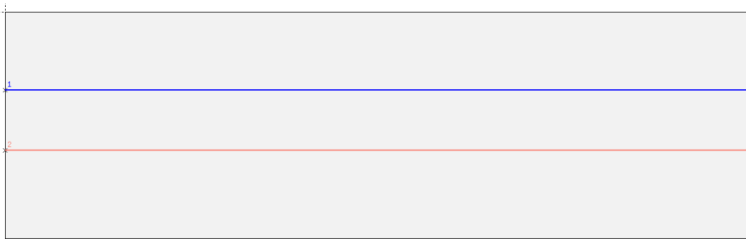


Fig. 4.48. Observation lines

- Check if the model is ready to run – **Problem Summary** (Fig. 4.49).

Problem Summary Okay

DESCRIPTORS:

FILE NAME	Przyklad 3.fem (BINARY 5.2)
PROBLEM TITLE	Ruch wody - profil trojwarstwowy
RECENT UPDATING	Thu Nov 26 11:15:57 2009
DIMENSION	Two-Dimensional
TYPE	Unsaturated
NUMBER OF LAYERS	Irrelevant
NUMBER OF SLICES	Irrelevant
PROBLEM MEASURE	10,9588 [m]
VERTICAL EXAGGERATION :	1,0000 : 1
PROJECTION	Vertical
PROBLEM CLASS	Separate flow process
TIME CLASS	Unsteady flow
TIME STEPPING SCHEME .:	Forward Euler/Backward Euler (FE/BE) predictor-corrector
UPWINDING	No upwinding (best-accurate Galerkin-based formulation)
NUMBER OF SPECIES	0

MESH DATA:

ELEMENT TYPE	3-noded triangle
MESH ELEMENTS	344
MESH NODES	199
MESH OPTIMIZATION :	Not done

FLOW CONDITIONS:

BOUNDARIES	<input type="checkbox"/> Specified	<input type="checkbox"/> Unspecified
INITIALS	<input type="checkbox"/> Specified	<input type="checkbox"/> Default
MATERIALS	<input type="checkbox"/> Specified	<input type="checkbox"/> Default

READY TO RUN ?

Yes No

TRANSPORT CONDITIONS:

BOUNDARIES	<input type="checkbox"/> Specified	<input type="checkbox"/> Unspecified
INITIALS	<input type="checkbox"/> Specified	<input type="checkbox"/> Default
MATERIALS	<input type="checkbox"/> Specified	<input type="checkbox"/> Default

Fig. 4.49. Summary of model creation

Save the created numerical model as *.fem and go to calculation processor.

- Select the way of saving of output data files – record of complete data with the filename extension *.dac.
- Run the simulation selecting the button **(Re-)Run Simulator** according to Fig. 4.50.

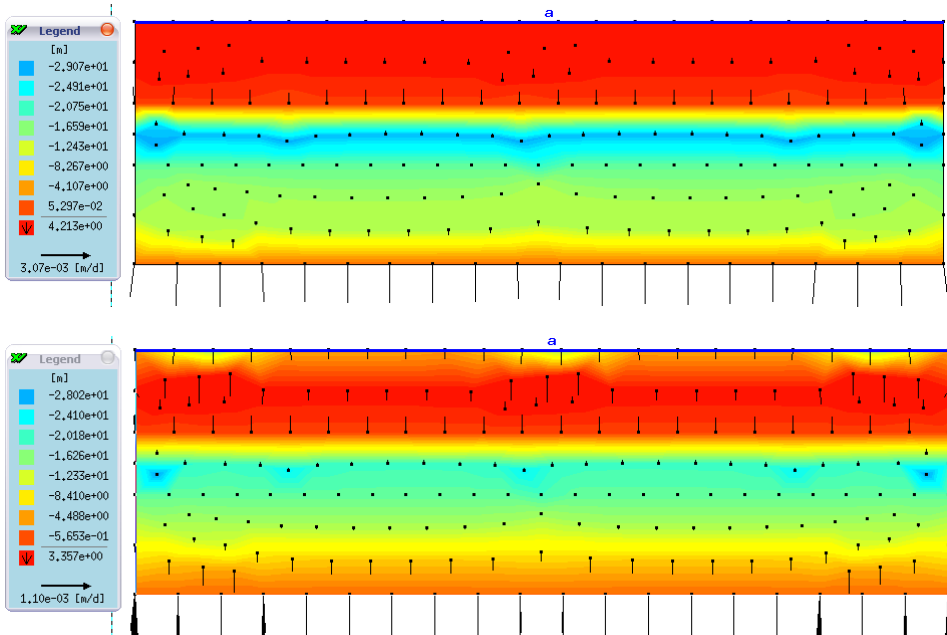


Fig. 4.50. Simulation calculation of water movement in three-layered soil profile

- After calculating go to the postprocessor.
- Load the saved output data file.
- Select **Fluid flux analyzer** to verify the volume of water flux through the observation lines 1-1 and 2-2 according to Fig. 4.51 and Fig. 4.52.

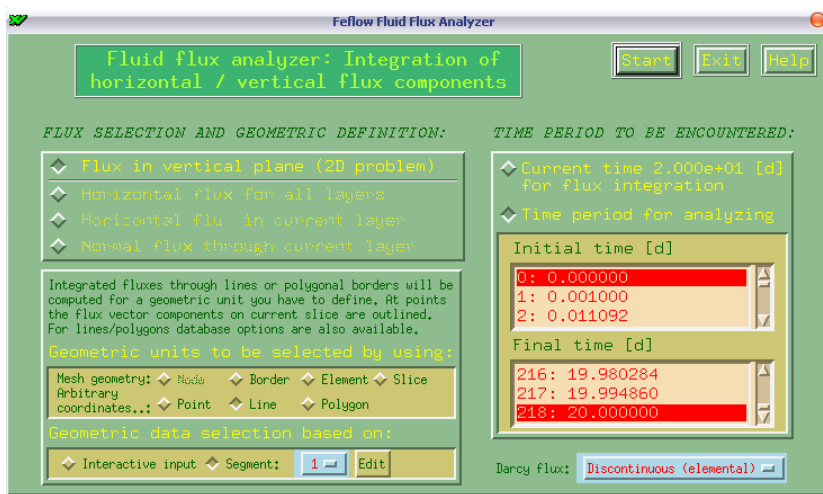


Fig. 4.51. Calculations of intensity of water flux through the selected observation lines

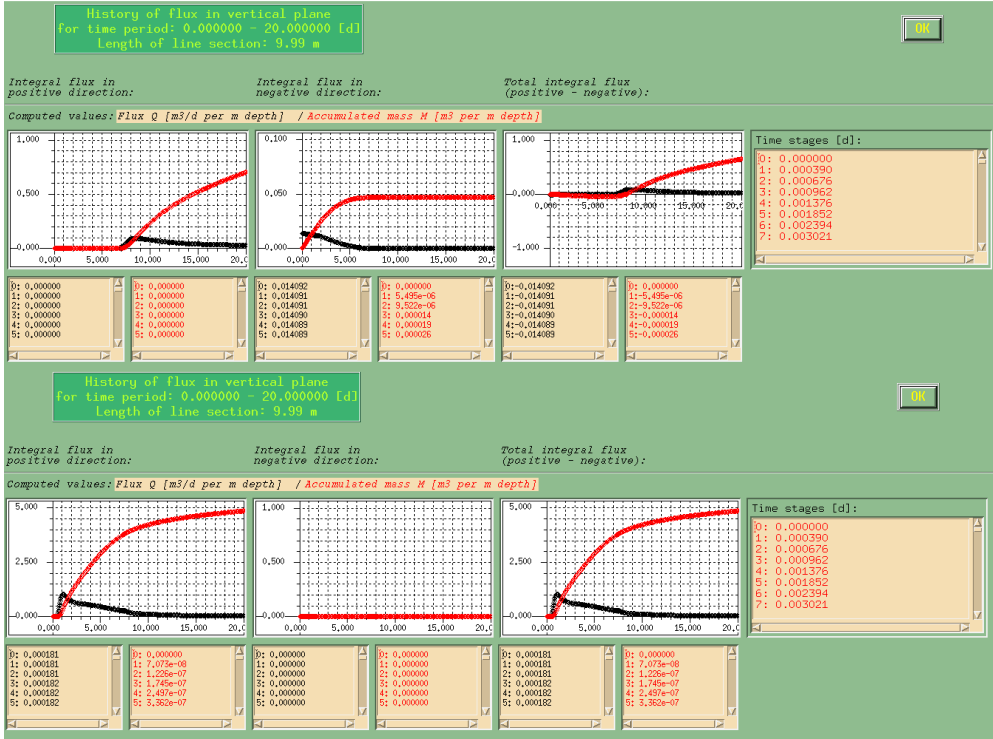


Fig. 4.52. Results of calculations of intensity of water flux through the selected observation lines

4.4 Simulation of cadmium transport in fine sand column wetting by capillary rise

Perform numerical calculations of cadmium transport in a soil column of dimensions 100x30 cm for time duration $t = 10$ days (variable time step, Euler/Euler scheme) for the data according to Table 4.5.

Table 4.5. Soil characteristics for example of numerical calculations

Material	Layer	K_s [cm/d]	θ_s [-]	α [1/cm]	n [-]
Sand	0–100 cm	769.0000	0.4200	0.0100	1.9600

Apply the parameters of the contaminant transport according to Table 4.6.

Table 4.6. Input data required for simulation of cadmium transport in soil column

Sorption Henry coeff. [-]	Molecular diffusion coeff. [m^2/s]	Decay rate coefficient [$1/\text{s}$]	Longitudinal dispersivity [m]	Transverse dispersivity [m]
78.97	$1.0 \cdot 10^{-9}$	$1.727 \cdot 10^{-8}$	7.60	0.5

Initial and boundary conditions:

Initial condition for water – saturation of sand column – 20%.

Top boundary condition – constant evapotranspiration 0.2 mm/d.

Bottom boundary condition – constant pressure head – 100 cm.

Initial condition for mass transport: contaminant concentration $0.01 \text{ mg}/\text{dm}^3$.

Boundary conditions: the boundary condition of the first type – Mass = $0.1 \text{ mg}/\text{dm}^3$, on the upper edge (10 cm in width) of soil profile.

The contaminant distribution for time duration $t = 10$ days should be analyzed.

Assumptions for calculations:

- variable time step,
- maximum length of time step – 0.1 d,
- unsaturated hydraulic conductivity model – van Ganuchten,
- three observation points in the vertical axis of the column,
- no pF curve hysteresis included (pF),
- residual saturation (S_r) equal to 0 [-],
- porosity equal to maximal saturation.

Solution

- Create the mesh of finite elements of dimensions $1.0 \times 0.3 \text{ m}$ (Fig. 4.53).

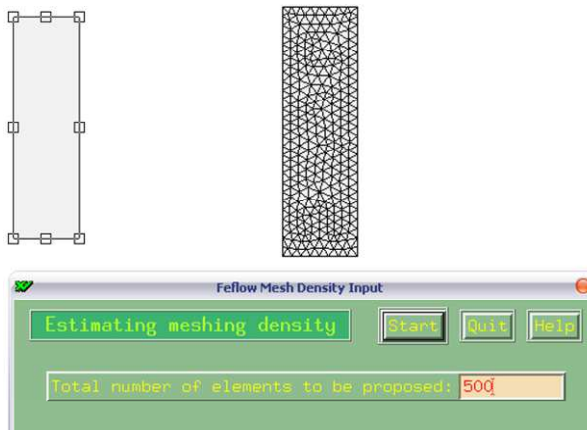


Fig. 4.53. Generation of finite elements mesh

- Move the origin of coordination system to the upper corner of the modeled domain according to Fig. 4.54.

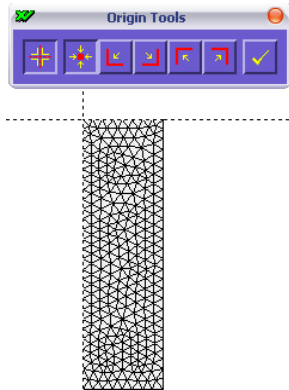


Fig. 4.54. Shift of coordination system origin

- Using **Menu Edit – Edit problem attributes** to open the preprocessor.
- Change the parameters of a simulation – in the window **Problem Class**, set the option of modeling single-species transport – transient flow of water and transient transport of contaminants according to Fig. 4.55.

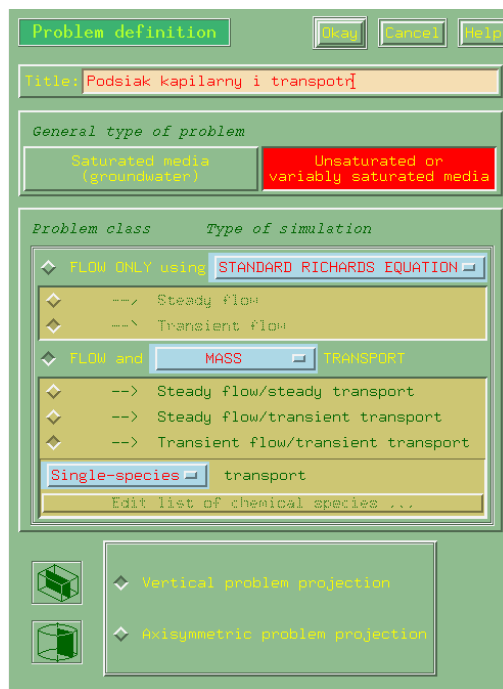


Fig. 4.55. Basic settings of contaminant mass transport model

- Set the time duration of simulation and select the model of time step control according to Fig. 4.56.

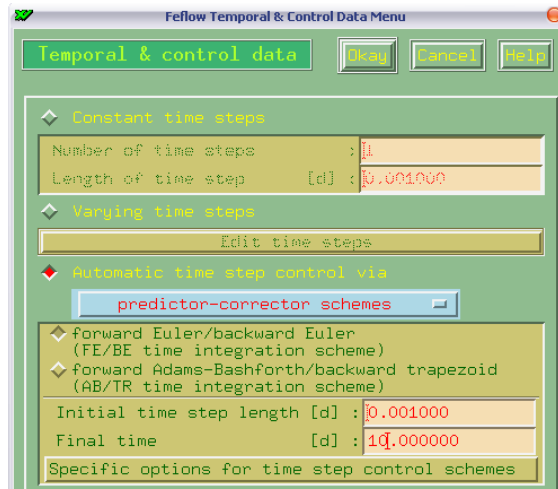


Fig. 4.56. Selection of time duration and time step control options

- Limit the allowable time step length to 0.1 day (Fig. 4.57).

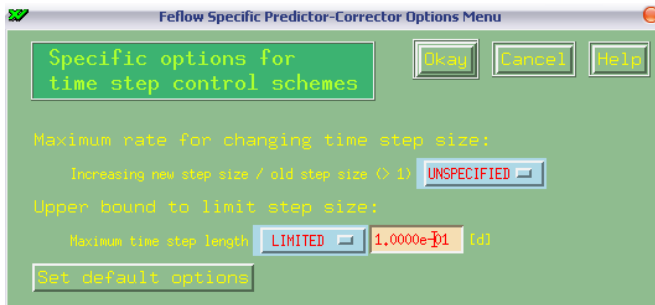


Fig. 4.57. Limit of the maximum allowable time step

- Assign saturated and unsaturated characteristics of soil to mesh (Fig. 4.58).

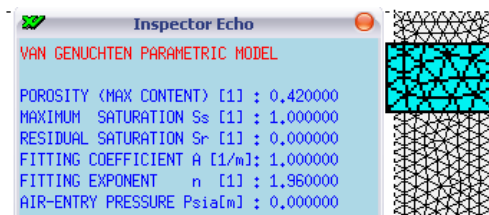


Fig. 4.58. Assignment of soil parameters to finite elements mesh

- Set the initial condition – saturation 20% (Fig. 4.59).

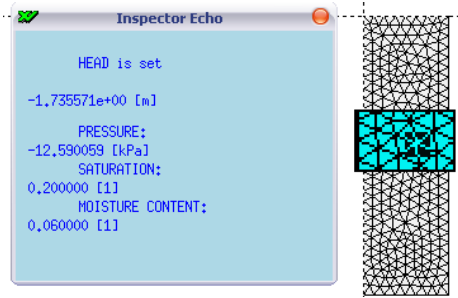


Fig. 4.59. Determination of the initial conditions

- Assign the bottom boundary condition for water HEAD equal to -1.0 m, according to Fig. 4.60.

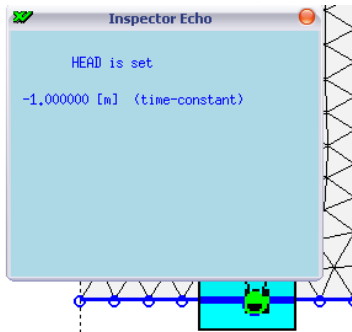


Fig. 4.60. Bottom boundary condition

- Set the top boundary condition for water as FLUX 0.002 m/d (Fig. 4.61).

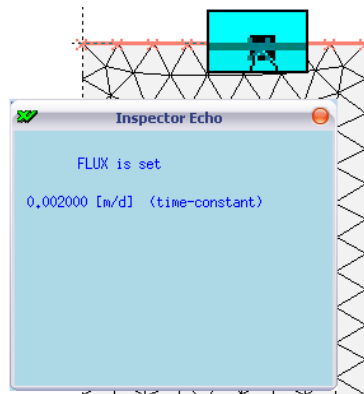


Fig. 4.61. Top boundary condition for water

- Assign transport parameters of the selected contaminant to the elements of the mesh according to Fig. 4.62.

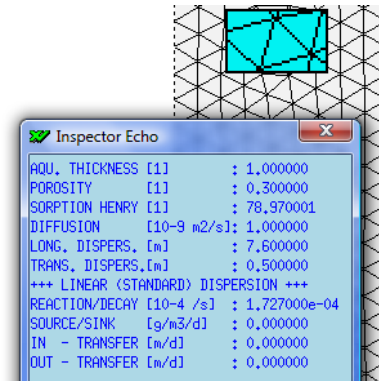


Fig. 4.62. Assignment parameters of transport of contaminant mass

- Assign an initial condition according to Fig. 4.63 – Mass = 0.01 mg/dm³.

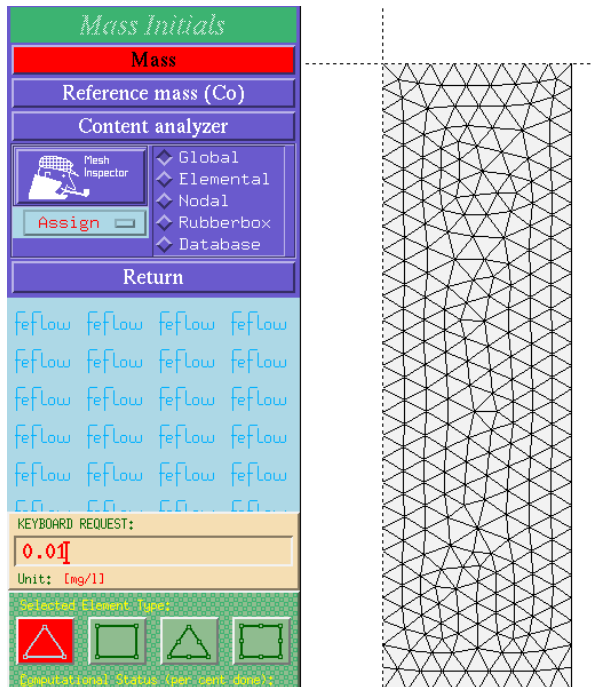


Fig. 4.63. Assignment of initial condition of transport of contaminant mass

- Assign the time-constant boundary condition – Mass = 0.1 mg/dm^3 , on the upper edge (10 cm in width) of the simulation domain (Fig. 4.64).

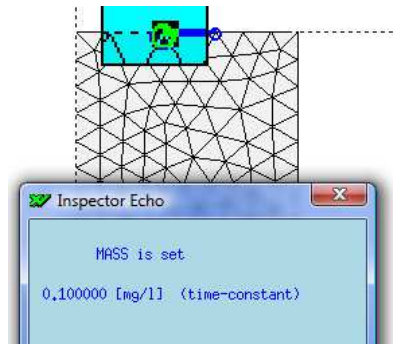


Fig. 4.64. Upper boundary condition of transport of contaminant mass

- Set three reference points according to Fig. 4.65.

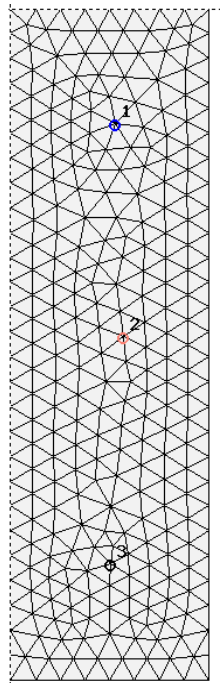


Fig. 4.65. Reference points

- Go to the main menu, enter **Run – Start simulator** and select **Problem Summary** according to Fig. 4.66, to verify basic settings of the model and its readiness to run.

Problem Summary Okay

DESCRIPTORS:

FILE NAME	Przyklad 1 Transport.fem (BINARY 5,2)
PROBLEM TITLE	Podsiak kapilarny i transpotr
RECENT UPDATING	Wed Dec 02 12:36:57 2009
DIMENSION	Two-Dimensional
TYPE	Unsaturated
NUMBER OF LAYERS	Irrelevant
NUMBER OF SLICES	Irrelevant
PROBLEM MEASURE	4,55 [m]
VERTICAL EXAGGERATION :	1,00 : 1
PROJECTION	Vertical
PROBLEM CLASS	Combined flow and MASS transport
TIME CLASS	Unsteady flow - unsteady MASS transport
TIME STEPPING SCHEME :	Forward Euler/Backward Euler (FE/BE) predictor-corrector
UPWINDING	No upwinding (best-accurate Galerkin-based formulation)
NUMBER OF SPECIES	1 (single-species transport)

MESH DATA:

ELEMENT TYPE	3-noded triangle
MESH ELEMENTS	508
MESH NODES	290
MESH OPTIHZIZATION :	Not done

FLOW CONDITIONS:

BOUNDARIES	<input type="checkbox"/> Specified	<input type="checkbox"/> Unspecified
INITIALS	<input type="checkbox"/> Specified	<input type="checkbox"/> Default
MATERIALS	<input type="checkbox"/> Specified	<input type="checkbox"/> Default

READY TO RUN ?

Yes No

TRANSPORT CONDITIONS:

BOUNDARIES	<input type="checkbox"/> Specified	<input type="checkbox"/> Unspecified
INITIALS	<input type="checkbox"/> Specified	<input type="checkbox"/> Default
MATERIALS	<input type="checkbox"/> Specified	<input type="checkbox"/> Default

Fig. 4.66. Summary of created model

- Save the developed model as *.fem.
- Go to the processor of the FEFLOW software.
- Select the way of saving of output data files – record of complete data with filename extension *.dac.
- Run the simulation selecting the button **(Re-)Run Simulator** according to Fig. 4.67.

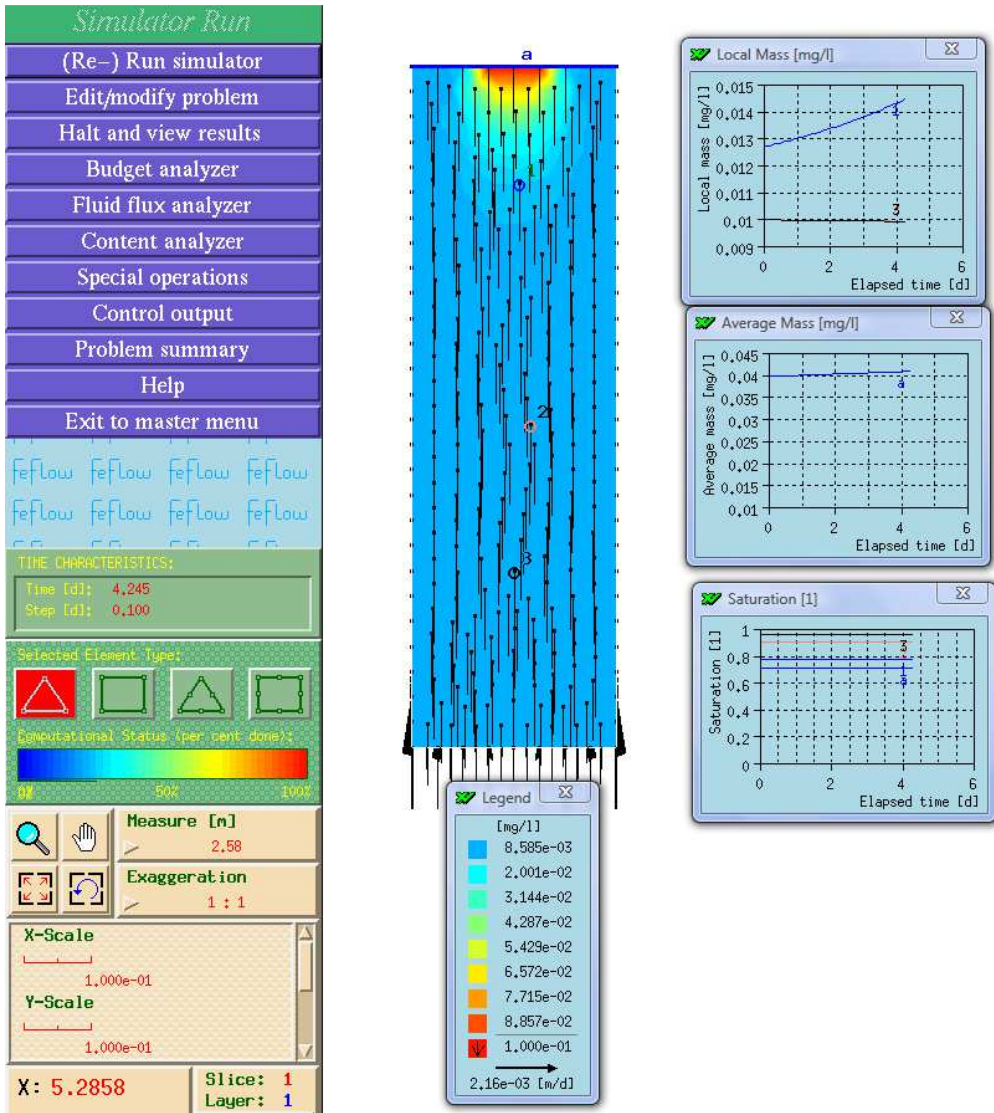


Fig. 4.67. Numerical calculation of water flow and contamination transport in the processor

- After calculating go to the postprocessor.
- Load the saved output data file *.dac.
- Enter **Browse file** and select a time step.
- Enter **View results at...** to see results of calculation for the assumed time step.
- Generated diagrams can be exported in any format (Fig. 4.68).



Fig. 4.68. Diagram of results of calculation of contaminant intensity in soil column

4.5 Simulation of chromium transport in two-layered soil profile

Perform numerical calculations of transport of a contaminant (chromium) in a two-layered soil column of dimensions 0.3x1.0 m during 10 days of experiment (variable time step – the Euler/Euler scheme).

Input data should be applied according to Table 4.7 for water transport and Table 4.8 for mass transport.

Table 4.7. Soil characteristics applied as input data for water transport

Layer	Depth	K_s [cm/d]	θ_s [-]	α [1/cm]	n [-]
Layer 1	0–50 cm	18	0.433	0.00596	1.24892
Layer 2	50–100 cm	2	0.37	0.00113	1.2946

Table 4.8. Input data required for Exercise of simulation of chromium transport in two-layered soil column

No	Sorption Henry coefficient [-]	Molecular diffusion coefficient [m^2/s]	Decay rate coefficient [1/s]	Longitudinal dispersivity [m]	Transverse dispersivity [m]
1	0.20	$1.0 \cdot 10^{-9}$	$2.886 \cdot 10^{-7}$	36.00	0.5
2	0.191	$1.0 \cdot 10^{-9}$	$2.886 \cdot 10^{-7}$	2.50	0.5

Initial and boundary conditions:

- initial condition for water flow – saturation of soil – layer I – 50%, layer II – 60%,
- top boundary condition (water flow) – constant value of infiltration equal to -1.8 mm/d during first three days of a simulation and then constant value of evapotranspiration equal to 1.2 mm/d ,
- bottom boundary condition for water transport – constant pressure head equal to -200 cm ,
- initial condition for mass transport – constant background concentration – 0.7 mg/dm^3 ,
- entry of a contamination to the profile through the left half of the top edge,
- top boundary condition – constant intensity of contaminant inflow to the profile $\text{Flux} = 5 \text{ mg/dm}^3$, during first three days of a simulation,
- reference concentration $c_0 = 0.0 \text{ mg/dm}^3$.

Modeling assumptions:

- variable time step,
- maximum length of time step – 0.1 d ,
- unsaturated hydraulic conductivity model – van Ganuchten,
- two observation points in the vertical axis of the column and observation line between two layers,
- no pF curve hysteresis included (pF),
- residual saturation (S_r) equal to $0 [-]$,
- porosity equal to maximal saturation.

Check a contamination distribution for time duration of simulation 5 and 10 days.

Solution

- Go to **Menu Edit – Edit problem attributes** to run the preprocessor.
- Create the finite elements mesh of dimensions 1.0 x 0.3 m for two-layers profile (at least approx. 300 elements, 150 for each layer) according Fig. 4.69.

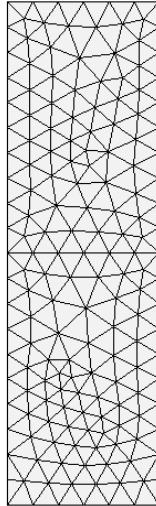


Fig. 4.69. Finite elements mesh

- Set the location of coordination system origin – Fig. 4.70.

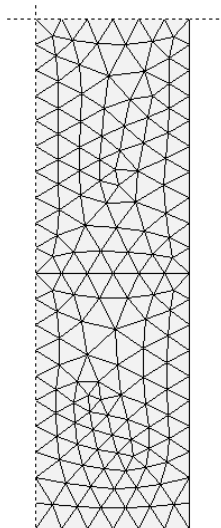


Fig. 4.70. Shifted origin of coordination system

- Set the parameters of a simulation – in the window **Problem Class**, set the option of modeling single-species transport – transient flow of water and transient transport of contaminants.
- Assign the initial conditions for water flow: layer I – saturation 0.5 [-], layer II – saturation 0.6 [-] according to Fig. 4.71.

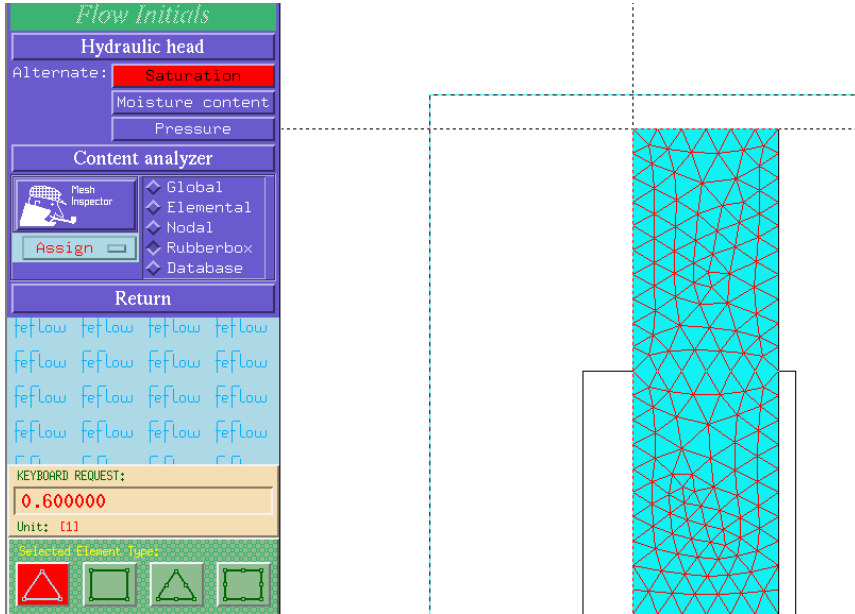


Fig. 4.71. Initial conditions for soil water flow

- Assign the saturated and unsaturated soil characteristics (Fig. 4.72).

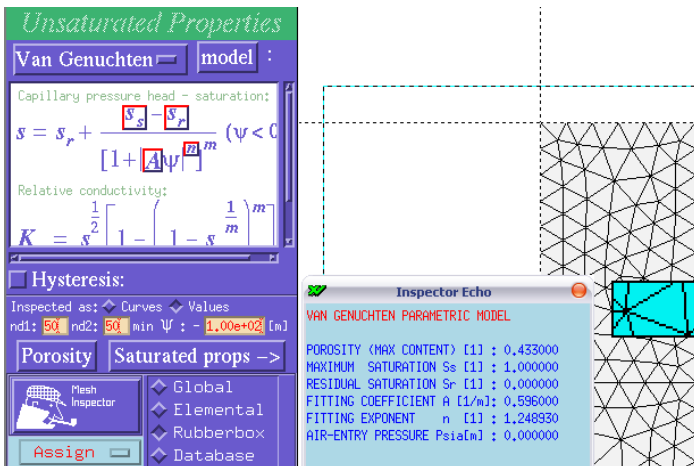


Fig. 4.72. Unsaturated soil characteristics

- Set the bottom boundary condition for water flow according to Fig. 4.73, as $\text{HEAD} = -2.0$ m.

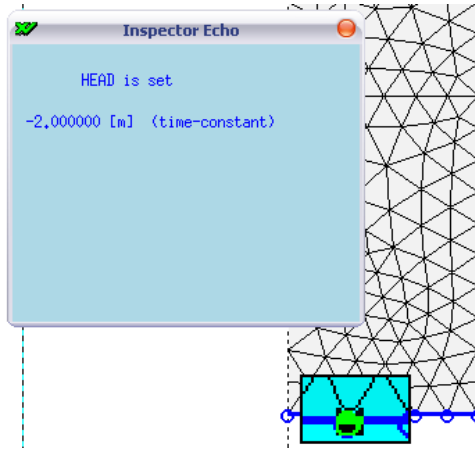


Fig. 4.73. Bottom boundary condition for water flow

- Assign the top boundary condition for water – enter **Time varying functions' ID** to create a function reflecting the assuming top boundary condition, and assign the new boundary condition on the top edge of the simulation domain, according to Fig. 4.74 and Fig. 4.75.

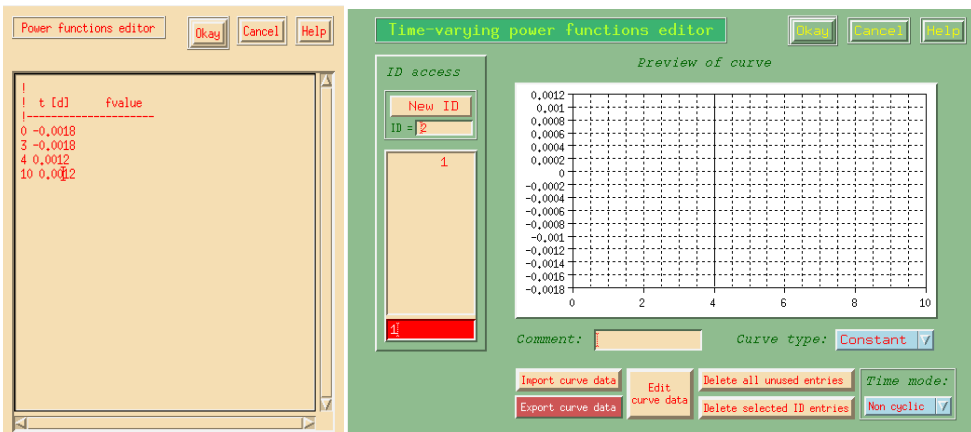


Fig. 4.74. Time-varying function of top boundary condition

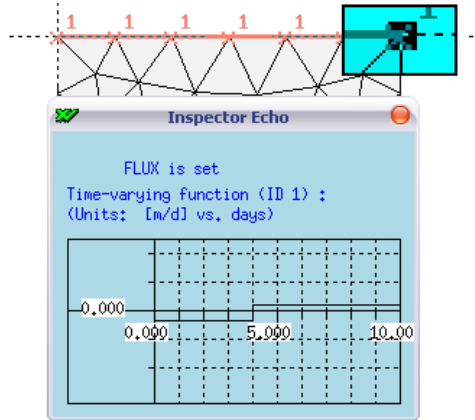


Fig. 4.75. Time-varying top boundary condition assigned on the border of model

- Determine the initial condition of the contaminant concentration Mass = 0.7 mg/dm³ using the command **Transport Data, Mass Transport Initials, Mass** according to Fig. 4.76.

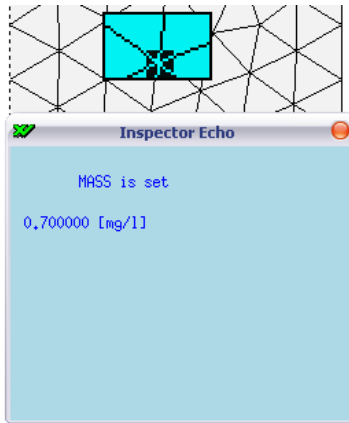


Fig. 4.76. Initial condition of calculations of contaminant transport

- Define a time-varying function reflecting the top condition of mass transport (**Transport Data, Mass Transport Boundaries, Time varying functions' ID**) and assign time-varying condition of the second type (**Flux**) on the left half of the top edge of the calculation domain (Fig. 4.77 and Fig. 4.78).
- Next, assign the requested parameters of the contaminant transport to the finite elements mesh (Fig. 4.79).

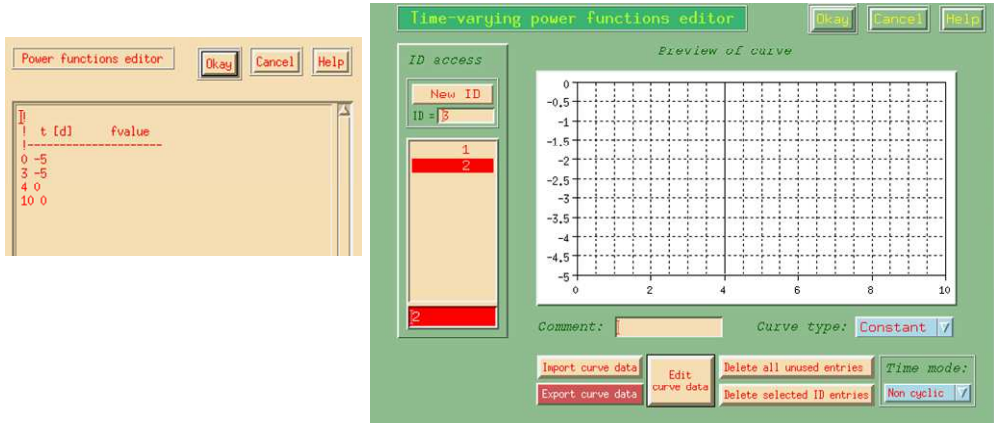


Fig. 4.77. Time-varying function of top boundary condition of mass transport

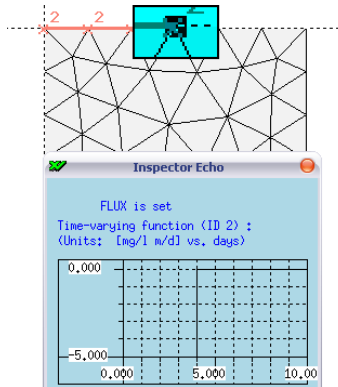


Fig. 4.78. Time-varying top boundary condition of contaminant transport

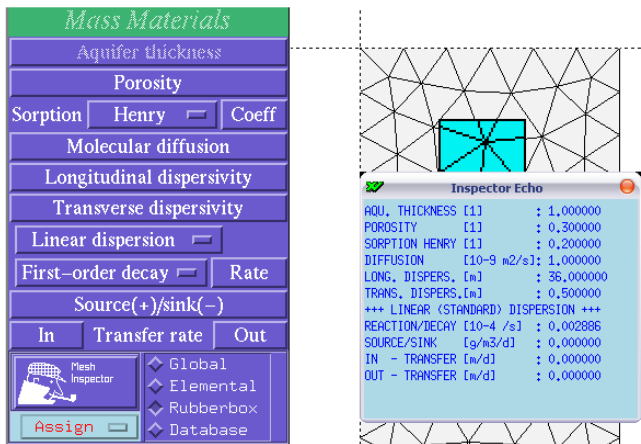


Fig. 4.79. Transport parameters of soil medium assigned to finite elements mesh

- Set two reference points and observation line – Fig. 4.80.

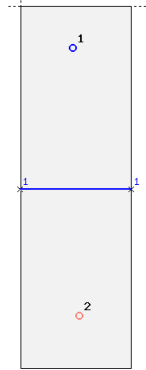


Fig. 4.80. Observation points and reference line

Problem Summary
Okay

DESCRIPTORS:

FILE NAME	Przyklad 2 Transport.fem (BINARY 5,2)
PROBLEM TITLE	Transport - kolumna duuwarstwowa
RECENT UPDATING	Sat Dec 05 21:03:14 2009
DIMENSION	Two-Dimensional
TYPE	Unsaturated
NUMBER OF LAYERS	Irrelevant
NUMBER OF SLICES	Irrelevant
PROBLEM MEASURE	1.26 [m]
VERTICAL EXAGGERATION :	1,00 : 1
PROJECTION	Vertical
PROBLEM CLASS	Combined flow and MASS transport
TIME CLASS	Unsteady flow - unsteady MASS transport
TIME STEPPING SCHEME .:	Forward Euler/Backward Euler (FE/BE) predictor-corrector
UPWINDING	No upwinding (best-accurate Galerkin-based formulation)
NUMBER OF SPECIES	1 (single-species transport)

MESH DATA:

ELEMENT TYPE	3-noded triangle
MESH ELEMENTS	292
MESH NODES	173
MESH OPTIMIZATION :	Not done

FLOW CONDITIONS:

BOUNDARIES	<input type="checkbox"/> Specified	<input checked="" type="checkbox"/> Unspecified
INITIALS	<input type="checkbox"/> Specified	<input checked="" type="checkbox"/> Default
MATERIALS	<input type="checkbox"/> Specified	<input checked="" type="checkbox"/> Default

READY TO RUN ?

Yes
 No

TRANSPORT CONDITIONS:

BOUNDARIES	<input type="checkbox"/> Specified	<input checked="" type="checkbox"/> Unspecified
INITIALS	<input type="checkbox"/> Specified	<input checked="" type="checkbox"/> Default
MATERIALS	<input type="checkbox"/> Specified	<input checked="" type="checkbox"/> Default

Fig. 4.81. Summary of the model

- Enter **Problem Summary** to verify settings of the model and its readiness to run – Fig 4.81.
- Save the created model as *.fem and go to the processor.
- Select the way of saving of output data files – record of complete data with filename extension *.dac.
- Run the simulation selecting the button **(Re-)Run Simulator** (Fig. 4.82).
- After calculating go to the postprocessor.

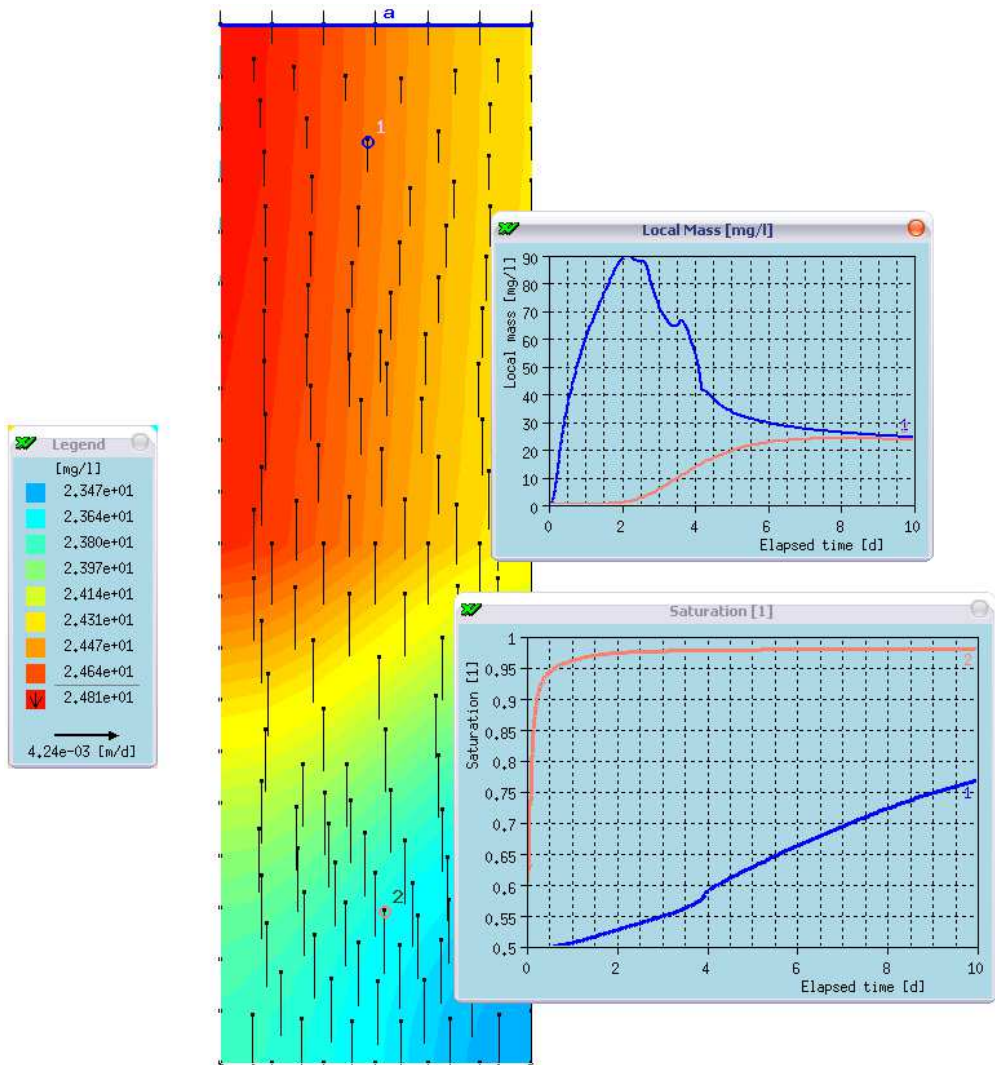


Fig. 4.82. Numerical calculations in the FEFLOW processor

- In **Postprocessor** load the saved output data file – *.dac.
- Enter **Browse file** and select a time step.
- Enter **View results at...** to see results of calculation for the requested time step.
- Generated diagrams can be exported in any format (Fig. 4.83).

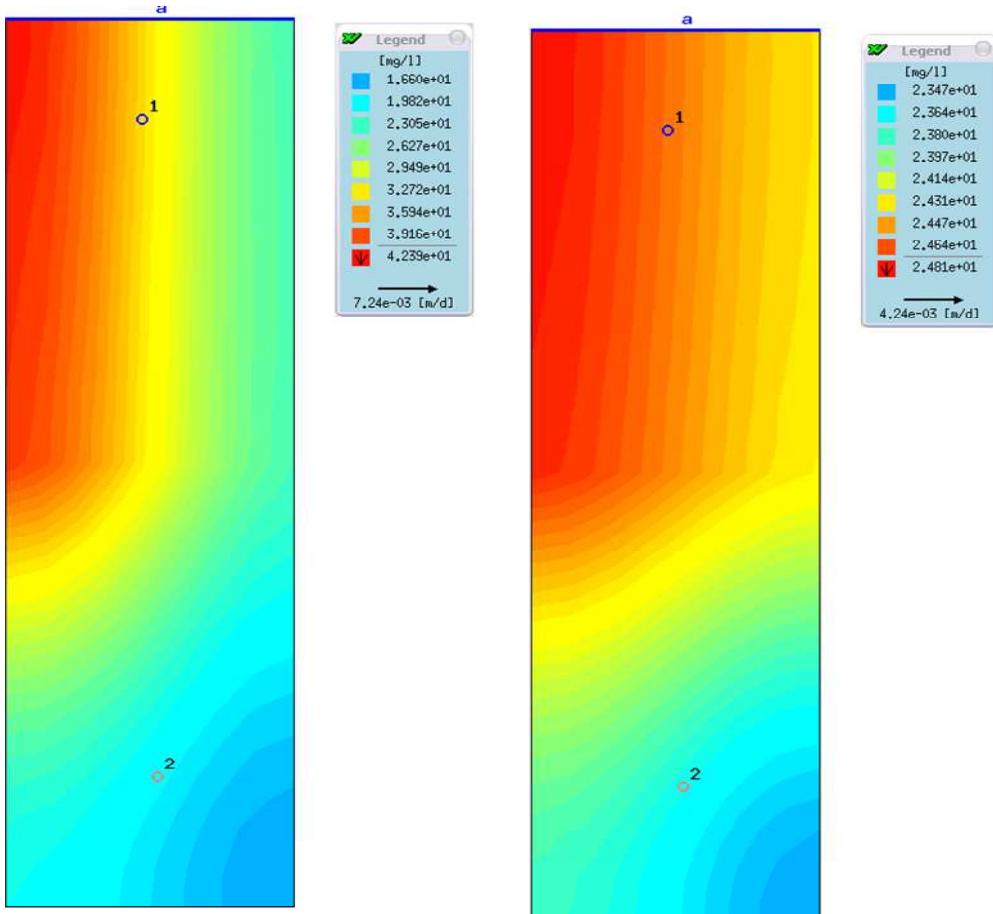


Fig. 4.83. Distribution of contaminant (chromium) in modeled domain in requested time steps

4.6 Simulation of water and contaminant balance for the soil profile consisting of four layers

Perform numerical calculation of water and contaminant balance for the soil profile of dimensions 10.0x3.0 m consisting of four layers of soil. Simulation should cover 60 day time duration. The source of pollution is a failure of underground pipeline starting after 30th day of simulation and lasting 4 days. The water

inflow to the modeled domain from the single point was 100 L/day with concentration of pollution equal to 120 mg/L while background concentration was 20 mg/L. The initial saturation of modeled soil profile was equal to 70%. Bottom boundary condition should allow free gravitational drainage of water to the lower layers of soil. Top boundary condition should reflect water stream consisting of rainwater infiltration and evapotranspiration according to the table below.

Table 4.9. Top boundary condition values

Time [day]	Flux [m ³ /day]	Time [day]	Flux [m ³ /day]	Time [day]	Flux [m ³ /day]
0	0.0002354	21	5.69e-05	42	-0.0038136
1	0.000202	22	9.21e-05	43	-0.0012932
2	0.0001699	23	5.82e-05	44	-0.0009291
3	0.0002305	24	-0.0005137	45	-0.0033021
4	0.0003539	25	-0.00071	46	-0.0002819
5	0.0003729	26	-0.0014386	47	-6.1e-06
6	0.0001245	27	0.0002964	48	-0.0002589
7	0.0001047	28	0.000253	49	-0.0002064
8	0.0002024	29	-0.0001185	50	-0.0002521
9	0.000102	30	-0.0008418	51	-0.0005631
10	3.85e-05	31	-0.0044778	52	-0.0007701
11	1.74e-05	32	-0.0027086	53	-0.0032719
12	3.03e-05	33	-0.0045881	54	-0.0005357
13	0.0001267	34	-0.0030664	55	-6.66e-05
14	-3.95e-05	35	-0.0005851	56	-0.0001106
15	0.0001508	36	-0.002909	57	-0.0002498
16	0.0001545	37	-0.0034462	58	-0.0063844
17	7.15e-05	38	-0.0026084	59	-0.0005289
18	7.39e-05	39	-0.0023687	60	-0.0001073
19	5.84e-05	40	-7.53e-05		
20	-0.0003279	41	-0.0006574		

Table 4.10. Required input soil data

Soil layer	Saturated water content θ_s [-]	Residual water content θ_r [-]	Saturated hydraulic conductivity K_s [m/d]	WRC fitting parameter A [1/cm]	WRC fitting parameter n [-]
Layer 1	0.3895	0.07	0.492	0.0051	1.4245
Layer 2	0.4428	0.051	0.62	0.0082	1.3664
Layer 3	0.4434			0.0090	1.3572
Layer 4	0.4428			0.0082	1.3572

Table 4.11. Mass transport data

Soil layer	Sorption Henry coeff. [-]	Diffusion coeff. $E-9$ [m ² /s]	Longitudinal dispersivity [m]	Transverse dispersivity [m]	Decay rate coefficient $E-4$ [1/s]
Layer 1	0.1485	1.0	36.0	0.5	0.0146
Layer 2	0.1408		1.5		
Layer 3					
Layer 4					

We assume

- soils applied to modeling are an isotropic material,
- no hysteresis for pF (WR) curves,
- porosity equal to maximum saturation,
- automatic time step control.

Simulation

- Create the finite element mesh (or load existing, developed earlier) representing the modeled soil profile – four layers of soil in 10.0x3.0 m profile according to Fig. 4.84.

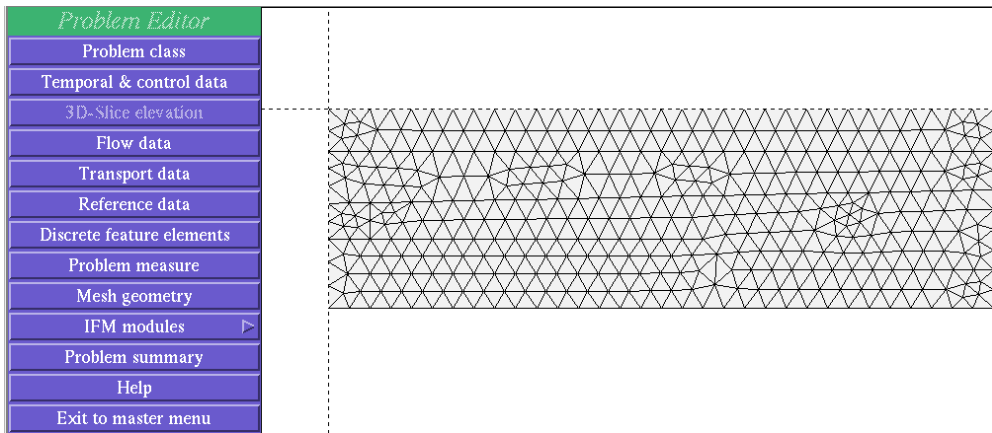


Fig. 4.84. Finite element mesh for modeled soil profile

- Set type of simulation (Fig. 4.85), time duration (Fig. 4.86) and time control options (Fig. 4.87).

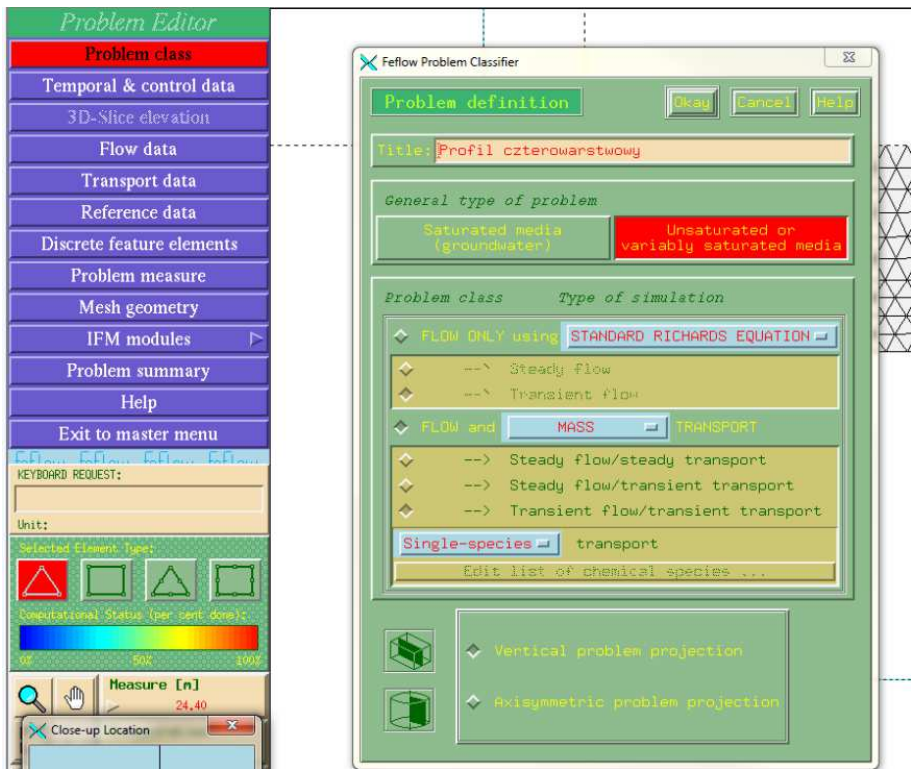


Fig. 4.85. Problem class setting

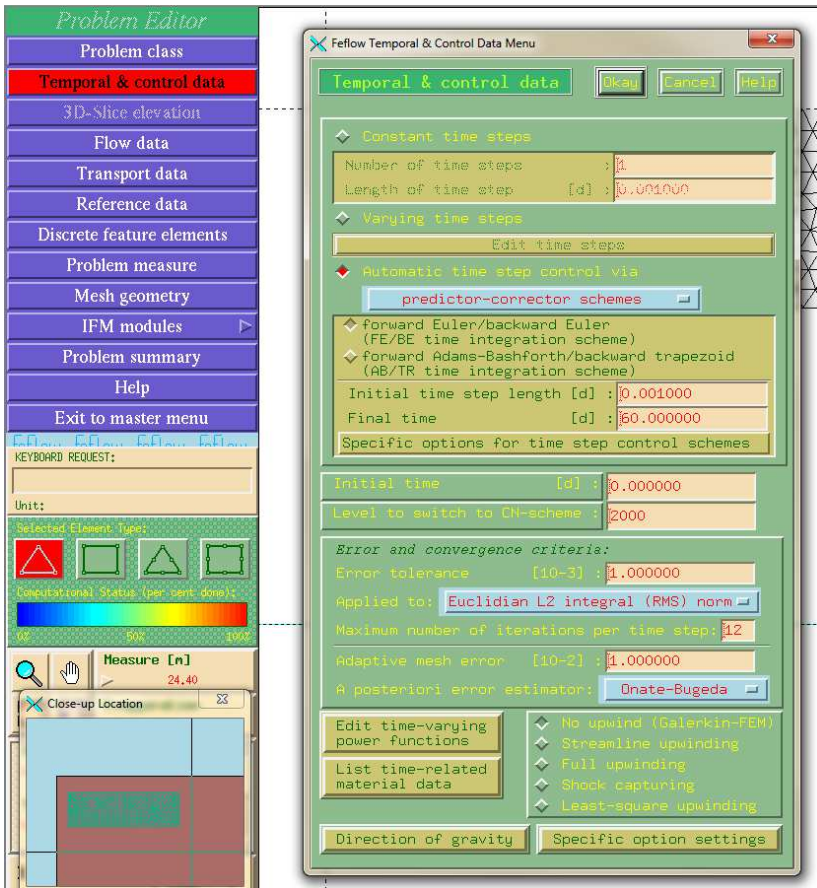


Fig. 4.86. Temporal and control data

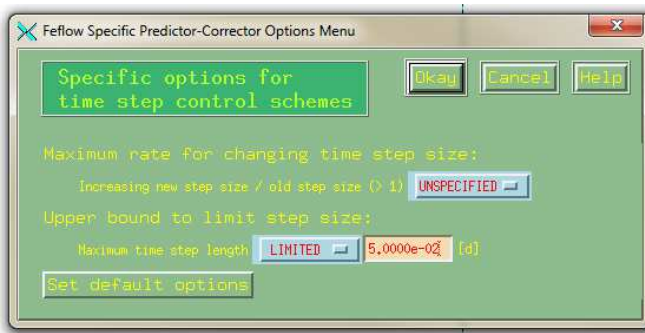


Fig. 4.87. Setting the maximum allowable time step length

- In **Flow data** menu (Fig. 4.88) assign saturated and unsaturated hydraulic characteristics to soil profile, separately for each layer, saturated conductivity and water retention curve (pF) parameters.

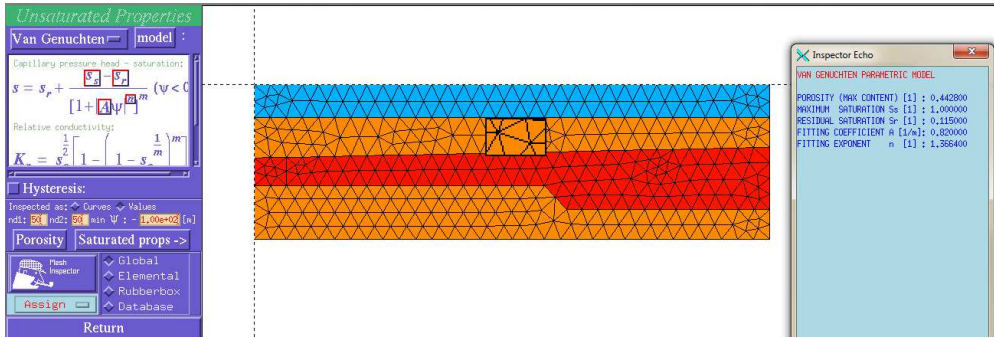


Fig. 4.88. Assigned soil parameters to various layers of modeled profile

- Go back to **Flow data** and select **Flow initials** (Fig. 4.89). Then select **Saturation** and assign 0.7 [-] representing 70% of saturation for time $t = 0$ to the whole modeled soil profile.

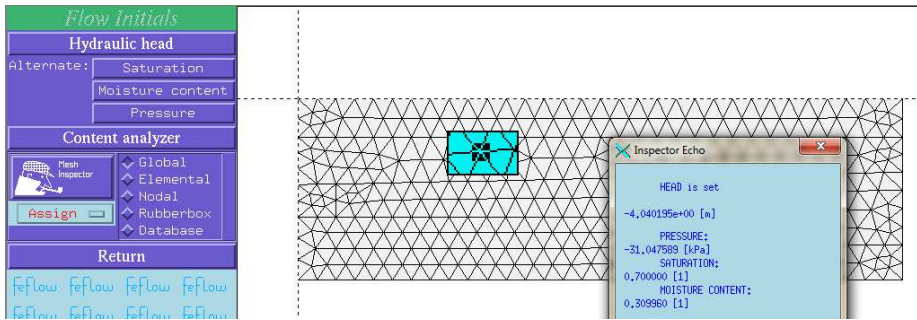


Fig. 4.89. Initial conditions for water flow

- Go to **Flow boundaries** (Fig. 4.90) and assign the gradient type **Flux** bottom boundary condition of value equal to K_s .

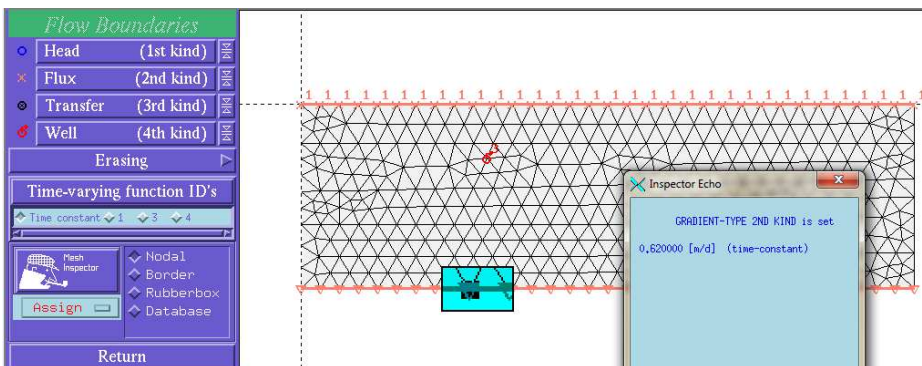


Fig. 4.90. Gradient type FLUX bottom boundary condition

- Enter **Time-varying function ID**, then create the new function (Fig. 4.91), press button Edit curve data and input data from Table 4.7.

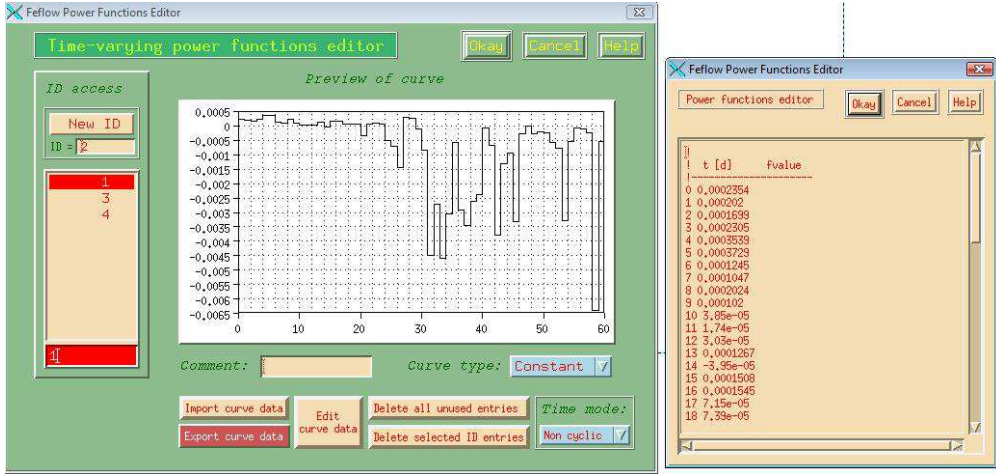


Fig. 4.91. Curve and table for top FLUX boundary condition

- Assign the time dependant function of FLUX boundary condition to the upper boundary of the modeled domain according to Fig. 4.92.

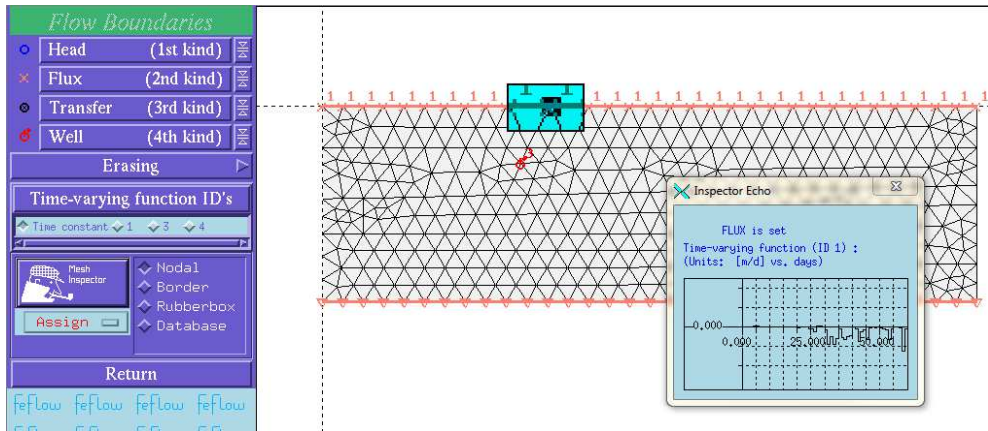


Fig. 4.92. Assigned top time varied FLUX boundary condition

- Enter **Time-varying function ID**, then create the new function, press button **Edit curve data** and input data representing water flux for the pipeline failure, according to Fig. 4.93 – be careful about the sign.

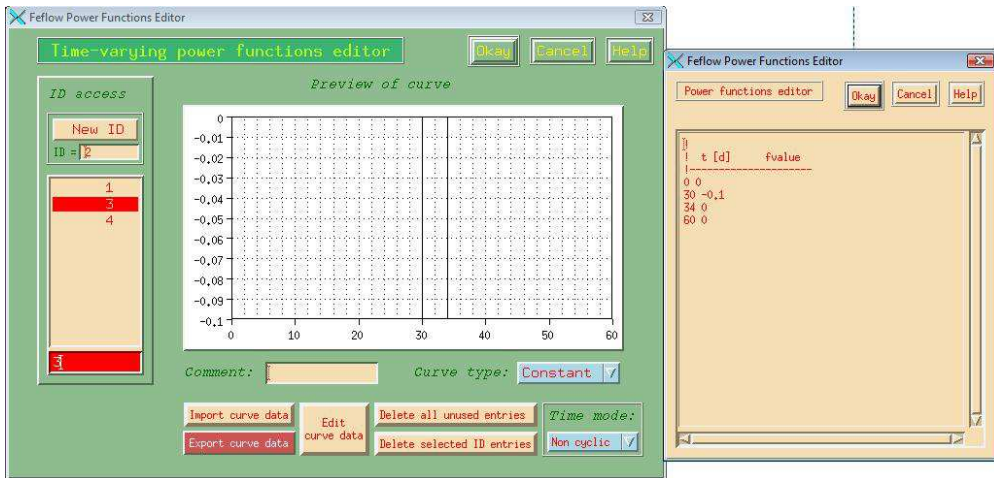


Fig. 4.93. Graph and table for time dependent FLUX for pipeline failure

- Assign the time dependant function of **WELL** boundary condition to the selected node of the modeled domain according to Fig. 4.94.

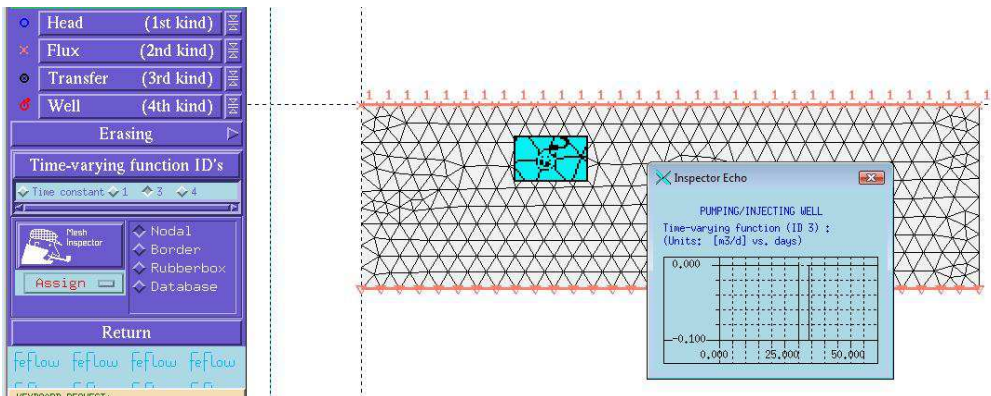


Fig. 4.94. Assigned WELL boundary condition for water flow

- Enter **Transport data** and select **Mass transport materials**, then input the all required mass transport parameters to the modeled domain (Fig. 4.95) according to the Table 4.8.

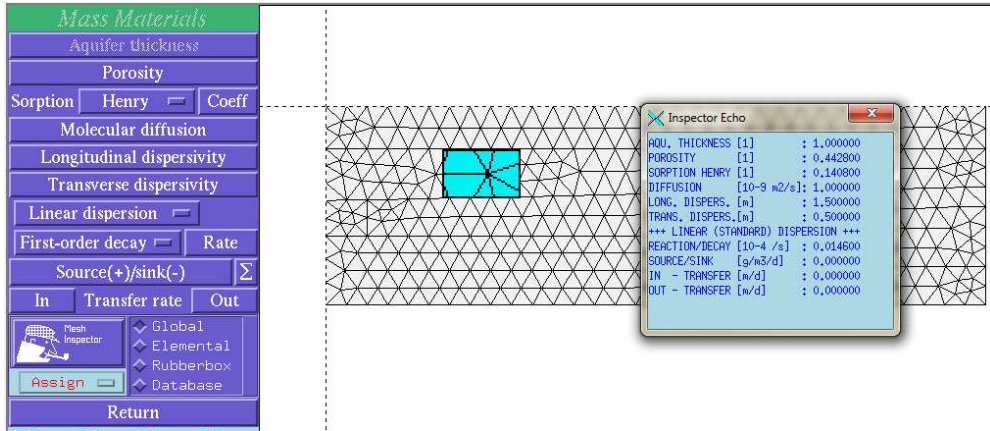


Fig. 4.95. Mass transport materials parameters

- Go to **Mass Initials** and set initial condition for mass transport modeling (Fig. 4.96) – concentration of 20 mg/L.

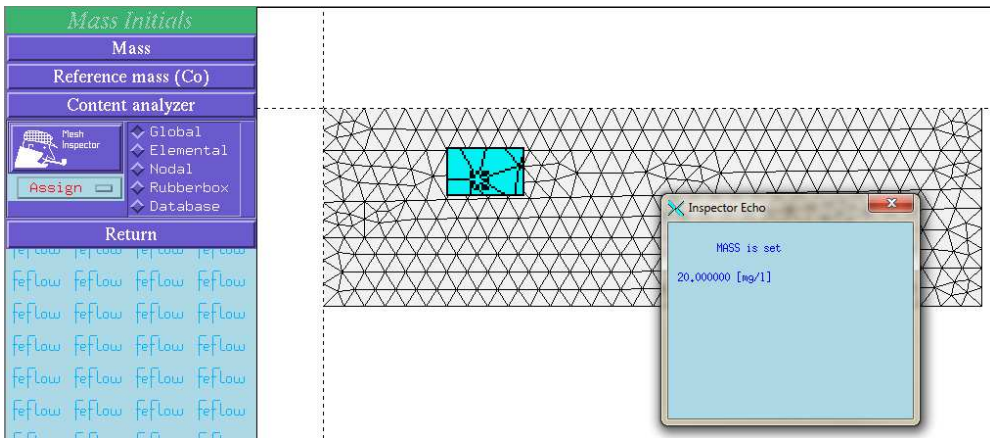


Fig. 4.96. Mass transport initial condition

- Enter **Mass transport boundaries** and select **Time-varying function ID**, then create the new function, press button **Edit curve data** and input data representing changes of pollutant concentration during pipeline failure according to Fig. 4.97.

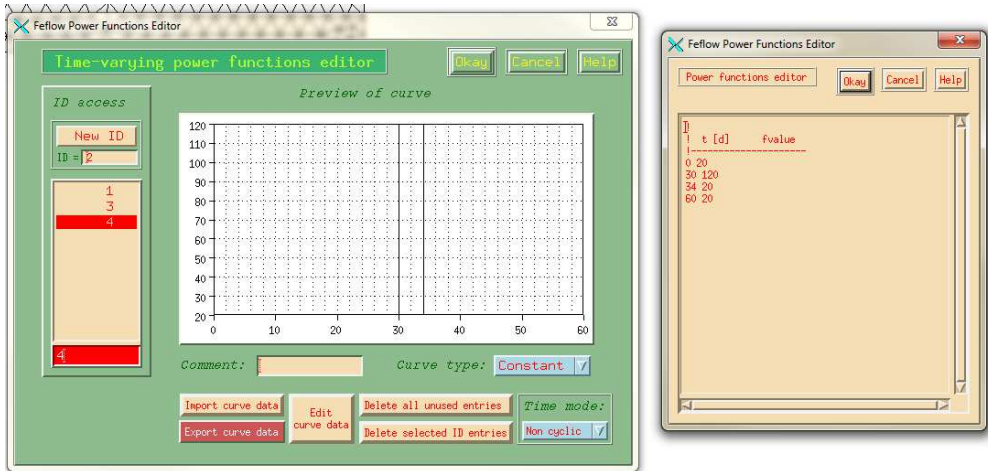


Fig. 4.97. Graph and table for time dependent concentration for WELL boundary condition of mass transport

- Assign the recently created curve as WELL mass transport boundary condition exactly in the location of WELL condition for water flow (Fig. 4.98).

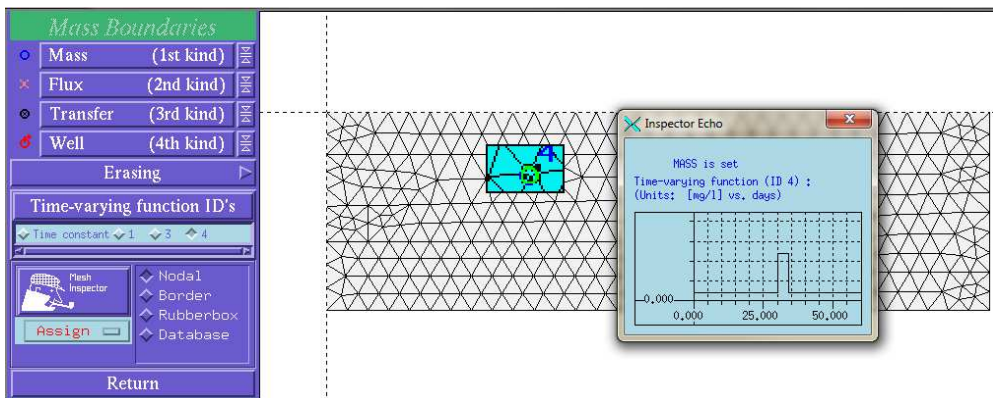


Fig. 4.98. Assigned WELL boundary condition for mass transport

- Now go to the **Reference data – Observation single points** and set observation points, according to Fig. 4.99.

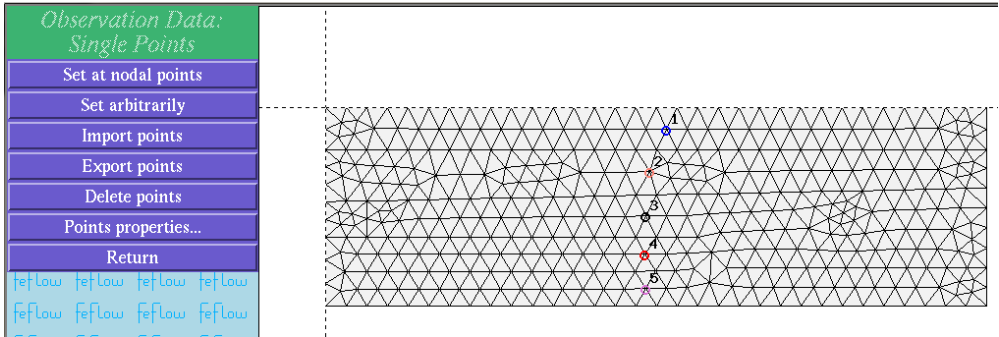


Fig. 4.99. Observation single points

- Save finite element problem (Fig. 4.100), go to the **Simulator**, input **Control output** settings and run the simulation (Fig. 4.101).

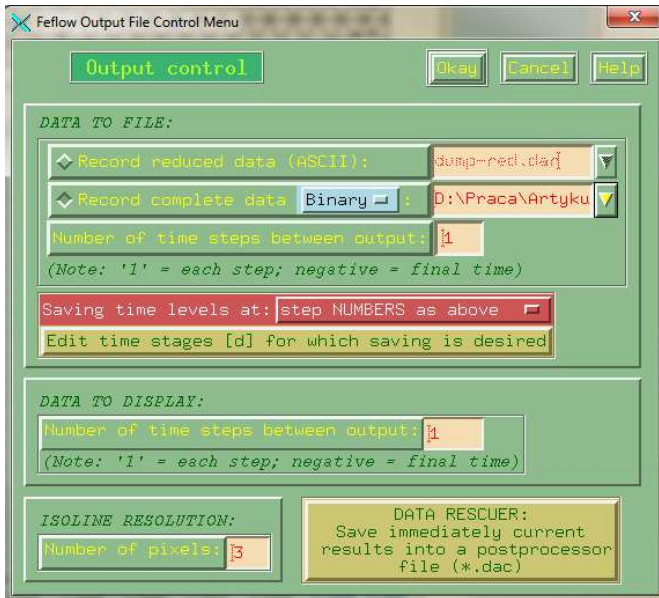


Fig. 4.100. Settings for output control

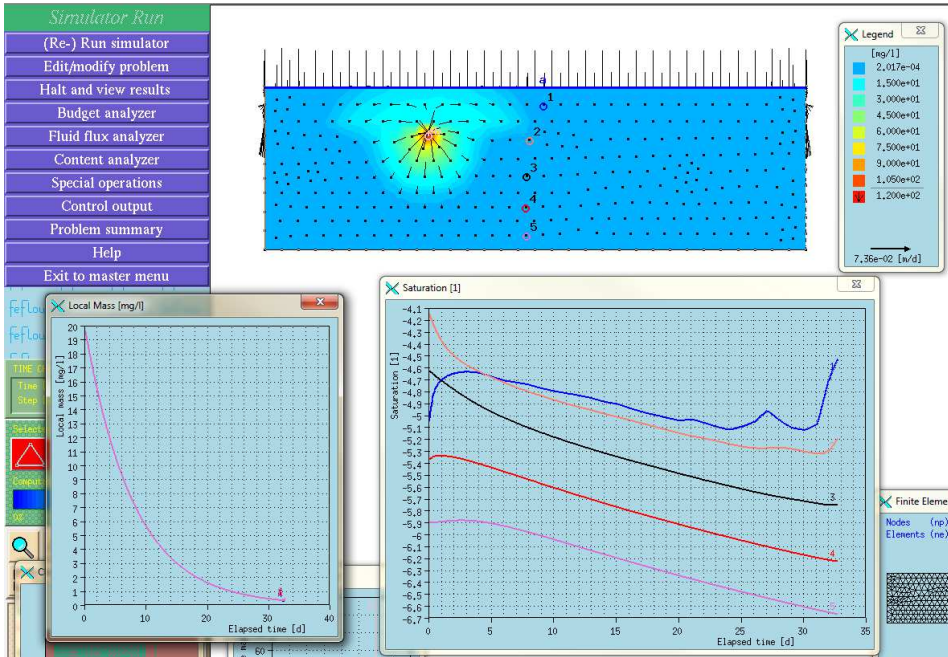


Fig. 4.101. Simulation run

- After finishing the calculation at **Postprocess** load results data (Fig. 4.102).

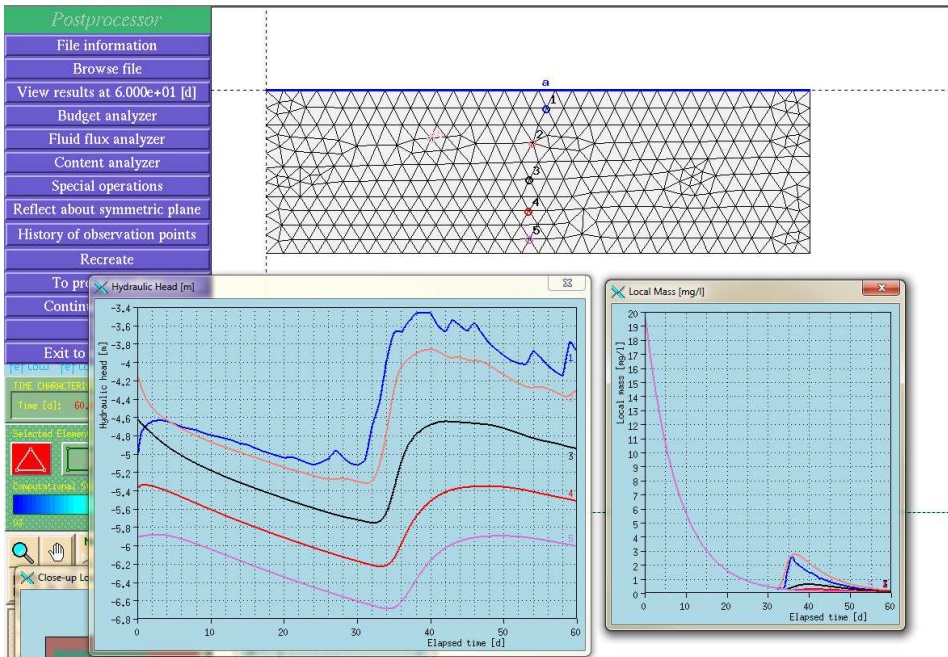


Fig. 4.102. Postprocess

- Enter **Budget analyzer** (Fig. 4.103) and perform balance calculations (select **Total balancing...**) for water after selecting the whole period of simulation for calculations (Fig. 4.104).

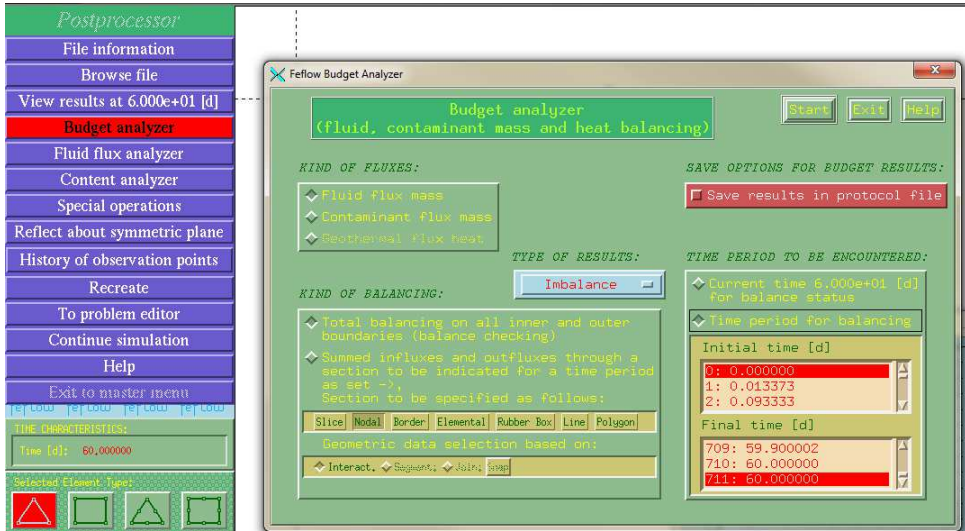


Fig. 4.103. Settings for water budget calculations

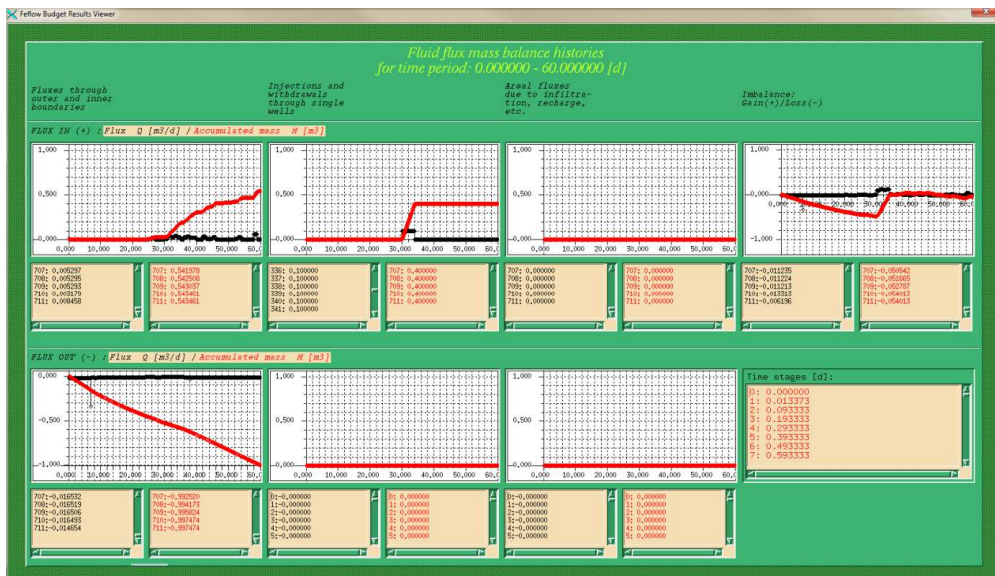


Fig. 4.104. Calculated water balance

- Then perform budget calculations for **Contaminant flux mass** (Fig. 4.105).

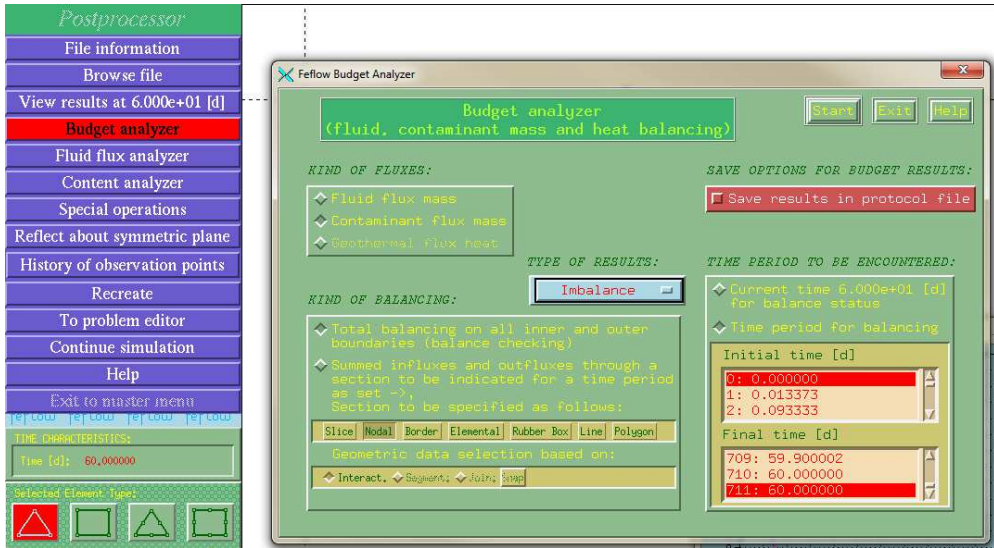


Fig. 4.105. Settings for mass budget calculations

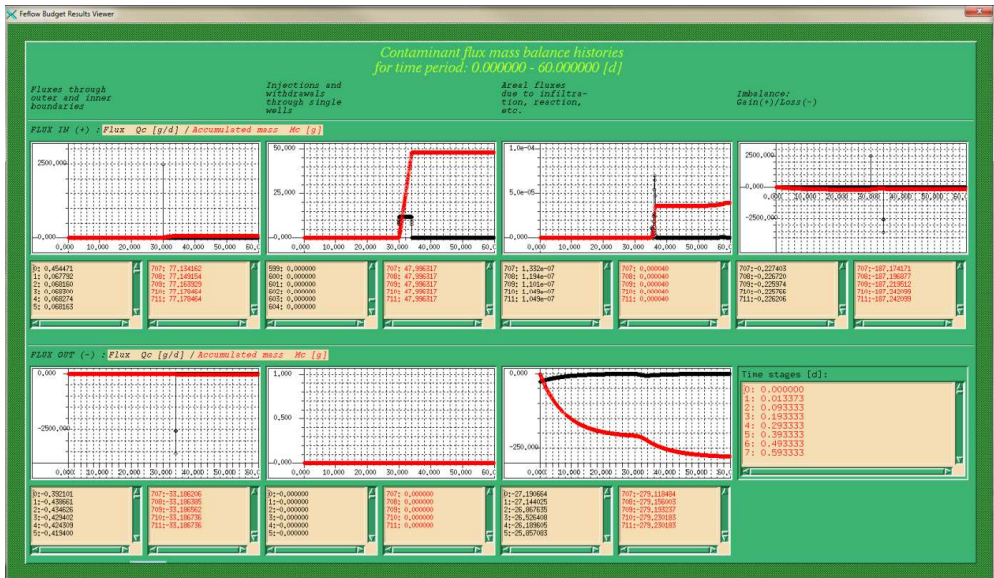


Fig. 4.106. Calculated mass balance

Now the water flux and accumulated volume and contaminant flux and accumulated mass are ready to export (Fig. 4.106) – both as table data and as graphs.

5 Bibliography

1. ASTM D 5298. Standard test method for measurement of soil potential (suction) using filter paper.
2. Bear J., Beljinb M.S., Rossc R.R.: Fundamentals of ground-water modeling. EPA. Ground Water Issue. 1992.
3. Birkeland P.W.: Soils and Geomorphology, 3rd Edition. Oxford University Press, New York 1999.
4. Bohne K., Olszta W.: Application of the van Genuchten's relations to determine the hydraulic prosperities of unsaturated soils. *Polish Journal of Soil Science*, 21(2), 83–88, 1988.
5. Brakensiek D.L., Rawls W.J., Stephenson G.R.: Determining the saturated hydraulic conductivity of a soil containing rock fragments. *Soil Science Society of America Journal*, 50, 834–835, 1984.
6. Brooks R.H., Corey A.T.: Hydraulic properties of porous media. Hydrology Papers 3. Colorado State University, Fort Collins 1964.
7. Brzostowski E., Olszta W.: An assessment of hysteresis in studies on the hydraulic conductivity of peat soils. *Zeszyty Problemowe Postępów Nauk Rolniczych*, 436, 5–11, 1996.
8. Chesworth W (ed.): Encyclopedia of Soil Science. Springer Dordrecht, Berlin, Heidelberg, New York 2008.
9. Cook R.D.: Concepts and applications of finite element analysis. John Wiley & Sons, New York 2002.
10. Cosby B.J., Hornberger G.M., Clapp R.B., Ginn T.R.: A statistical exploration of the relationship of soil moisture characteristics to the physical properties of soil. *Water Resources Research*, 20(6), 682–690, 1984.
11. Dagan G.: Flow and Transport in Porous Formations. Springer-Verlag, Berlin 1989.
12. Darcy H.: Les fontaines publiques de la ville de Dijon. Dalmont, Paris, 1856.
13. de Wit C.T., Goudriaan J.: Simulation of ecological processes. PUDOC, Wageningen 1978
14. Diersch H.J.G., Kolditz O.: Variable-density flow and transport in porous media: approaches and challenges. *Advances in Water Resources*, 25(8–12), 899–944, 2002.
15. Diersch H.J.G.: FEFLOW 5.2 Finite Element Subsurface Flow and Transport Simulation System, Reference Manual. WASY Ltd., Berlin 2005.
16. Diersch H.J.G.: FEFLOW 5.2 Finite Element Subsurface Flow and Transport Simulation System, User's Manual. WASY Ltd., Berlin 2005a.
17. Encyklopedia nauki i techniki. Praca zbiorowa – tłumaczenie. McGraw-Hill Concose of Science & Technology, fourth edition. Prószyński i spółka, Warszawa 2002.
18. Gardner W.R.: Some steady state solutions of unsaturated moisture flow equations with application to evaporation from a water table. *Soil Science*, 85, 228–232, 1958.
19. Glinski J., Horabik J., Lipiec J. (eds.): Encyclopedia of Agrophysics. Springer 2011.

20. Grabarczyk Cz.: Modele w naukach technicznych. W: Problemy inżynierii środowiska u progu nowego tysiąclecia. Oficyna Wydawnicza Politechniki Wrocławskiej, Wrocław 2000.
21. Gromiec J. (red.): Modelowanie matematyczne wód podziemnych – przykłady zastosowań. Biblioteka Jakości Polskiego Komitetu IWA, tom 23, Europejskie Centrum Ekologiczne, Polski Komitet IWA, Warszawa 2007.
22. Hassanizadeh S.M.: Derivation of basic equations of mass transport in porous media, Part 2. Generalized Darcy's and Fick's laws. *Advances in Water Resources*, 9(4), 207–222, 1986.
23. Heinrich J.C., Pepper D.W.: Intermediate finite element method: fluid flow and heat transfer applications / Series in Computational and Physical Processes in Mechanics and Thermal Sciences. Taylor & Francis, Philadelphia 1999.
24. Hillel D.: Introduction to soil physics. Academic Press, San Diego 1982.
25. Huebner K.H.: The finite element method for engineers. John Wiley & Sons, New York 2001.
26. ISO 11276:1995. Soil quality. Determination of pore water pressure. Tensiometer metod.
27. Jillavenkatesa A., Dapkunas S.J., Lin-Sien Lum: Particle Size Characterization. NIST Special Publication 960-1, 2001.
28. Karafiat A. (red.): Adaptive finite element method in fluid mechanics problems / Seria Monografia – Politechnika Krakowska im. Tadeusza Kościuszki, Podstawowe Nauki Techniczne CUT, Kraków 2000.
29. Knapik K.: Dynamiczne modele w badaniach sieci wodociągowych. Politechnika Krakowska, Kraków 2000.
30. Kowalik L.: Zarys fizyki gruntów. Wydawnictwo Politechniki Gdańskiej, Gdańsk 2007.
31. Kowalik P.: Obieg wody w ekosystemach lądowych. Monografie Komitetu Gospodarki Wodnej PAN, Zeszyt nr 9, Warszawa 1995.
32. Król K.: Metoda elementów skończonych w obliczeniach konstrukcji. Wydawnictwo Politechniki Radomskiej, Radom 2006.
33. Kulbik M.: Komputerowa symulacja i badania terenowe miejskich systemów wodociągowych. Politechnika Gdańska 2004.
34. Maciejewski S.: Procesy przepływu rozpuszczonych w wodzie substancji w gruncie nienasyconym. IBW PAN, Biblioteka Naukowa Hydrotechnika nr 26., Gdańsk 1998.
35. Maqsood A., Bussiere B., Mbonimpa M., Aubertin M.: Hysteresis effects on the water retention curve: A comparison between laboratory results and predictive models. 57th Canadian Geotechnical Conference, Quebec, 3A. 8–15, 2004.
36. Mazzia A., Putti M.: Three-dimensional mixed finite element – finite volume approach for the solution of density-dependent flow in porous media. *Journal of Computational and Applied Mathematics*, 185, 347–359, 2006.
37. Olszta W., Zaradny H.: Modelowanie transportu wody w glebach dla potrzeb doskonalenia regulacji stosunków wodnych oraz prognozowania nawodnień. Materiały Informacyjne IMUZ 26, Falenty 1994.

38. Orzechowski Z., Prywer J., Zarzycki R.: *Mechanika płynów w inżynierii środowiska*. Wydawnictwa Naukowo-Techniczne, Warszawa 1997.
39. Pachepsky Y., Timlin D., Rawls W.: Generalized Richards' equation to simulate water transport in unsaturated soils. *Journal of Hydrology*, 272, 3–13, 2003.
40. Prutton M.: *Introduction to Surface Physics*. Oxford University Press, Oxford 1994.
41. Raats P.A.C.: Development in soil-water physics since the mid 1960s. *Geoderma*, 100, 355–387, 2001.
42. Rajkai K., Kabos S., van Genuchten M.Th.: Estimating the water retention curve from soil properties: comparison of linear, nonlinear and concomitant variable methods. *Soil & Tillage Research*, 79, 145–152, 2004
43. Rijtema, P.E.: *Analysis of actual evapotranspiration*. Agricultural Research Reports. No. 69, Wageningen. 1965.
44. Richards L.A.: Capillary conduction of liquids through porous mediums. *Physics*, 1, 318–333, 1931.
45. Sawicki J.M.: *Migracja zanieczyszczeń*. Wydawnictwo Politechniki Gdańskiej, Gdańsk 2003.
46. Saxton K.E., Rawls W.J., Romberger J.S., Papendick R.I.: Estimating generalized soil water characteristics from texture. *Soil Science Society of America Journal*, 50, 2031–2036, 1986.
47. Schaap M.G., van Genuchten M.Th.: A modified Mualem-van Genuchten formulation for improved description of the hydraulic conductivity near saturation. *Vadose Zone Journal*, 5, 27–34, 2006.
48. Sheindorf Ch., Rebhun M., Sheintuch M.: A Freundlich-type multicomponent Isotherm. *Journal of Colloid and Interface Science*, 79(1), 136–142, 1981.
49. Sobieraj J.A., Elsenbeer H., Vertessy R.A.: Pedotransfer functions for estimating saturated hydraulic conductivity: implications for modeling storm flow generation. *Journal of Hydrology*, 251, 202–220, 2000.
50. Stauffer F., Kinze W.: Cyclic hysteretic flow in porous medium column: model, experiment, and simulations. *Journal of Hydrology*, 240, 264–275, 2001.
51. Tietje O., Hennings V.: Accuracy of the saturated hydraulic conductivity prediction by pedo-transfer functions compared to the variability within FAO textural classes. *Geoderma*, 69, 71–84, 1996.
52. Trefry M.G., Muffels Ch.: FEFLOW: a finite-element ground water flow and transport modeling tool. *Ground Water*, 45, 525–528, 2007.
53. van Genuchten M.Th.: A closed-form equation for predicting the hydraulic conductivity of unsaturated soils. *Soil Science Society of America Journal*, 44, 892–898, 1980.
54. Wagner B., Tarnawski V.R., Hennings V., Muller U., Wessolek G., Plagge R.: Evaluation of pedo-transfer functions for unsaturated soil hydraulic conductivity using an independent data set. *Geoderma*, 102, 275–279, 2001.
55. Werner A.D., Lockington D.A.: Influence of hysteresis on tidal capillary fringe dynamics in a well-sorted sand. *Advances in Water Resources*, 26, 1199–1204, 2003.

56. Widomski M.K.: Ocena wpływu zabezpieczeń przeciwoerozyjnych na warunki wilgotnościowe w profilu glebowym. Monografie Komitetu Inżynierii Środowiska PAN 43, Lublin 2007.
57. Widomski M., Iwanek M., Stępniewski W.: Implementing anisotropy ratio to modeling of water flow in layered soil. *Soil Science Society of America Journal*, 2013, 77(1), 8–18.
58. Widomski M., Kowalski D., Łagód G.: Modelowanie ruchu wody i transportu zanieczyszczeń w ośrodku porowatym, Przykłady zastosowania programu FE-FLOW. red. L. Pawłowski, Monografie Komitetu Inżynierii Środowiska PAN vol. 73, Lublin 2010.
59. Widomski M.K., Sobczuk H., Olszta W.: Sand-filled drainage ditches for erosion control: effects on infiltration efficiency. *Soil Science Society of America Journal*, 74(1), 213–220, 2010.
60. Wieczysty A.: Hydrogeologia inżynierska. Arkady, Warszawa 1982.
61. Wilson J.L., Gelhar L.W.: Analysis of Longitudinal Dispersion in Unsaturated Flow. 1. The analytical method. *Water Resources Research*, 17(1), 122–130, 1981.
62. Wind G.P.: Analog modeling of transient moisture flow in unsaturated soil. PUDOC, Wageningen 1979.
63. Wind G.P.: Field experiment concerning capillary rise of moisture in heavy clay soil. *Netherlands Journal of Agricultural Science*, 3, 60–69, 1955.
64. Zand-Parsa Sh., Sepaskhah A.R.: Soil hydraulic conductivity function based on specific liquid-vapor interfacial area around the soil particles. *Geoderma*, 119, 143–157, 2004.
65. Zangwill A.: Physics at surfaces. Cambridge University Press, Cambridge 1988.
66. Zaradny H.: Matematyczne metody opisu i rozwiązań przepływu wody w nienasyconych i nasyconych gruntach i glebach. Praca IBW PAN 23, 1990.
67. Zhao Ch., Wang Y., Chen X., Li B.: Simulation of the effects of groundwater level on vegetation change by combining FEFLOW software. *Ecological Modelling*, 187, 341–351, 2005.
68. Zienkiewicz O.C., Taylor R.L., Nithiarasu P.: The finite element method for fluid dynamics. Elsevier Butterworth-Heinemann, Oxford 2005a.
69. Zienkiewicz O.C., Taylor R.L., Zhu J.Z.: The finite element method. Its basis and fundamentals. Elsevier Butterworth-Heinemann, Oxford 2005b.